

IDENTIFICATION OF HB-EGF POSITIVE AND HB-EGF RESPONSIVE CELL
POPULATIONS IN ZEBRAFISH OLFACTORY EPITHELIUM

by

Kardelen GÜLER

B.S., Molecular Biology and Genetics, Boğaziçi University, 2018

Submitted to the Institute of Graduate Studies in
Science and Engineering in partial fulfillment of the
requirements for the degree
Master of Science

Graduate Program in Molecular Biology and Genetics
Boğaziçi University
2021

ACKNOWLEDGEMENT

I would like to thank various people who supported and contributed to the process of preparing this thesis. My very special gratitude goes to Dr. Stefan H. Fuss for the fact that he never left me alone not only in the process of writing the thesis, but also during my experiments, for being an admirable role model as a supervisor and for his valuable guidance, critiques, enthusiastic encouragement during this research. He helped me improve myself a lot and if he wouldn't showed me a great patience and understanding, I think I wouldn't be where I am now. In this respect, he will hold a very special place for me throughout my life. I would also like to thank former lab member, S. Elif for being a great friend and very professional teacher during the experiments that we performed together. I would like to state that I respect Yiğit Kocagöz for his intellectual and scientific character and I would like to thank him very much for being a very valuable mentor student and for always answering all my scientific questions. In addition, I would like to thank the other members of our laboratory Mehmetcan, Aysu, Zeynep, Şiran, and Sinay for all their help during the time that we worked together and for their friendship. And, of course, I would like to thank Gökberk for all the times that he hosted me and for being such a good friend. I would also like to thank Barış for his honest friendship, who is a member of Fly Lab, and to my jury members for their patience and understanding, along with all the other MBG members. Additionally, I would like to thank dear Ümit Bayraktar, since she did her best to convince me to continue and finish my work when I decided to leave. I would like to thank her for being very supportive. And lastly but very specially, I would like to thank my very beloved parents and my beautiful sister for all the sacrifices and support they have shown for me. I acknowledge with great thanks the support, patience, encouragement, and most importantly the love from my family. Thank you for being such an amazing family.

Work on this thesis has been supported by the Scientific and Technological Research Council of Turkey (TÜBİTAK) under Grant Number 119Z081 (Zebra balığı koku epitelinde rejeneratif nörogenez sırasında heparin bağlayıcı epidermal büyüme faktörü (HB-EGF) sinyalinin rolü) to SHF.

ABSTRACT

IDENTIFICATION OF HB-EGF POSITIVE AND HB-EGF RESPONSIVE CELL POPULATIONS IN ZEBRAFISH OLFACTORY EPITHELIUM

The peripheral olfactory epithelium (OE) is an exception to the limited capacity of the adult nervous system to undergo neurogenesis, which supports structural repair in response to traumatic injury. It continuously and lifelong generates new olfactory sensory neurons (OSNs) at high rate to replace dying cells. Additionally, the OE is capable of regenerating efficiently following severe structural damage. Similar to the mammalian OE, maintenance and regenerative neurogenesis in zebrafish are associated with the selective activity of globose (GBC) and horizontal basal cells (HBC), respectively, which have distinctive structural and functional characteristics. Transcriptome analysis of the regenerating OE suggested that the diffusible signaling factor heparin-binding epidermal growth factor-like growth factor (HB-EGF) may play a critical role at the onset of regenerative neurogenesis. In response to tissue damage, expression levels of HB-EGF are transiently and rapidly upregulated as an early damage response. HB-EGF stimulates mitotic activity in HBCs through the epidermal growth factor receptor (EGFR) signaling pathway. However, the tissue expression of both HB-EGF and EGFR in the zebrafish OE were not known. The studies described in this thesis identified HB-EGF-expressing and HB-EGF-responsive cells by selective *in situ*-hybridization against *hbegfa* and *egfra* transcripts. *Hbegfa* is expressed largely by Sox2-positive basal cells, including tp63-positive HBCs, in addition to HuC/D-positive OSNs and additional cells that may comprise sustentacular glial cells. In response to injury, the number of *hbegfa*-positive cells increases across all cell populations. In contrast, *egfra* is expressed by two cell types with distinct tissue distribution, which include HBCs occupying basal OE layers and a subpopulation of OSNs that are restricted to the apical surface of the zebrafish OE. The expression analysis complements previous findings on the proposed role of HB-EGF during OE regeneration and suggests a model of signaling that includes paracrine stimulation between basal cells and other resident OE cells onto injury-responsive HBCs.

ÖZET

ZEBRABALIĞI KOKU ALMA EPİTELİNDEKİ HB-EGF POZİTİF VE HB-EGF'E YANIT VEREN HÜCRELERİN TANIMLANMASI

Periferik olfaktör epitel (OE), yetişkin sinir sisteminin, travmatik yaralanmaya karşın yapısal onarımı destekleyen nörogenez geçirme konusundaki sınırlı kapasitesinin bir istisnasıdır. Sürekli ve ömür boyu, ölmekte olan hücrelerin yerini almak için yüksek oranda yeni koku alma duyu nöronları (OSN'ler) üretir. Ek olarak, OE, ciddi yapısal hasarın ardından verimli bir şekilde yenilenme yeteneğine sahiptir. Memeli OE'ine benzer şekilde, zebra balığındaki onarım ve rejeneratif nörogenez, ayırt edici yapısal ve fonksiyonel özelliklere sahip olan sırasıyla küresel (GBC) ve yatay bazal hücrelerin (HBC) seçici aktivitesi ile ilişkilidir. Yenileyici OE'in transkriptom analizi, difüz edilebilir sinyal faktörü olan heparin bağlayıcı epidermal büyüme faktörü benzeri büyüme faktörünün (HB-EGF) rejeneratif nörogenezin başlangıcında kritik bir rol oynayabileceğini öne sürdü. Doku hasarına yanıt olarak, HB-EGF'nin ekspresyon seviyeleri, erken bir hasar yanıtı olarak geçici ve hızlı bir şekilde yukarı doğru regüle edilir. HB-EGF, epidermal büyüme faktörü reseptörü (EGFR) sinyal yolu aracılığıyla HBC'lerde mitotik aktiviteyi uyarır. Bununla birlikte, zebra balığı OE'sinde hem HB-EGF hem de EGFR'nin doku ekspresyonu bilinmiyordu. Bu tezde açıklanan çalışmalar, *hbegfa* ve *egfra* transkriptlerine karşı seçici *in situ*-hibridizasyon yoluyla HB-EGF eksprese eden ve HB-EGF'ye yanıt veren hücreleri tanımladı. *Hbegfa*, HuC/D-pozitif OSN'lere ve sustantaküler glial hücreler içerebilen hücrelere ek olarak tp63-pozitif HBC'ler dahil olmak üzere Sox2-pozitif bazal hücreler tarafından büyük ölçüde eksprese edilir. Yaralanmaya yanıt olarak, tüm hücre popülasyonlarında *hbegfa*-pozitif hücrelerin sayısı artar. Buna karşılık, *egfra*, bazal OE katmanlarında bulunan HBC'leri ve zebra balığı OE'nin apikal yüzeyi ile sınırlı olan bir OSN alt popülasyonunu içeren, farklı doku dağılımına sahip iki hücre tipi tarafından ifade edilir. Ekspresyon analizi, OE rejenerasyonu sırasında HB-EGF'nin önerilen rolüne ilişkin önceki bulguları tamamlar ve bazal hücreler ile diğer yerleşik OE hücreleri arasında yaralanmaya duyarlı HBC'ler üzerinde parakrin uyarımı içeren bir sinyal modeli önerir.

TABLE OF CONTENTS

ACKNOWLEDGEMENT	iii
ABSTRACT	iv
ÖZET	v
TABLE OF CONTENTS	xiii
LIST OF FIGURES.....	ix
LIST OF TABLES	xiii
LIST OF SYMBOLS	xiv
LIST OF ACRONYMS/ABBREVIATIONS	xv
1. INTRODUCTION	1
1.1. Adult Neurogenesis	2
1.2. Two modes of Adult Neurogenesis	3
1.3. Zebrafish as a Regenerative Research Model	5
1.4. Anatomical structure and function of the olfactory epithelium.....	8
1.5. Molecular regulation of the dynamic neurogenesis.....	12
1.5.1. The role of HB-EGF signaling pathway on neurogenesis.....	14
2. PURPOSE	18
2.1. Identification of <i>hbegfa</i> -expressing cells in the intact and injured OE.....	18
2.2 Identification of HB-EGF-responsive cells.....	18
2.3 Analysis of the induction of transient GBCs in response to injury.....	19
3. MATERIALS AND METHODS	20
3.1. Materials.....	20
3.1.1. Fish	20
3.1.2. Equipment and supplies	20

3.1.3. Chemicals, reagents, and solutions	20
3.2. Methods	20
3.2.1. Maintenance of zebrafish	20
3.2.2. Polymerase Chain Reaction (PCR) amplification and cloning strategy.....	21
3.2.3. Restriction Digestion	23
3.2.4. Agarose gel electrophoresis	23
3.2.5. Antisense Riboprobe synthesis via <i>In vitro</i> Transcription.....	24
3.2.6. Chemical lesion on the olfactory epithelium with Triton X-100	25
3.2.7. Dissection of olfactory epithelium	26
3.2.8. Cryosectioning of olfactory epithelium	26
3.2.9. <i>In situ</i> -hybridization	27
3.2.10. Combining <i>In situ</i> -hybridization with Immunohistochemistry on OE sections	29
3.2.11. Imaging.....	30
3.2.12. Data analysis	30
4. RESULTS.....	32
4.1. Expression pattern of <i>hbegfa</i> in the intact zebrafish OE.....	34
4.2. Expression pattern of <i>hbegfa</i> in the damaged zebrafish OE.....	35
4.3. Summary Conclusion.....	38
4.4. Identification of <i>hbegfa</i> -expressing cells in the intact OE.....	38
4.4.1. Expression of <i>hbegfa</i> in Sox2-positive cells.....	38
4.4.2. Expression of <i>hbegfa</i> in Tp63-positive cells.....	40
4.4.3. Expression of <i>hbegfa</i> in Krt5-positive cells.....	41
4.4.4. Expression of <i>hbegfa</i> in CKII-positive cells.....	43
4.4.5. Expression of <i>hbegfa</i> in HuC/D-positive cells.....	44
4. 5. Summary Conclusion.....	45

4. 6. Identification of hbegf-expressing cells in damaged OE.....	46
4.6.1. Expression of <i>hbegfa</i> in Sox2-positive cells [4hpl].....	47
4.6.2. Expression of <i>hbegfa</i> in CKII-positive cells [4hpl].....	49
4.6.3. Expression of <i>hbegfa</i> in Tp63-positive cells [4hpl].....	51
4.6.4. Expression of <i>hbegfa</i> in HuC/D-positive cells [4hpl].....	53
4. 7. Summary Conclusion.....	55
4. 8. Generation of an <i>erbb1/ egfra</i> - specific riboprobe.....	58
4. 9. Expression pattern of <i>erbb1/egfra</i> in the intact zebrafish OE.....	64
4.9.1. Expression of <i>erbb1/egfra</i>	65
4.9.2. Expression of <i>erbb1/ egfra</i> combined with IHC	66
4. 10. Summary Conclusion.....	67
4. 11. Induction of <i>ascl1a</i> -expressing cells in the lesioned OE.....	68
4.11.1. Expression of <i>ascl1</i> in intact OE.....	68
4.11.2. Expression of <i>ascl1</i> -expressing cells in damaged (1% TrX Lesioned) OE..	70
5. DISCUSSION.....	74
5.1. HB-EGF as a molecular signal in tissue regeneration.....	78
5.2. EGFR expression in the zebrafish olfactory system.....	79
5.3. Relationship between EGF signaling and other signaling pathways in the context of regeneration.....	82
REFERENCES.....	84
APPENDIX A: EQUIPMENTS, CHEMICALS and REAGENTS.....	105

LIST OF FIGURES

Figure 1.1. Morphological and anatomical structure of peripheral zebrafish olfactory epithelium.....	10
Figure 1.2. Overview of HB-EGF signaling.....	16
Figure 4.1. Expression of the paralogous <i>hbegfa</i> and <i>hbegfb</i> zebrafish genes.....	33
Figure 4.2. <i>In situ</i> -hybridization of the zebrafish OE using a <i>hbegfa</i> antisense riboprobe.....	34
Figure 4.3. ISH against <i>hbegfa</i> (red) transcript on OE sections under physiological and different injury conditions.....	37
Figure 4.4. Quantification of <i>hbegfa</i> signal in the control and 4-hour post lesioned OE.....	37
Figure 4.5. <i>In situ</i> -hybridization against <i>hbegfa</i> transcript non-neuronal cells immunoassayed with Sox2.....	40
Figure 4.6. Combination of <i>in situ</i> -hybridization against <i>hbegfa</i> transcript and immunohistochemistry against the transcription factors Tp63.....	41
Figure 4.7. Anti-Krt5 (the HBC marker) and anti- HuC/D immunohistochemistry on intact OE.....	42
Figure 4.8. Immunohistochemistry against the SC marker CKII.....	43
Figure 4.9. Combination of <i>in situ</i> -hybridization against <i>hbegfa</i> transcript and immunohistochemistry against the SC marker CKII.....	44

Figure 4.10. Combination of <i>in situ</i> -hybridization against <i>hbegfa</i> transcript and immunohistochemistry against the pan-neuronal marker HuC/D.....	45
Figure 4.11. Combination of <i>in situ</i> -hybridization against <i>hbegfa</i> transcript and immunohistochemistry against the HBC marker Tp63 and pan-neuronal marker HuC/D on the intact OE.....	46
Figure 4.12. <i>In situ</i> -hybridization against <i>hbegfa</i> transcript and immunohistochemistry against Sox2 marker.	48
Figure 4.13. ISH against <i>hbegfa</i> transcript and IHC against Sox2 marker.....	49
Figure 4.14. Combination of <i>in situ</i> -hybridization against <i>hbegfa</i> transcript and IHC against SC marker CKII.	50
Figure 4.15. ISH against <i>hbegfa</i> transcript and IHC against SC marker CKII	51
Figure 4.16. Combination of <i>in situ</i> -hybridization against <i>hbegfa</i> transcript and immunohistochemistry against transcription factor tp63.	52
Figure 4.17. Combination of <i>in situ</i> -hybridization against <i>hbegfa</i> transcript and immunohistochemistry against transcription factor tp63.	53
Figure 4.18. ISH against <i>hbegfa</i> transcript and IHC against the pan-neuronal marker HuC/D.....	54
Figure 4.19. ISH against <i>hbegfa</i> transcripts and IHC against the pan-neuronal marker HuC/D, and general stem cell marker Sox2.	56
Figure 4.20. <i>In situ</i> -hybridization against <i>hbegfa</i> transcripts and immunostaining against the pan-neuronal marker HuC/D, and the transcription factor tp63.....	57

Figure 4.21. A. B. ISH against <i>hbegfa</i> transcripts and IHC against HuC/D, tp63 and Sox 2. C. Quantification of the number of <i>hbegfa</i> -positive cells per epithelial fold at 4 hpl.....	58
Figure 4.22. Representation of <i>egfra</i> transcript.....	59
Figure 4.23. Amplification of <i>egfra</i> target region by polymerase chain reaction (PCR) with OneTaq® and Titanium Taq® Polymerases.....	60
Figure 4.24. Gel image of specifically designed <i>egfra</i> primer pairs.....	61
Figure 4.25. <i>EcoRI</i> -HF restriction digestion for <i>egfra</i> colonies	62
Figure 4.26. Representation of pGEMT-easy vector map with <i>egfra</i> probe region reverse-ly inserted	63
Figure 4.27. Agarose gel image of linearized <i>egfra</i> template in pGEMT-easy vector.....	63
Figure 4.28. Gel electrophoresis of the synthesized <i>egfra</i> riboprobe.....	64
Figure 4.29. A. Baseline expression levels of EGF receptor family members in the intact zebrafish OE B. Logarithmic fold changes in expression levels of EGF receptor family members upon 1% TrX 100 induced chemical lesion to OE.....	65
Figure 4.30. <i>Egfra</i> expression in the intact hemi-OE.	66
Figure 4.31. ISH with <i>egfra</i> antisense RNA riboprobe and IHC against the HBC marker tp63 and the OSN marker HuC/D.	67
Figure 4.32. Expression of <i>ascl1a</i> proneuronal gene and IHC against stem cell marker Sox2.....	69

Figure 4.33. Expression pattern of <i>ascl1a</i> and immunohistochemistry against HBC marker Tp63.....	70
Figure 4.34. Expression pattern of <i>ascl1a</i> and immunohistochemistry against Sox2 stem cell marker.	71
Figure 4.35. <i>In situ</i> -hybridization against <i>ascl1a</i> combined with immunohistochemistry against HuC/D in intact and damaged OE at 24 and 48 hpl.....	72

LIST OF TABLES

Table 1. Primers used in this study.....	21
Table 2. The standard PCR setups.....	22
Table 3. Genes analyzed in this study.....	23
Table 4. Riboprobe synthesis reaction.....	25
Table 5. Hybridization mixture.....	29
Table A.1. List of equipment.....	105
Table A.2. List of chemicals and reagents.....	108
Table A.3. Solutions and Buffers.....	112

LIST OF SYMBOLS

bp	Base pair
kb	Kilobase
h	Hour
d	Day
g	Gram
L	Liter
M	Molar
min	Minute
sec	Second
ml	Milliliter
mM	Millimolar
μg	Macrogram
μl	Microliter
μm	Micrometer
μM	Micromolar
mg/l	Milligram / liter
ng	Nanogram
v	Volume
w	Weight
nm	Nanometer
rpm	Revolution per minute
°C	Celcius

LIST OF ACRONYMS/ ABBREVIATIONS

BrDU	5'- Bromo-2'Deoxyuridine
BSA	Bovine Serum Albumin
cDNA	Complementary DNA
CNS	Central Nervous System
DIG	Digoxigenin
DG	Dentate Gyrus
DMSO	Dimethyl Sulfoxide
DNA	Deoxyribonucleic Acid
dpf	Days Post Fertilization
DT	DEPC- treated
FA	Formamide
GBC	Globose Basal Cell
GPCR	G protein -Coupled Receptor
HBC	Horizontal Basal Cell
hpf	Hours Post-Fertilization
IHC	Immunohistochemistry
ILC	Inter-lamellar Curve
ISH	<i>In situ</i> -Hybridization
LCR	Locus Control Region
Mdn	Median
mRNA	Messenger RNA
nt	Nucleotide
OB	Olfactory Bulb
OE	Olfactory Epithelium
OMP	Olfactory Marker Protein
OR	Olfactory Receptor
OSN	Olfactory Sensory Neuron
PBS	Phosphate Buffered Serine
PBST	Phosphate Buffered Serine with Tween

PCR	Polymerase Chain Reaction
PFA	Paraformaldehyde
pH	Power of Hydrogen
PNS	Peripheral Nervous System
RNA	Ribonucleic Acid
RT	Room Temperature
S/NS	Sensory/ Non-Sensory
SC	Sustentacular Cell
Sc	Sensory Central
SEM	Standard Error Mean
Sp	Sensory Peripheral
UV	Ultraviolet

INTRODUCTION

Every living organism receives and responds to stimuli from the external and internal environment. The proper communication between the organisms and the external environment has great importance for its survival and allows it to choose the right mating partner for reproduction, to feed on appropriate food, and to avoid predators (Dangles et al., 2009). In this regard, chemosensation as an ancient and conserved sense exists in both higher organisms and lower organisms. Depending on their evolutionary stage, different groups of organisms have developed unique structures and signaling pathways for sensing environmental stimuli (Libert & Pletcher, 2007). As organismal complexity increases over evolution, receiving, adapting, and responding to these stimuli becomes more organized into dedicated sensory structures (Edlund et al., 2011). In addition, increasingly complex higher neural structures become involved in the process compared to the simpler structures of organisms that can sense and respond to environmental chemicals directly (Erulkar & Lentz, 2020). One of the more complex, yet widely conserved sensory systems across species is the olfactory system, which allows for the conscious perception of smell in response to chemical stimuli.

The term chemosensation refers to the events that take place during the reception of a chemical input by a neuronal chemoreceptor cell and the transduction of that input into molecular or electrical signals that are further communicated to the brain as a response (Prasad & Reed, 1999). Chemosensation and the olfactory system have been studied extensively in mammals, insects, and other species (Prasad & Reed, 1999). In the study presented in this thesis, the small freshwater teleost *Danio rerio*, commonly known as the zebrafish, was used as a model organism. Compared to mammals, the zebrafish olfactory system is easier to study because it is less complex and more easily accessible, which make the zebrafish a suitable model for different types of experimental manipulations.

1.1. Adult Neurogenesis

Neurogenesis is defined as the process of generating neurons from lineage restricted neuronal precursors or progenitor cells (Ming and Song, 2005). Until the second half of the 20th century, it was believed that neurogenesis only occurs during the early development of an organism and that the adult nervous system has no capacity to compensate for the loss of neurons via regenerative processes (Owji and Shoja, 2020). It was believed that the nervous system is too complex in its structural morphology and function for newly born neurons to be successfully integrated into the already existing neural connections of the adult brain (Ramon y Cajal, 1928).

However, the above-mentioned ‘central dogma of neurobiology’ was invalidated in the 1960s by studies of Robert Altman, who demonstrated the presence of newborn neurons in specific regions of the regenerating hippocampus and olfactory bulb after damage in the postnatal rat brain (Altman and Das, 1965). These results posed the first pioneering evidence for the existence of adult neurogenesis, i.e., the generation of new nerve cells in the post-developmental brain. Subsequent research provided further supportive evidence for adult neurogenesis by confirming that certain central nervous system components have proliferative capacity (Altman, 1969). Early studies conducted in songbirds (Paton and Nottebohm, 1984) and subsequent research reporting the functional integration of newly generated neurons into the central nervous system of monkeys (Gould et al., 1999) demonstrated that adult neurogenesis exists in different species. However, different organisms show differential neurogenic potential in terms of mitotically active sites in the brain at old organismal age (Eriksson et al., 1998). Nevertheless, these pioneering studies were received as a major breakthrough in neuroscience because of their important therapeutic implications and finally resulted in the wider acceptance of the phenomenon of adult neurogenesis. The field was further developed upon the introduction of new methodologies to detect newborn cells in tissue samples. Various dyes and chemicals such as bromodeoxyuridine (BrdU), a thymidine analogue that is incorporated into DNA during replication, is often used as a simple birth marker and lineage tracing agent (Kuhn et al., 1996).

Even though adult neurogenesis also occurs in mammals, the capacity of the CNS to generate adult-born neurons is relatively low and highly restricted to two distinct regions of

the brain. The subgranular zone (SGZ) of the hippocampus and the ventricular-subventricular zone (V-SVZ) of the lateral ventricles are the two prominent regions in which neurogenesis occurs persistently in the mammalian brain. (Altman, 1969; Kaplan and Hinds, 1977; Gage, 2000). However, species-specific differences exist, and the neurogenic potential may be lower in some species. For instance, one recent study has shown that hippocampal neurogenesis ceases during early adulthood in primates and humans and becomes undetectable at old age (Sorrells et al., 2018). In contrast, lower vertebrates generally show a much higher rate of adult neurogenesis. Studies conducted in three different teleost species, the stickleback *Gasterosteus aculeatus* (Ekström et al., 2001), the electric knife fish *Apteronotus leptorhynchus* (Zupanc and Horschke, 1995), and the zebrafish *Danio rerio* (Grandel et al., 2006), reported up to 16 sites that were identified to be active in generating new neurons. These active sites include the olfactory bulb, the telencephalon, the hypothalamus, the cerebellum, and the spinal cord, to name only the most prominent ones. It appears that the capacity of an organism to generate new neurons seems to be inversely proportional to the level of evolution and development of that organism (Kaslin et al., 2008). Thus, simpler organisms, such as amphibians and fish, have a larger capacity to regenerate and harbor additional neurogenic sites that are active in the adult compared to higher level organisms like mammals (Alunni et al., 2016).

1.2. Two modes of adult neurogenesis

Adult neurogenesis refers to a sequence of complex steps, which includes the proliferation and expansion of neural stem and progenitor cells, the specification of neuronal precursors, the differentiation of specific neurons, and ultimately the integration of new information-processing nerve cells into pre-existing neural circuits (Ming, 2011). The process can be conceptually subdivided into two distinct modes, constitutive and regenerative neurogenesis, depending on the tissue conditions (Alunni et al., 2016). Constitutive neurogenesis, also referred as maintenance neurogenesis, describes the process by which active stem/progenitor cells proliferates continuously in the intact nervous system and generate a constant stream of adult-born neurons. Constitutive neurogenesis contributes to neuronal turnover and tissue maintenance under physiological conditions but also to plastic changes in brain function (Ma et al., 2009). In contrast, regenerative (or repair) neurogenesis, depends on dormant stem/progenitor cells that are transiently induced to

undergo mitotic proliferative activity to restore neurons that have been lost because of traumatic injury to the tissue. Both modes of neurogenesis are tightly regulated and controlled by a large number of signaling factors that control the rate of cell proliferation but also the different steps of neuronal differentiation and specification (Alunni and Bally-Cuif, 2016). Interactions between cells, chemical factors, and physical properties that form the neurogenic niche and neural stem/progenitor cells (NSCs) have a crucial regulatory role in maintaining the homeostasis of adult neurogenesis throughout the life of organism. Niche-derived signals control quiescence and senescence of NSCs and regulate their mode and rate of cell division (Morrison and Spradling, 2008; Miller and Gauthier-Fisher, 2009). In this regard, adult neurogenesis is a highly dynamic process and extensively regulated by a large variety of physiological, pathological, and pharmacological stimulants (Ming and Song, 2011). Similar to other epithelial tissues, constitutive neurogenesis occurs at a high proliferation rate, while regenerative neurogenesis is typically inactive under physiological conditions. It depends on latent, also referred to as dormant or quiescent, progenitor/stem cell populations that are transiently engaged to undergo active divisions to repair lesioned tissue and to regenerate a large number of lost neurons. In addition to regenerating neurons, it was reported that upon a traumatic injury, both processes also contribute to the generation of non-neuronal cell populations in accordance with the need of the lesioned tissue for structural repair (Goldman, 2005; Zhang et al., 2005).

Both forms of adult neurogenesis occur in the mammalian nervous system but typically with low capacity, while non-mammalian vertebrate species show a much higher capacity. Among those, the zebrafish is one of the more widely used experimental models to study the regenerative capacity of the CNS in response to injury. The zebrafish brain shows both high constitutive turnover during maintenance neurogenesis in up to 16 distinct regions of the nervous system (Grandel et al., 2006) but also responds efficiently to injury (Kaslin et al., 2008; Alunni and Bally-Cuif, 2016). In addition to the brain, other studies also demonstrated the persistent constitutive neurogenesis in the fish retina (Stenkamp, 2007) and in the olfactory epithelium (Bayramlı et al., 2017). Taken together, these studies illustrate that zebrafish is a remarkable model for regenerative research on the nervous system.

1.3. Zebrafish as a Regenerative Research Model

Zebrafish (*Danio rerio*) is a tropical fish that belongs to the minnow family of freshwater teleost and is an inhabitant to Southeast Asia, predominantly territories around the Himalayan Mountains (Engeszer et al., 2007). It has been established as a common vertebrate animal research model since the 1970s and its popularity has accelerated scientific research in developmental and regenerative biology (Streisinger et al., 1981). The zebrafish was first introduced as a biological model organism by George Streisinger at the University of Oregon because it was easier to manipulate genetically compared to the mouse. Others were fascinated by the idea of using the zebrafish embryo to study the development of nervous system. In the 1990s, the zebrafish was used to develop genetic mutants by the Nobel Prize winning studies of Christiane Nusslein-Volhard, Wolfgang Driever, and Mark Fishman (FR Khan, 2018).

Zebrafish has significant advantages which made it a prominent laboratory model over the years. In the laboratory, it is easy to maintain in simple aquatic systems even with limited space and low costs, which make it an affordable model organism to study. The rapid embryonic development and high fecundity provide large sample sizes for developmental studies (Gemberling et al., 2013). External fertilization and external development of optically clear embryos make zebrafish even a more valuable model, which allow the direct observation of developmental process in real time (Veldman and Lin, 2008). Since the zebrafish genome was sequenced in 2013 and has been updated at regular intervals, an increasing number of genetic tools and engineering methods have been developed. The fish also has benefits for discovering the molecular causes of disease phenotypes, such as muscular dystrophy (Spinazzola et al., 2016) and cancer, as well as other conditions, such as aging (Dooley and Zon, 2000; Ghosh and Hui, 2016; Gurtner et al., 2008).

One of the first studies demonstrating technical advantage of investigating regeneration in adult zebrafish were conducted by Johnson and Weston in 1995. The authors used a temperature-sensitive screen to identify mutations disrupting the regeneration of tailfins (Gemberling et al., 2013). In addition to its ability to regenerate fins, zebrafish has also a natural capability to regenerate heart tissue (Poss et al., 2002). Several injury models, cryoinjury being the most widely used, allowed scientists to study myocardial infarctions to

gain a better understanding of the mechanisms that are involved in repair of cardiac muscle upon experimental damage (Wang et al., 2011).

Furthermore, by using zebrafish for chemical screening in a regeneration context, scientists have identified compounds that activate the adenosine pathway as enhancers of β -cell regeneration, that were subsequently confirmed in a mouse model of diabetes, which further would be useful for developing novel therapeutic approaches (Andersson et al., 2012). In addition to chemical screening studies and the advance of genetic screens in zebrafish, novel tools for interfering with gene function have been developed. For instance, larvae injected with *dnmt1* morpholino oligonucleotides showed increased capacity for pancreatic beta cell regeneration, which poses an inducible model of pancreatic beta cell ablation as well (Anderson et al., 2009).

Scientists have also reported evidence showing that the zebrafish is capable of regenerating renal tissue (McCampbell et al., 2014). They traced the source of new nephrons in the adult zebrafish to small cellular aggregates containing nephron progenitors and demonstrated that the zebrafish kidney harbors self-renewing nephron stem/progenitor cells. The identification of these cells paved the way for isolating or engineering analogous cells in mammals and developing novel renal regenerative therapies (Diep et al., 2011). Another study in this field has also demonstrated that liver tissue of the zebrafish regenerates by a compensatory growth mechanism, utilizing proliferation of existing hepatocytes in uninjured liver lobes (Stoick-Cooper et al., 2007; Kan et al., 2009; Curado and Stainier, 2010). Other studies revealed that intrinsic and extrinsic signals modulate blastemal progenitors to repair bony structure and mesenchymal segmentation in the zebrafish lower jaw, which again, highlight the importance of zebrafish as a regenerative research model (Wang et al., 2012; reviewed by Gemberling et al., 2013).

The regenerative ability of the fish is not limited to somatic tissues but also extends to central and peripheral nervous system structures (Becker and Becker, 2008). Hair cells in the zebrafish lateral line have been investigated for their regenerative ability in live animals, showing that hair cell regeneration is robust and rapid thanks to their position on the surface of the body and the stereotyped positions of neuromasts, (Williams and Holder, 2000; Harris et al., 2003; Hernandez et al., 2006; Lopez-Schier and Hudspeth, 2006; Ma et al., 2008).

According to these studies, it has been shown that hair cells regenerated within only 48 h and reestablished mechano-transduction, hair cell bundle polarity, and synapses with the auditory nervous system (Hernandez et al., 2006; Lopez-Schier and Hudspeth, 2006; Brignull et al., 2009).

Zebrafish also provides an excellent model for studying retina regeneration (Wan and Goldman, 2016). Investigations of mechanisms underlying retina regeneration in zebrafish have revealed important signaling pathways that are involved in the process and which may be translated to human eye conditions (Gorsuch and Hyde, 2014). The comparisons of retinal injury responses in zebrafish and mammals may allow the identification of factors that could potentially trigger mammalian retina regeneration, and which would be beneficial for finding therapeutic treatments for people suffering from blinding eye disease (Wan J and Goldman, 2016; reviewed by Gemberling et al., 2013).

In contrast to mammalian models of spinal cord injury, zebrafish regeneration unfolds in the absence of a glial scar (Goldshmit et al., 2012). Unlike the dense network of glial processes that is formed from hypertrophic stellate glia in mammals, zebrafish glia adopts an elongated morphology joining the amputated regions of the spinal cord. These glia structures form a bridge over which regenerating axons can actively grow to re-innervate regions caudal to the injury. Goldshmit and her colleagues showed that glial activation and formation of an environment that is permissive for regeneration is regulated by Fgf signaling and they proposed that differences in Fgf expression and responsiveness could determine the distinct responses of mammal and zebrafish to spinal cord injury (Goldshmit et al., 2012).

Remarkably, not only peripheral nervous system structures but also the brain itself can undergo substantial regeneration (Fleisch et al., 2010). Studies have revealed that zebrafish brain effectively regenerates, replenishes lost neurons, and restores the tissue architecture. With the use of conditional CreER^{T2}-loxP lineage-tracing (Hans et al., 2009), scientists demonstrated that ventricular radial glia cells expressing *her4.1* (an orthologue of mammalian *hes5*) serve as the main neuronal progenitors responding to the lesion (Kroehne et al., 2011). In response to blunt traumatic brain injury, these cells increase proliferation, upregulate neuronal fate determining gene transcription, and form neuroblasts that migrate into the periventricular zone and deeper into the parenchyma to the site of injury, where they

differentiate into mature neurons (Kroehne et al., 2011). Understanding the ability to produce long lasting neurons after a lesion to the adult brain bears fundamental importance and could serve as a pioneering development for the establishment of new therapeutic strategies for the degenerative, diseased, or injured human brain (Becker & Becker, 2008).

Thus, the zebrafish has a remarkable capacity for the repair of somatic and neural tissues, making the zebrafish a conspicuous model that can serve as a guide for the comprehensive understanding of tissue renewal across species and for the discovery of novel regenerative strategies that can be utilized for higher organisms, including humans (Marques et al., 2019).

1.4. Anatomical structure and function of rodent and zebrafish olfactory epithelium

The zebrafish olfactory epithelium (OE) is organized into lamella structures that are formed by folding of the flat multilayered neuroepithelium onto itself around 33 days post fertilization (dpf) during early development (Hansen and Zeiske, 1993). The apical surface of the OE is exposed to water-filled spaces and the basal parts of the epithelium join at the lamina propria between two epithelial sheets, which includes blood vessels, fat cells, pigment cells, and olfactory sensory neuron (OSN) axon fascicles (Fig. 1 B). The intricate folding gives the OE a rosette-like overall appearance. Two separate olfactory organs lie dorsally on each side of the head and each projects a short nerve to the olfactory bulbs of the rostral telencephalon (Fig. 1.1. A). An adult OE contains about 16 to 20 lamellae and its dimensions vary between 350 – 600 μm in length and 250- 350 μm in width depending on the age of the organism (Hansen and Zeiske, 1998; Calvo-Ochoa et al., 2021). Owing to the rosette-shaped OE, which is analogous to the turbinate organization in mammals, the sensory surface area is increased for interaction with environmental chemicals and odorant perception (Green et al., 2012; reviewed by Calvo-Ochoa et al., 2021).

The OE is composed of different neuronal and non-neuronal cell populations with different characteristic functions and morphologies giving rise to a pseudostratified tissue. OSNs occupy the central sensory region of the OE (Celik et al., 2001; Bayramlı et al., 2017), while mucus producing cells and cells with motile cilia occupy the outer edge of the tissue

defining the non-sensory region (Hansen and Zeiske, 1998). The apical layer of the OE harbors the cell bodies of neurons, while basal layer accommodates the cell bodies of olfactory stem and progenitor cells in addition to sustentacular glial cells (Demirler et al., 2020).

The neuronal population of the OE consists of specialized OSNs that have the capacity to detect odorant compounds (Sato et al., 2005). OSNs make direct contact with the external environment and are unprotected against environmental toxicants and infectious agents, which is probably the reason for their relatively short lifespan of only 30 – 90 d in mammals (Moulton, 1974; Mackay-Sim and Kittel, 1991) and 19 days in zebrafish (Bayramli et al., 2017). Therefore, the OE has a high regenerative capability to replace the dying neurons continuously to preserve olfactory sensory function throughout the lifespan of the organism (Schultz, 1941).

OSNs project their axons to the OB glomeruli where they form synapses with periglomerular interneurons and mitral cell projection neurons to transmit odorant information to the piriform cortex and other higher cortical areas in the brain (Mori et al., 1999; Tham et al., 2009). Each OSN expresses only a single (or a few) olfactory receptor (OR) belonging to the family of seven transmembrane G protein-coupled receptors (Song et al., 2008). Because they only express a limited subset of possible receptors from a vast genomic repertoire of ORs (Weth et al., 1996), the population of OSNs is capable of detecting a huge number of structurally distinct odorants. In zebrafish, OSNs occupy the inner two thirds of each lamella starting from the interlamellar curve (ILC) towards the outer edge of the epithelium. This area is referred to as the sensory region and comprises five different types of OSNs, namely microvillous, ciliated, crypt (Hansen and Finger, 2000), pear (Wakisaka et al., 2017) and kappe neurons (Ahuja et al., 2014; reviewed by Calvo-Ochao et al., 2020). The outer non-sensory epithelium mostly harbors respiratory cells, mucus-producing goblet cells and cells with motile cilia (Hansen and Zeiske, 1998). The ILC and the border that separates the sensory and non-sensory region (SNS) are the sites of active cell proliferation in the intact OE (Bayramli et al., 2017), which contributes to maintenance neurogenesis and compensate for the loss of dying neurons. Because new OSNs are generated outside the sensory region, new-born cells migrate towards to the middle of the epithelium as they mature and age (Bayramli et al., 2017). The sensory region of the OE

can be visualized by immunostaining against HuC/D which is a pan-neuronal marker (Kim et al., 1996) or the mature OSN-specific marker olfactory marker protein (OMP) on cross sections of OE (Celik et al., 2002; Bayramlı et al., 2017; Fig. 1.1.C).

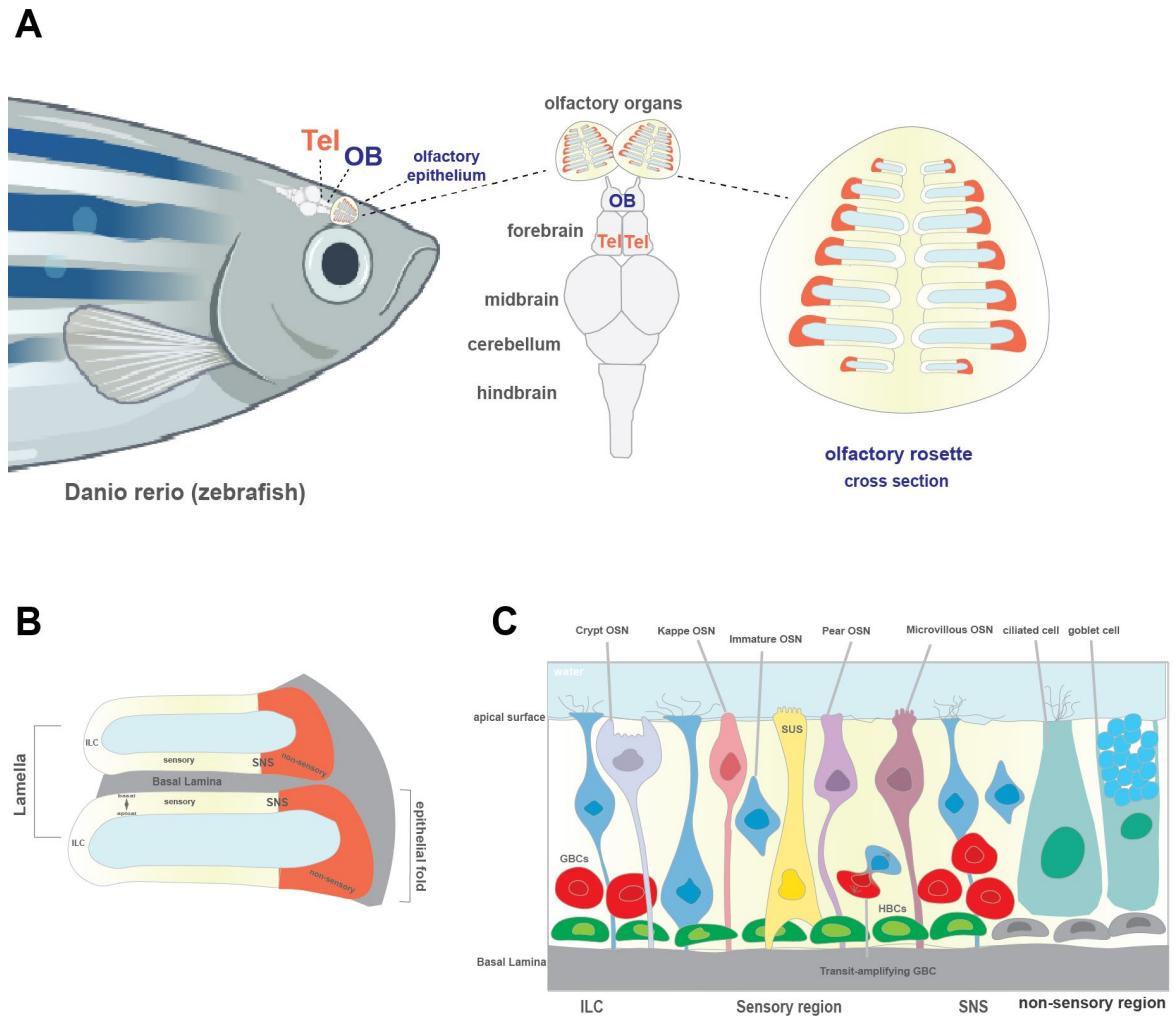


Figure 1.1. Morphological and anatomical structure of peripheral zebrafish olfactory epithelium. **A.** The zebrafish olfactory system. **B.** Structure of individual lamellae. **C.** Cellular composition of zebrafish OE.

Analogous to the rodent OE, the zebrafish tissue comprises different non-neuronal cells that have direct role in OSN neurogenesis or support the OE structure. Also, the peripheral edge of the epithelium harbors columnar epithelial cells (Hansen and Zeiske, 1998), which resemble cells in the respiratory OE of mammals (Morrison and Castanzo,

1992). Goblet cells, which produce mucus are functionally analogous to Bowman's glands in the mammalian OE (Hansen and Zeiske, 1998). Similar to the mammals, the zebrafish OE also harbors two types of stem/progenitor cells, the globose (GBCs) and horizontal basal cells (HBCs), that are located in the basal layer of OE (Schwob et al., 2017; Demirler et al., 2020). GBCs are a group of spherical cells that form a heterogeneous populations of stem cells, transit-amplifying cells, committed progenitors, and mitotically active immediate precursors. GBCs are constitutively active and are responsible for the regular turnover of olfactory OSNs in the intact tissue (Schwob et al., 2017; Guo et al., 2010; Chen et al., 2014; Leung et al., 2007; Demirler et al., 2020). Different transcription factors are transiently and sequentially expressed in the GBCs lineage during the generation of OSNs, which enable the identification and characterization of different GBC subgroups. GBC progenitors are Sox2 (Sry-box containing gene 2) and Pax6 (Paired box 6) double-positive (Guo et al., 2010; Packard et al., 2016), while transit-amplifying cells also express the basic helix-loop-helix transcription factor Ascl1 (Achaete- scute homolog 1; Krolewski et al., 2012), which determines the neuronal fate. In addition, immediate neuronal precursors express NeuroD1 and Neurog1, which drives OSN differentiation forward (Cau et al., 1997). Simplified, it could be said that Sox2 expression represents the stemness in this context and Ascl1 expression is a reliable neuronal commitment marker. GBCs lie in suprabasal layers and slightly more apically than HBCs. While they are evenly distributed in the mammalian OE, they are found to be exclusively located around the ILC and the SNS at the outer edge of the sensory area in zebrafish (Fig. 1 C). Under intact tissue condition, constitutive neurogenesis by GBC proliferative activity is observed exclusively in these defined areas but not in sensory region that is occupied by OSNs and HBCs.

Unlike GBCs, HBCs are flat in shape and occupy the basal-most layer of the OE uniformly in rodents (Leung et al., 2007) and zebrafish (Demirler et al., 2020; Fig. 1C). HBCs can be discriminated from GBCs by their expression of Keratin 5 together with the transcription factor tumor protein 63 (tp63; Demirler et al., 2020). Zebrafish and rodent HBCs are quiescent reserve stem cells under physiological (undamaged) conditions (Schwob et al., 2017; Demirler et al., 2020). However, HBCs are rapidly activated when the tissue integrity is disturbed or cell-to-cell connections between sustentacular glial cells (supportive non-neuronal glial cells) and HBCs is broken (Herrick et al., 2017). HBCs undergo transient activation of mitotic divisions and regenerate both neuronal and non-neuronal cell types of

the OE (Leung et al., 2007). A common method to damage the OE of aquatic organisms is nasal irritation with the non-ionic cytotoxic detergent Triton X-100 (TrX) (Iqbal and Byrd-Jacobs, 2010). High concentrations of TrX cause acute damage to the tissue, while lower concentrations result in milder lesion (Capar, 2015; Iqbal and Byrd-Jacobs, 2010). Although other chemical reagents, such as the organobromide compound methybrumide gas, can be used to damage the OE of air-breathing terrestrial animals, TrX has been shown to affect both progenitor cell types (Iqbal and Byrd-Jacobs, 2010; Calvo-Ochoa and Byrd-Jacobs, 2019). Both strong and mild damage created by TrX give rise to increased mitotic activity especially in the sensory region which is equivalent to an HBC response because of the lack of GBCs in these positions (Kocagöz et al., 2021). Thus, it can be stated that HBCs serve as a stem cell reservoir of the OE and that is in charge of repair neurogenesis under damage conditions. Resembling previous findings, our research group has demonstrated that upon TrX damage, the OE undergoes degeneration causing the death of almost all neuronal cells by 24 hours post lesion (hpl; Kocagöz et al., 2021). Remarkably, the OE appears to be fully regenerated by only 5 to 7 d after the lesion. However, the functional and lineage relationships between HBCs and GBCs are complicated as activated HBCs generate transient GBC-like cells during regeneration (Calvo-Ochoa et al., 2021).

Together with HBCs and GBCs, the sustentacular glial cells (SCs or SUSs) contribute to the non-neuronal population of the OE and provide support to OE and act as a tissue-specific glial cell (Hansen and Zeiske, 1998). SCs are characterized by cytokeratin II but also express Sox2 (Demirler et al., 2020). Unlike mammals, the sustentacular glial cells show an inverted morphology with cell bodies that are positioned basally instead of forming a monolayer within the apical border of the OE. (Demirler et al., 2020).

1.5. Molecular regulation of the dynamics of neurogenesis

The limited ability of the adult CNS to produce new neurons largely contributes to the progression of neurodegenerative diseases and limits recovery after traumatic brain injury (Zambusi, 2020). To develop and design therapeutic drugs to cure or improve CNS related diseases and injuries, deciphering the dynamics and molecular nature of neurogenesis bear vital importance. It is assumed that both extrinsic and intrinsic factors regulate neural stem cell activity, however, to what extent and which factors contribute to regulation of

neurogenesis and knowledge of the underlying detailed mechanism is still missing (Knobloch and Jesseberger, 2011). Notch, FGF, Wnt, and cytokine signaling and their related signaling cascades have all been shown to have a role in regulating neural stem cell activity similar to their role during embryonic development (Ihunwo et al., 2016).

Previous studies have indicated that Notch signaling is prominent in the regulation of neural stem cell activity during the adulthood of both mammals and zebrafish through preserving the balance between quiescent and proliferating progenitors (Chapouton et al., 2010). Notch signaling was shown to be endogenously active in quiescent radial glial cell progenitors and overexpression of Notch gives rise to increased dormancy of radial glial cells in the zebrafish telencephalon (Chapouton et al., 2010). On the other hand, blocking of Notch in these progenitors shift them towards the neuroblasts and postmitotic neuronal states. Thus, it can be stated that the proliferative activity of telencephalic progenitors is negatively regulated by Notch signaling. Likewise, bone morphogenetic protein (BMP) signaling has also been found to modulate stem cell activity through restricting proliferation of stem cells in the adult hippocampus (Mira, 2010; Kızıl et al., 2011).

On the other hand, fibroblast growth factor (FGF) signaling has been shown to modulate proliferation in the adult mouse SVZ (Gritti et al., 1996; Kuhn et al., 1997) and subsequent research has demonstrated that FGF signaling is required to activate telencephalic progenitor proliferation in the adult zebrafish telencephalon (Ganz et al., 2010). Furthermore, epidermal growth factor receptor (EGFR) has been shown to play an important role in the development of nervous system and is involved in the perpetuation of neural stem cell growth and differentiation (Currais et al., 2009). In addition, one member of the EGF family, HB-EGF, has been reported to play a crucial role in dedifferentiation and proliferation of Müller glia cells of zebrafish retina (Wan et al., 2012) and to induce regenerative processes after CNS injury (Jin et al., 2003; Todd et al., 2015).

Other than the factors described above, inflammatory responses have also been shown to be involved in the regulation of NSC activity and proliferation (Carpentier et al., 2009). CNS degeneration induces inflammatory responses through activation of microglia cells, which are CNS macrophages (Das and Basu, 2008). Activated microglia cells eliminate dying neurons in the damaged area and induce neuro-inflammation by the release

of certain chemokines, cytokines, and reactive oxygen species (Rock et al., 2004). These released factors have been revealed to have an impact on neurogenic cell proliferation from local stem/progenitors or functional differentiation of neurons. Also, most recent findings have demonstrated that, in the injured zebrafish retina, cytokines IL6, IL11 and leptin synergistically stimulate regenerative neurogenesis from Müller glia cells through activation of STAT and β -catenin signaling (Wan et al., 2014; Zhao et al., 2014).

1.5.1. The role of HB-EGF signaling pathway on neurogenesis

The signaling molecule heparin-binding epidermal growth factor-like growth factor (HB-EGF) is a transmembrane glycoprotein protein composed of 208 amino acids and initially synthesized as pro-HB-EGF, which is the inactive form (Raab et al., 1997). HB-EGF is a potent mitogen and chemotactic factor on epithelial cells (Feng et al., 2005). It selectively binds to epidermal growth factor receptors that are formed by ErbB1 homodimers or ErbB1/4 heterodimers of the ErbB family of EGF receptor subunits (Iwamoto et al., 2017). It induces downstream signal transduction pathways, predominantly mitogen-activated protein (MAP) kinase, phosphatidylinositol 3-kinase (PI3K/AKT), and signal transducer and activator of transcription (STAT) signaling in target cells (Wee and Wang, 2017; Fig. 1. 2). Pro HB-EGF undergoes ectodomain shedding by ADAM metalloproteinases, particularly ADAM 9, 10, 12, and 17 (Taylor et al., 2014) to produce soluble HB-EGF as the active ligand.

ErbB receptors are members of the receptor tyrosine kinase (RTKs) family, and they were discovered initially during 1950s just after the discovery of nerve growth factor (NGF) by Rita Levi-Montalcini and the epidermal growth factor ligand (EGF) by Stanley Cohen (Cohen, 2008). The formal confirmation regarding the existence of specific receptors that bind to epidermal growth factors was reported in 1975 by Graham Carpenter and colleagues and defined as epidermal growth factor receptors, EGFRs (Eierhoff et al., 2010). This ErbB family involves four members: ERBB1, ERBB2, ERBB3, and ERBB4 (also known as HER1-4). The ErbB1 homodimer is also known as the epidermal growth factor receptor (EGFR; Hynes, 2005). Since the focus of this study will be on the expression of HB-EGF, the known primary receptor of HB-EGF, which is EGFR transcribed from the *egfra* gene in zebrafish, was also analyzed to identify HB-EGF target cells.

Through binding of HB-EGF to EGFR in the target membrane, MAP kinase signal transduction pathway and/or PI3K/AKT signaling is activated, which results in receptor dimerization and cross-phosphorylation. JAK kinase auto-phosphorylates the cytoplasmic tail of ErbB receptor subunits by using phosphates from ATP to form docking sites for STAT resulting in STAT dimerization (Miyoshi et al., 1997; Fang et al., 2001;). Dimerized STAT acts as a transcription factor and translocate into the nucleus to ultimately bind to DNA and regulate transcription of target genes that are related to growth, survival, and proliferation (Singh and Harris, 2005; Wee and wang, 2017; Abud et al., 2021; Fig. 1. 2.) Activated and phosphorylated EGF receptor also recruits PI3 kinase resulting in the conversion of PIP2 into PIP3 and PIP3 serves as a kinase for TOR stimulating translation (Mattoon et al., 2004). EGF receptor activation also leads to activation of the MAP kinase pathway by creating sites for recruitment of the GRB2/SOS/RAS complex, which results in phosphorylation of MEK and ERK (Saito et al., 2004). Phosphorylated ERK further phosphorylates downstream proteins and stimulate translation as well as transcription of genes regulating growth, survival, or proliferation of target cells (Fang et al., 2001; reviewed by Dao et al., 2018).

HB-EGF has been reported to be involved in a variety of developmental and physiological processes in addition to its significant role in the regulation of neural stem cell activity (Tolino et al., 2011; Taylor et al., 2014; Puschmann et al., 2014; Jin et al., 2003; Jin et al., 2005). Previous studies have demonstrated the potential therapeutic role of HB-EGF in combating against various type of cancers since HB-EGF has been found to induce tumorigenesis particularly in ovarian cancer lines (Shen et al., 2019). HB-EGF has also been associated with tumor growth and angiogenesis (Ongusaha et al., 2004). In addition, HB-EGF has been proven to be a prominent therapeutic candidate for certain type of gastrointestinal diseases due to its ability to promote regeneration in the intestinal tissue (Radulescu, 2009).

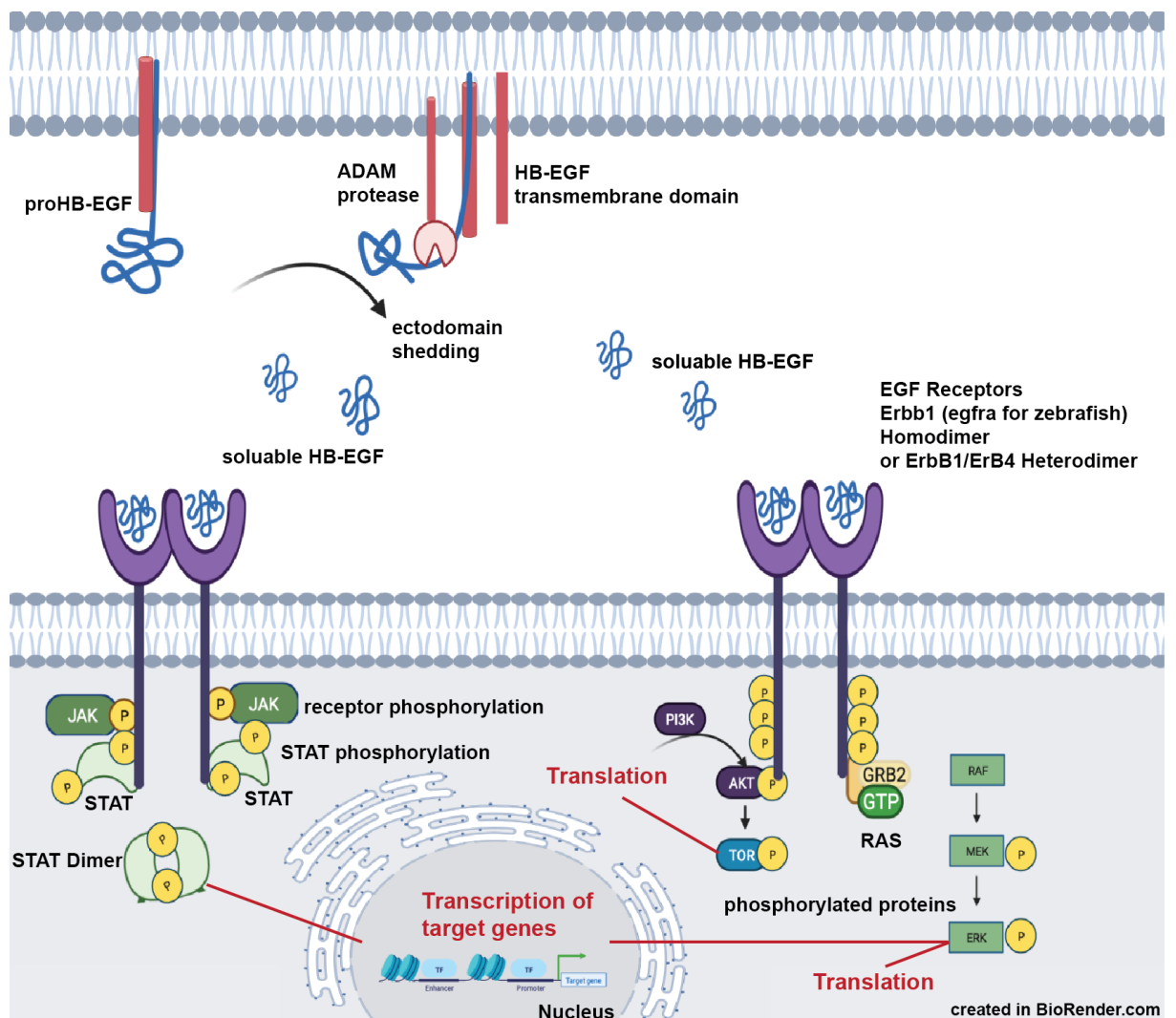


Figure 1.2. Overview of HB-EGF signaling (created in BioRender.com).

HB-EGF expression has been observed in neuron and glia cell populations in several regions of the adult brain (Mishima et al., 1996). Although HB-EGF has been detected to induce neurogenic activity in the active SGZ and SVZ of the brain, it has also been shown that HB-EGF promotes neurogenic activity in the retina of fish and chicken (Wan et al., 2012; Todd et al., 2015). The direct effect of HB-EGF on maintenance and regenerative neurogenesis has been examined in detailed in zebrafish retina and it has been reported that HB-EGF stimulate Müller glia cell reprogramming and subsequent proliferation to repair the loss of nerve cells (Jin, et al., 2003; Wan et al., 2012; Inoue et al., 2013; Todd et al., 2015).

In addition to aforementioned studies, our research group has identified HB-EGF as a candidate signaling molecule that is transiently upregulated during the early tissue response to experimental injury of the zebrafish OE (Kocagöz et al., 2021). Transcriptome profiling by RNA-seq showed that the zebrafish *hbegfa* gene is upregulated 15-fold at 4 h post lesion (hpl) but decreases to basal expression levels around 24 hpl. Therefore, HB-EGF is proposed as a potential and eminent candidate factor promoting the induction of OE regeneration when the tissue integrity is disturbed and that HB-EGF directly or indirectly leads to the activation of dormant neuronal progenitor cells to repair the tissue after traumatic injury. However, the tissue expression of *hbegfa* and its cognate *egfra* receptor in the zebrafish OE were not known.

2. PURPOSE

The heparin-binding growth factor-like growth factor (HB-EGF) has been suggested to be a potent inducer for regenerative neurogenesis in the zebrafish OE. The *hbegfa* gene is highly upregulated immediately following experimental lesions to the OE (Kocagöz et al., 2021). Exogenous stimulation of the OE with recombinant HB-EGF stimulates cell proliferation and neurogenesis (Kocagöz et al., 2021). In contrast, inhibition metalloprotease activity, direct inhibition of HB-EGF, and inhibition of EGFR signaling prevent injury-induced HBC proliferation and OE regeneration (Kocagöz et al., 2021; Şireci and Alkiraz, unpublished). Thus, HB-EGF either directly or indirectly stimulates dormant HBC progenitors in response to tissue damage. However, the identity of *hbegfa*-expressing and HB-EGF-responsive cell populations in the zebrafish OE is not known. Identification of these cells would be required to further elucidate the molecular mechanisms and signaling events that are involved in regenerative OE neurogenesis.

2.1. Identification of *hbegfa*-expressing cells in the intact and injured OE

As a first aim, the expression of the zebrafish *hbegfa* gene was analyzed at mRNA level in the intact OE and immediately after Triton X-100-induced experimental damage to confirm the upregulation *hbegfa* expression that has been observed by transcriptome analysis. For this purpose, an antisense RNA probe specific to the *hbegfa* transcript was synthesized and *in situ*-hybridization experiments were conducted on intact control OEs and at different time points after Triton X-100-induced tissue damage. *In situ*-hybridization against the *hbegfa* transcript were combined with immunohistochemistry against cell type-specific markers for neurons, glia cells, and horizontal basal cells to further identify *hbegfa*-expressing cells under both conditions.

2.2. Identification of HB-EGF-responsive cells

To identify and to further characterize HB-EGF-responsive cell populations in the zebrafish OE an expression analysis of the relevant EGFR subunit ErbB1/Egfra was conducted. For this aim, a specific antisense riboprobe against the *egfra* transcript was

designed, synthesized, and used in *in situ*-hybridization experiments in the intact OE. The *egfra*-expressing cell types were further characterized by immunohistochemistry against cell type-specific markers for neurons, glia cells, and horizontal basal cells.

2.3. Analysis of the induction of transient GBCs in response to injury

Injury-induced HBC proliferation in the core-sensory OE results in tissue regeneration by OSN neurogenesis (Kocagöz et al., 2021; Dokuzluoglu, unpublished). To understand whether HBC activity results in the induction of a transient population of *Ascl1*-positive GBC intermediates, intact and Triton X-100-lesioned OEs were analyzed by *in situ*-hybridization against *ascl1a* transcripts in combination with immunohistochemistry against markers for progenitor cells and neurons. The analysis can be extended to investigate whether the induction of OSN neurogenesis by exogenous stimulation of the OE with recombinant HB-EGF follows the same cellular events as the response to injury.

3. MATERIALS AND METHODS

3.1. Materials

3.1.1. Fish

Throughout of this study, adult zebrafish that are older than 6 months were used, and fish were supplied/ purchased from local pet shops. Some zebrafish used in this study were in AB/AB genetic background and received from a zebrafish research group in Qatar. The maintenance of the fish was accomplished in the zebrafish facility at Vivarium of Boğaziçi University for Life Sciences and Technologies and required permission for the use of zebrafish was given by the Boğaziçi University committee on animal ethics.

3.1.2. Equipment and supplies

The complete list of laboratory equipment with their manufacturers were shown in Appendix A.

3.1.3. Chemicals, Reagents and Solutions

The complete list of all chemicals, buffers, reagents, and solutions used in this study including all the primers and oligonucleotides synthesized by MacroGene and antibodies in IHC and ISH together with the certain molecular reaction kits were provided in Appendix A and Appendix B with their manufacturers.

3.2. Methods

3.2.1. Maintenance of zebrafish

Adult zebrafish were maintained at zebrafish facility at Vivarium of Boğaziçi University for Life Sciences and Technologies in either 1, 3, or 10 l tanks filled with artificial fresh fish water with constant room temperature at ~28°C. Artificial fresh fish water was prepared by

dissolving 2 g sea salt, 0.84 g calcium sulphate and 7.5 g sodium bicarbonate in reverse osmosis water up to 100 l. At the zebrafish facility, all the tanks were associated with the automated housing system (Stand Alone System, Aquatic Habitats) thereby circulating fish water was filtrated, aerated, UV sterilized and kept in constant temperature with that five-stage housing system at daily light cycle of 14 hours light/10 hours of darkness. Fish were fed twice a day with dry crushed flake food in the morning and frozen *Artemia* brine shrimp dissolved in fresh fish water combined with crushed flake in the evening. For the breeding pairs, extra pre-boiled frozen egg yolk was given in the evening.

3.2.2. Polymerase Chain Reaction (PCR) and cloning strategies

The targeted gene sequences were amplified using polymerase chain reaction with the specifically designed primers shown in Table 1. The specific primers were designed by the help of OligoAnalyzer and ncbi/primer blast software. PCR reaction was set according to the providers' manual and OneTaq® (NEB) and Titanium Taq (ClonTech Laboratories, Inc) polymerases were used. Thermocycler protocol was set as follows; Initial denaturation at 95°C for 3 min, per cycle denaturation is 30 sec at 95°C, annealing temperatures were determined according to designed primers for 30 sec and elongation temperatures were detected as 68°C for both OneTaq® and Titanium polymerases for 1 min and in each cycle 3 sec extension was added. As for final elongation, the temperature was set to 68°C for 5 min. 35 cycles of amplification were performed, and similar approach was followed for colony PCR to screen bacterial colonies. The standard PCR setups can be seen in Table 2.

Table 1. Primers used in this study

Primers	Sequences
zOMP cds F	ATGTCTCTGGAGTTGACGTTCAATCCTG
zOMP cds R	ATTATAACTTAAATTTAATTTTATACATATTTAGGAACAC
hbegfa_F	TGAGGAGGAGGATGAAGAGTATTA
hbegfa_R	CTACATTCCCAACCCTGAAGAG
egfra_F2	GCTCTCCACAAAGCCCTTCT
egfra_R2	GTCCGAACACTTTTCAGCGG
egfra_F3	TGAACCAGAATGAGTCCAGCA
egfra_R3	CACTGGCGTAAATTGCCGAT
T7	TAATACGACTCACTATAGGG
SP6	ATTTAGGTGACACTATAGAAT

Table 2. The standard PCR setups

Ingridients	Standard PCR	Advantage 2 PCR	Colony PCR
Template (Zebrafish gDNA)	2 μ l	2 μ l	10 μ l tip touched to a single colony
Polymerase Buffer	10 μ l (5X OneTaq® Buffer)	5 μ l (10X Titanium Taq Buffer)	2 μ l (5X OneTaq® Buffer)
dNTPs (100 mM each)	1 μ l	1 μ l	0.2 μ l
Forward Primer (10 pM)	2.5 μ l	2.5 μ l	0.5 μ l
Reverse Primer (10pM)	2.5 μ l	2.5 μ l	0.5 μ l
Polymerase	0.5 μ l OneTaq®	0.5 μ l Titanium Taq	0.1 μ l OneTaq®
dH ₂ O	up to 50 μ l	up to 50 μ l	up to 10 μ l

Amplified PCR products were purified using PCR purification kit and its instructions and purified product was quantified via nanodrop measurement and ligated into the pGEMT-easy vector (Promega) through TA cloning. The plasmid harboring the targeted sequence was transformed into DH5 α strain of *E.coli* competent bacterial cell culture via heat shock. 50 μ l of competent cells aliquot was melted on ice for 8 min. 10 μ l of ligation product was added into competent cell aliquot followed by 40 min of on ice incubation just after stirring gently. Heat shock was performed at 42°C for 60 sec and the mixture was immediately put on ice more than 2 min. Near the flame, 700 μ l LB Broth without any antibiotics in it added into the Eppendorf tube containing competent cell culture and ligation product. After 1 h incubation at 37°C while shaking, the mixture was centrifuged at 3000 rpm for 5 min and the pellet containing the heat shocked bacteria was spread onto the pre-warmed LB Agar plates with a specific antibiotic (amp: ampicillin in this study). The LB Agar plates with amp and heat shocked bacteria were incubated at 37°C overnight (16-18h). The antibiotic within the LB Agar plate was used as a selection marker thereby transformed bacteria could be able to be detected. Colony PCR was performed on selected colonies with different combination

of primer pairs so that the orientation of the insert was able to be detected. After detection of the construct harboring the targeted gene sequence in the desired orientation, the desired colony was amplified in 20 ml LB Broth with certain antibiotic, overnight at 37°C. Amplified plasmid was purified by using MIDIPrep kit (Roche) according to the manual provided by the manufacturer. The quantification of the purified plasmid was done by NanoDrop UV Spectrophotometer (ThermoFisher Scientific).

Table 3. Genes analyzed in this study

Gene name	Ensemble ID
<i>Hbegfa</i>	ENSDARG00000075121.4
<i>Egfra/ Erbb1a</i>	ENSDARG00000013847.15

3.2.3. Restriction digestion

To check the orientation of the targeted sequence in the pGEMT-easy plasmid, restriction digestion was performed for the MIDIPrep isolated plasmids with the suitable restriction digestion enzymes. The plasmid map visualized by SnapGene program and the determination of the use of certain restriction digestion enzymes which cuts the plasmid one at the insert site and one at the backbone of the plasmid giving the desired orientation was able to be done. The restriction enzymes that were used in this study were provided by NEB thereby the protocol provided by the NEB was followed during restriction digestion experiments.

3.2.4. Agarose gel electrophoresis

Visualization of both PCR products and products of restriction digestion was performed on 1 % agarose gels prepared in 1X TAE buffer. The concentration of the agarose gels was determined according to the size of the products. Visualization of the DNA fragments was enabled by the addition of 0.5 µg /ml ethidium bromide (0.01 %, v/v) to agarose gels. After mixing the samples with 6X DNA loading dye, samples were loaded into the wells of the agarose gel with the 1 kb and 100 bp ladders at the same time and gels were

run at 80-150 V (the voltage was arranged according to the size of the agarose gels) until the dye passed three fourths of the gel thereby separation of the DNA fragments were done. The bands corresponding to certain DNA fragments in size was detected under UV or under Bio-Rad Geldoc XR System or Syngene. Images were exported as TIFF files and analyzed accordingly.

3.2.5. Antisense riboprobe synthesis via *in vitro* transcription

Antisense riboprobes were synthesized according to the instructions of DIG RNA Labelling Kit provided by Roche to detect the RNA expression of the targeted genes via *in situ*-hybridization. Throughout the *in vitro* transcription followed by *in situ*-hybridization experiments, all solutions were prepared with DEPC-treated sterile distilled water (Polifarma) and autoclaved to preserve the RNase free environment, which is essential for the RNA related experiments. All of the DNA fragments that were transcribed were cloned into pGEMT-easy Vector (Promega) harboring the promoter sites for SP6 and T7 polymerases. The vectors containing the desired DNA fragments were linearized at suitable sites (restriction sites were detected according to the orientation of the template in the vector) via precisely selected one-cut restriction endonucleases (NcoI-HF, SpeI). Linearized plasmid vectors were used as templates for *in vitro* transcription and either SP6 or T7 RNA polymerases were able to transcribe antisense riboprobes *in vitro* from the template in the presence of DIG-UTP. Thus, every 20 to 25th nucleotide of the newly synthesized RNA transcript was expected to be labelled with DIG-UTP and following purification of the riboprobes were done by ethanol precipitation method.

The transcription reactions were prepared according to the Table 4 with the use of appropriate RNA polymerases (T7 or SP6 depending on the orientation of the interested template). The reaction mix was vortexed and spined down and incubated at 37°C for 2h. After the incubation, 2µl 0,2 M ethylene diamine tetra acetic acid (EDTA), 2,5 µl 4M lithium chloride (LiCl) and 75 µl 100 % ethanol were added into the reaction mix. The reaction mix was mixed well and incubated at -80°C for 1h. After incubation, the reaction was centrifuged at 4°C at 12,000g for 30 min. The supernatant was discarded very carefully by avoiding disturbing the white precipitation at the bottom which was desired transcript. Then the pellet was air-dried and re-suspended with 50 µl DEPC-treated dH₂O by pipetting. 1 µl RNase

inhibitor was added to the mix and 2 aliquots were taken for the following: 1 μ l for NanoDrop measurement to quantify the purified RNA transcript and another 5 μ l for running the sample on 1% agarose gel to detect the size of the transcript. 5 μ l of riboprobe was mixed with 5 μ l dH₂O_{DT} and 10 μ l Formamide and the transcript was denatured at 98°C for 10 min and immediately transferred to 4°C in the thermocycler. Then 2.2 μ l 10X RNA loading dye was added to the mixture and the sample was loaded into the well of the gel and was run at 80 V until the dye passed two thirds of the gel. The gel was again visualized under UV and the size of the transcript was confirmed.

The purified riboprobe was stored at -80°C for later experiments.

Table 4. Riboprobe synthesis reaction.

Ingredients	Concentration
10X Transcription Buffer	2 μ l
DIG-RNA Labeling Mix	2 μ l
Template DNA (purified, linearized)	1.0 μ g per 1.0 kb of probe to be transcribed
RNA Polymerase (either SP6 or T7)	2 μ l
RNase Inhibitor	0.75 μ l
dH ₂ O _{DT}	Up to 20 μ l

3.2.6. Chemical lesion on the olfactory epithelium with Triton X-100

The fish were anesthetized in Tricane methanesulfonate (MS-222) until the gill movement slowed down. Afterwards fish were placed between wet tissue papers under stereomicroscope (Zeiss). For strong damage 1% (v/v) Triton-X solution in 0.1 M PBS with 0.1 % (v/v) phenol red addition (as a pH indicator) was prepared in an Eppendorf tube and approximately 1-2 μ l Triton-X solution was injected into the right nasal cavity of the fish 3 times with 30 sec intervals by using an electronic microinjector. The right nose was washed with fresh fish water after 90 sec with the help of a Pasteur pipette and the fish were put back into the appropriately labelled tank and observed until it comes back to normal swimming routine. The same procedure was applied for mild damage with different concentration of

Triton-X that is 0.1% in concentration and application time was 4 times with 15 sec intervals which is 60 sec in total.

3.2.7. Dissection of olfactory epithelium

Depending on the experimental setup the fish that were lesioned or undamaged, were euthanized by submersion in approximately 4°C ice-water until the opercular movement stopped at time points (4h-8h) after damage. In order to dissect olfactory tissue from the adult zebrafish, the fish were decapitated with sterile surgical blade at the level of gills under the stereomicroscope (Zeiss). The head was placed on the dissection dish filled with ice-cold 1X PBS solution. The lower jaw and the eyeballs were removed at first by using dissection forceps and then the connective tissue was pulled out. The OE is attached to the nasal cavity bones on both sides and connected to olfactory bulb via axon bundle. With using of forceps OE tissue was detached from these nasal cavity bones and the axon bundle and the residual tissue was cleared away gently with fine and sharp dissection tools by preserving the morphological structure of the OE tissue.

For *in situ*-hybridization experiments, 1X PBS solution that was used during the dissection procedure was also DEPC-treated.

3.2.8. Cryosectioning of olfactory epithelium

Dissected OEs were carefully embedded at the bottom of molds filled with OCT (optimal cutting temperature) medium in proper orientation. Molds were frozen at -20°C until they were fully frozen and immediately transferred to the cryosection chamber. To be used in *in situ*-hybridization and immunohistochemistry experiments, OEs were sliced into 12-micron sections and fixed on positively charged glass slides (Superfrost Plus). Cryostat (Leica) was pre-cooled to -20°C and OEs that were removed from the molds were carefully positioned on the chamber thanks to the adhesive property of the OCT medium. After obtaining 12 µm horizontally cross-sections on the positively charged glass slides properly, the specimen was air-dried at pre-heated 65°C in a hybridization oven for 2-3 h. The specimen was either used immediately for following staining experiments or stored at -80°C

for later processing. For storage individual glass slides that were labeled appropriately were put in petri dish and covered by parafilm for slides to be safely stored.

3.2.9. *In situ*-hybridization

In situ-hybridization experiments were performed to detect the expression levels of gene of interest at the RNA level. The protocol for the *in situ*-hybridization was optimized for the sectioned OEs. The olfactory epithelium tissue was dissected and cross-sectioned as previously described in section 3.2.7 and 3.2.8. To avoid possible RNase contamination all solutions were prepared with DEPC-treated dH₂O and autoclaved unless otherwise is stated. All solutions were also prepared freshly from their stock solutions. The working area was also cleaned carefully with 75% ethanol or RNase ZAP cleaning agent. The glass slides harboring the specimen were processed with the relevant solutions in Coplin jars that were also carefully washed and autoclaved in each round of *in situ* hybridization.

At the first day of the whole process, if the glass slides were not used immediately after air-dried in hybridization oven but instead stored at -80°C, glass slides were dried with the help of hair dryer from back of the slides and slides were put in the freshly prepared 4% PFA solution (Paraformaldehyde) with exact pH:7.4 for 10 min at room temperature for tissue fixation. The slides were washed with 1X PBS_{DT} 1.30 min and 5 min respectively at RT. After PBS washes slides were treated with Proteinase K in Tris-HCl buffer (2 µl Proteinase K was added into the solution of 40 ml 0.1 M Tris-HCl pH: 8 pre-heated at 37°C) to degrade the proteins for exactly 7.30 min at 37°C. Another 4% PFA treatment was applied for 5min at RT that was followed by usual 1X PBS_{DT} washes for 1.30 and 5 min respectively at RT and then slides were treated with 0.2 M HCl solution for 10 min at RT. After PBS usual PBS washes following HCl treatment, slides were incubated in tri-ethanolamine buffer (TEA buffer: 662.5 µl TEA, 112.5 µl 1M HCl, 49.1 µl dH₂O_{DT} and 125 µl acetic anhydride (added lastly) for 10 min at RT and washed as usual with 1X PBS_{DT}.

The slides were put into fresh 1X PBS_{DT} solution while preparing hybridization mixture containing the previously synthesized riboprobe. The ingredients of hybridization mixture and their concentrations were shown in Table 5. Instead of using Coplin jars at this step due to the limitations in amount of riboprobes, hybridization mixture was directly put

on the slides. After preparing hybridization mixture without adding the riboprobe, the mixture was incubated at 85°C for 15 min in a heater. During this time interval, the very edges of the slides were drawn with liquid-repellent super PAP pen to prevent the waste of valuable hybridization mixture to be wasted and kept in defined area. Riboprobe was added into the hybridization mixture in certain concentration and the mixture was incubated 3 more min at 85°C in heater then 250 µl of hybridization solution with riboprobe in it was put on well-dried slides. The slides were covered with plastic cover slips without allowing any air bubble formation between the mixture and the cover slip and the slides were placed carefully in wet hybridization chamber (50% formamide and 50% dH₂O_{DT}) to prevent the vaporization of the hybridization mixture during the overnight hybridization process at 65°C in hybridization oven. The slides were placed in the hybridization chamber balanced and exactly horizontal for the mixture to be distributed evenly on each sectioned tissue.

After overnight hybridization of probes with the sections at 65°C in hybridization oven, on the second day of the procedure, the slides were washed with gradually concentrated saline-sodium citrate buffer (SSC) solutions in water bath at the same temperature that was setup for the hybridization. The slides were washed 5 times in total with gradually concentrated SSC buffer solutions. The first wash with 5X SSC was to just remove the cover slips from the slides and slides were put in the Coplin jar in water bath containing 2X SSC (50% formamide and 50% dH₂O_{DT}) for 30 min. Next 2X SSC washes followed the previous wash in the water bath for 20 min and 10 min respectively and lastly the slides were washed with 0.2 X SSC solution for 10 min. SSC was diluted in dH₂O_{DT} in each round of wash and the slides were incubated right away in DIG buffer (150 mM NaCl, 100 mM Tris-HCl pH:7.5) at RT for 5 min. Then for the blocking, the slides were incubated in 1X Blocking reagent diluted from 10X stock solution in maleic acid buffer pH:7.5, for 2h at RT. As a primary antibody for the later detection process, Alkaline Phosphatase (α -DIG-AP) was diluted in the ratio of 1:750 in 1X blocking reagent and the slides were incubated in primary antibody (400 ml 1° antibody/slide and slides were covered with plastic cover slips) either overnight (16-18h) at 4°C or 2h at RT in hybridization chamber. (Overnight incubation was preferable especially combining *in situ*-hybridization with immunochemistry experiments for better detection of the transcript).

Table 5. Hybridization mixture

Reagent	Stock Concentration	Final Concentration
Formamide	100%	50%
SSC	20X	5X
Heparin	50 mg/ml	50 µg/ml
Total yeast RNA	5 mg/ml	500 µg/ml
Citric acid	1M	9.2 mM
Tween	10%	0.05%
Riboprobe	250-350 ng/µl	3 ng/µl
dH ₂ O _{DT}		Up to 250 µl per slide

On the third day of the procedure, 1° antibody incubated slides were washed with DIG buffer supplemented with 0.05 % Tween for 3 min, 10 min and 10 min respectively at RT while shaking. After washes, HNPP (2-hydroxy-3-naphtoic acid-2'-phenylanilide phosphate) detection was applied. To do so prior to HNPP/Fast Red detection application, slides were incubated in detection buffer (100mM NaCl, 100mM Tris-HCl pH:8 and 10mM MgCl₂) for 10 min at RT. 10 ml of detection buffer was used for HNPP/Fast Red detection solution (10 µl 25µg/µl Fast Red and 10 ul HNPP from the stock was mixed well, vortexed and filtered through 0.22 µm filter). The slides were incubated with HNPP/Fast Red detection solution for 30 min at RT by putting the solution directly on the slides in a humidity chamber. After first 30 min, the development of the *in situ* signal was checked under confocal microscopy. If the signal was not enough, the slides were incubated more with the detection solution until a clear signal was able to be detected. Over-incubation was avoided due to the possible formation of high background. After detection, the slides were washed with dH₂O_{DT} for 15 min and stored at 4°C in dH₂O_{DT} as well for later imaging processes.

3.2.10. Combining *In situ*-hybridization with Immunohistochemistry on OE sections

To combine immunochemistry with *in situ*-hybridization on olfactory epithelium sections, at the primary antibody incubation step, other primary antibodies which are

compatible with each other were also diluted in 1X blocking reagent and previously optimized concentrations of different primary antibodies were freshly prepared and applied on the slides together with α -DIG-AP. The concentrations of the primary antibodies used in this study were as follows; mouse anti-human neuronal protein HuC/D in 1:500, rabbit Sox2 in 1:500, mouse CytII in 1:800, rabbit Tp63 in 1:400, rabbit Krt5 in 1:50. Especially when combining IHC with *in situ*-hybridization, overnight incubation of primary antibodies was applied. After the detection of *in situ* signal as explained in 3.2.10 section, secondary antibody incubation in appropriate combination of antibodies was applied on slides for 2h at RT in a dark humidity chamber. All secondary antibodies were used in 1:800 ratio diluted freshly in 1X blocking reagent and the secondary antibodies used in this study were as follows: anti-mouse Alexa Flour 647, anti-rabbit Alexa Fluor 488, anti-rat Alexa Fluor 555. The slides were washed in 1X PBST_{DT} and 1X PBS_{DT} for 10 min each at RT respectively and lastly with dH₂O_{DT} and stored at 4°C as previously mentioned.

3.2.11. Imaging

The stained sections were visualized under Leica TCS-SP5 AOBS laser-scanning confocal imaging system (Leica Microsystems) at 1024 x 1.024 or 2.048 x 2.048 pixel resolution. 20X objective lens were used to visualize the whole OE sections and 40X objective lens were most used to visualize zoom-in images of lamellae. Zoom-in images were required to discriminate individual cells or group of cells giving signals to obtain more detailed visualization.

3.2.12. Data analysis

In both immunochemistry and *in situ*-hybridization experiments, the samples were analyzed in detail. To detect which cells or cell groups are giving *in situ* signal under mild and strong damage conditions and undamaged/ control condition, single positive, double positive and if existed, triple positive cells were detected under confocal microscope and further processing was done by the Leica-LAS-AF (Leica Microsystems). To demonstrate the difference between different experimental conditions, at least 4 folds of 10 to 20 sections for each 2-3 different fish were quantified regarding the single, double or triple positivity. For detailed image analysis a custom macro in Fiji image analysis software by our laboratory

was used. The percentage of cells that were single, double or triple positive under different conditions were able to be defined and also just for the in-situ hybridization experiment, the normalized signal area covering the entire section was also calculated by Fiji image software. Positional cell counts were enabled by specific macro in Fiji written by Fuss, S and Demirler, M. (Demirler et al., 2021) and projected onto the radial axis between interlamellar curve and non-sensory region of olfactory epithelium of zebrafish. Non-specific signals and background noise were tried to be eliminated as much as possible to get more clear results. Fiji image analysis software also allowed brightness, contrast adjustments together with crop option. The whole quantitative data were used to create graphs on GraphPad, and R suite (R Core Team, 2020) and the standard error means were calculated accordingly. The final versions of images that are used in this study were organized and final png formats for thesis were created in Adobe Illustrator,2020.

4. RESULTS

Previous studies conducted in our lab demonstrated the cellular identity, tissue distribution, and specific functions of characterized stem/progenitor cell types that are involved in maintenance and regenerative neurogenesis under physiological and damage conditions in the zebrafish OE, respectively (Bayramlı et al., 2017; Demirler et al., 2020; Kocagöz et al., 2021). Both processes are largely independent from each other and involve different progenitor cell types that are regulated by distinct molecular cues. These studies revealed that maintenance neurogenesis is confined to two isolated regions: the interlamellar curve (ILC) and the sensory/non-sensory border (SNS) that flank the central and peripheral margins of the region occupied by olfactory sensory neurons (OSNs). Adult-born OSNs originate from *ascl1*-expressing fast cycling GBC progenitors at the ILC and SNS and migrate radially towards the core-sensory region under physiological conditions (Bayramlı et al., 2017; Kocagöz et al., 2021). In contrast, Krt5/Tp63 double-positive quiescent HBCs are uniformly distributed throughout the basal OE, are activated upon severe OE injury, and undergo mitotic activity, which contributes to regenerative neurogenesis (Iqbal and Byrd-Jacobs, 2010; Demirler et al., 2020, Kocagöz et al., 2021).

To better understand the regulation of HBC activation during regenerative neurogenesis, intact and regenerating OE tissue was analyzed by transcriptome profiling to identify candidate regulatory factors (Kocagöz et al., 2021). Among the differentially expressed genes, the HB-EGF signaling factor and associated activator metalloproteinases from a disintegrin, and metalloproteinase (ADAM) family showed an immediate upregulation at 4 hpl in response to tissue damage followed by rapid downregulation by 12 hpl. In Figure 4.1., the expression of the two zebrafish paralogs of the genes coding for HB-EGF, *hbegfa* and *hbegfb*, are shown. Both paralogs are expressed at equally moderate levels under physiological conditions. Upon severe lesion to the tissue, *hbegfa* expression is upregulated 15-fold at 4 hpl, whereas only a moderate induction can be observed for *hbegfb*. Induction of *hbegfa* and *hbegfb* expression is transient and returns to near baseline levels by 24 hpl. A similar upregulation of *hbegfa* upon tissue injury has been previously demonstrated in the zebrafish retina, where HB-EGF stimulates neurogenesis and regeneration (Wan et al., 2012). Exogenous stimulation of the OE with recombinant HB-EGF stimulates OSN

neurogenesis, while inhibition of metalloproteases or other components of HB-EGF/EGFR signaling prevents the unfolding of a full regenerative response (Kocagöz, Şireci, Alkiraz, Dokuzluoğlu, unpublished observations). Thus, the *hbegfa* gene was chosen for further analysis because it may constitute an important signaling molecule that is activated during the early damage response in the zebrafish OE to promote regenerative neurogenesis.

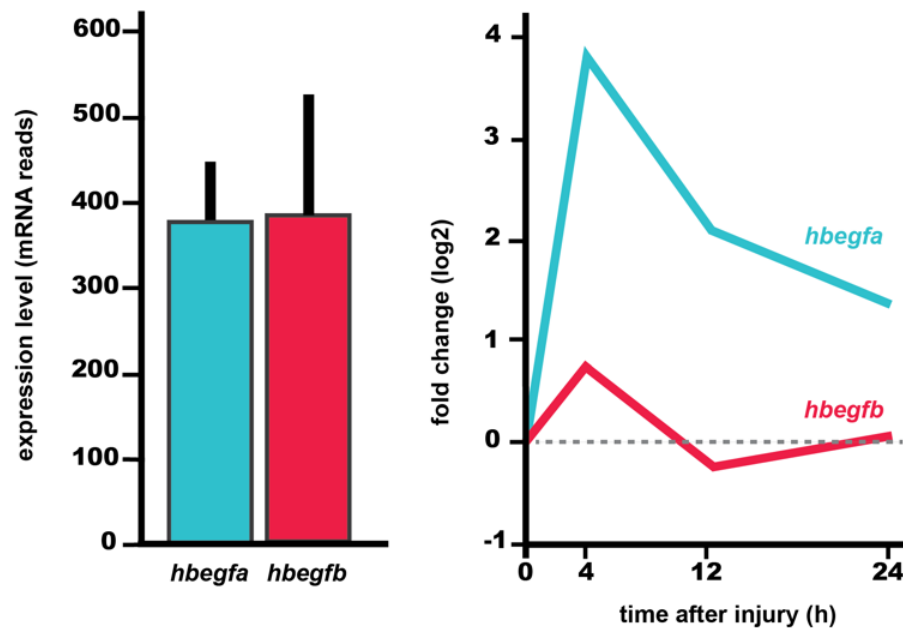


Figure 4.1. Expression of the paralogous *hbegfa* and *hbegfb* zebrafish genes. A. Baseline expression levels in the intact OE (mean \pm SEM of three independent biological replicates). B. Logarithmic fold changes in expression levels upon tissue injury.

HB-EGF has been shown to promote neurogenic activity in different injury models under different conditions (Jin, et al., 2003; Wan et al., 2012; Inoue et al., 2013; Todd et al., 2015), however, the expression pattern of the *hbegf* genes in the intact and injured zebrafish OE were not known. Therefore, the expression pattern of *hbegf*, in particular the highly upregulated *hbegfa* paralog, was investigated by *in situ*-hybridization to identify *hbegfa*-expressing and possible downstream target cell populations in the zebrafish OE. To do so, *in situ*-hybridization experiments combined with immunostainings against neuronal and non-neuronal cell type specific markers were performed at different time points under different tissue conditions.

4.1. Expression pattern of *hbegfa* in the intact zebrafish OE

Previous studies reported that, in the zebrafish model system, HB-EGF is sufficient to stimulate injury-responsive progenitor cell proliferation in the intact and damaged retina (Wan et al., 2012) and OE (Kocagöz et al., 2021). In the light of these findings, HB-EGF was considered as a candidate stimulatory factor that contributes to the initiation of injury responses in the zebrafish OE. To demonstrate the expression pattern of *hbegfa*, *in situ*-hybridization experiments were performed.

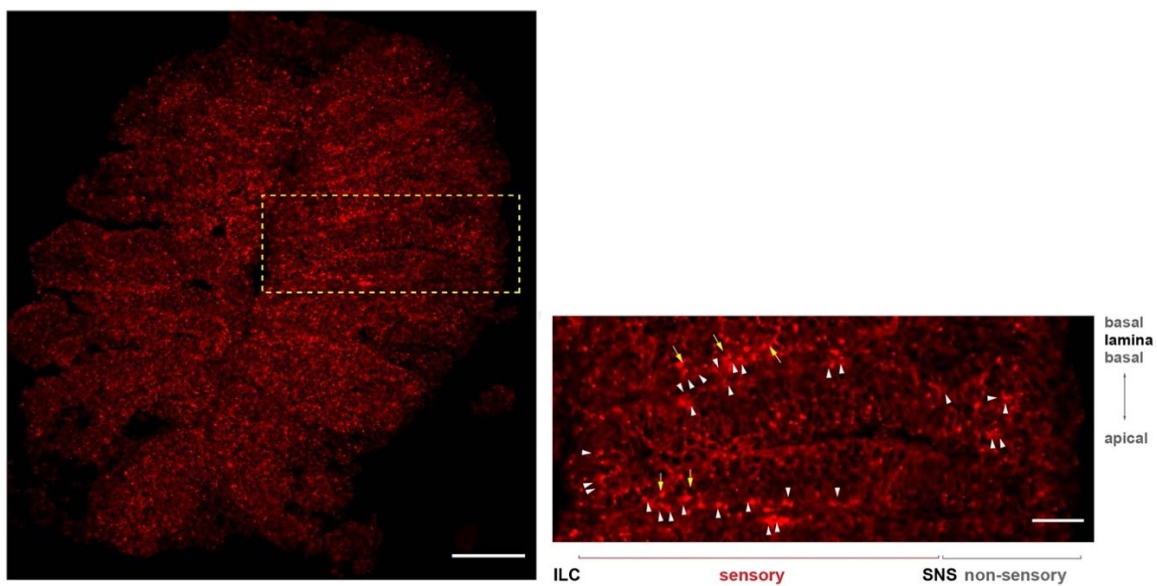


Figure 4.2. *In situ*-hybridization of the zebrafish OE using a *hbegfa* antisense riboprobe.

A full section of an intact OE is shown on the left and a higher power view of the region indicated by the yellow box is shown on the right. Scale bars: 240 μ m. Scale bars: 80 μ m.

In the intact OE, expression of *hbegfa* is low and mostly concentrated in cells close to the basal lamina (arrowheads in figure 4.2.). No obvious preference of the tissue distribution of the labeled cells could be observed and *hbegfa*-positive cells could be detected in all epithelial positions between the ILC and SNS. These epithelial regions harbor injury-responsive progenitors, the horizontal basal cells (HBCs). In addition, some cells expressing *hbegfa* occupy more suprabasal layers as indicated by yellow arrows in the figure 4. 2. Although the signal can be observed as red dots, probably in the cytoplasm of the expressing cells, at the basal layer of OE, modest staining and background of high intensity can also be seen above the basal lamina. Therefore, whether the dots demonstrate a true

biological signal or mostly background in upper layers of the sensory region of the epithelium is open to debate. Yet, some cells of the OE clearly express *hbegfa* under physiological conditions and the signal shows mostly a basal pattern.

4.2. Expression pattern of *hbegfa* in the damaged zebrafish OE

To assess changes of *hbegfa* expression in response to injury, an established chemical injury model was used (Kocagöz et al., 2021). The OE is efficiently injured by nasal irrigation with a 1% solution of the non-ionic detergent Triton X-100 (TrX) for 90 sec. In addition to the standard injury approach, a milder 0.1% TrX exposure was used, which triggers a robust proliferation response in HBC progenitors but does not disrupt the integrity of the tissue as severely (Kocagöz et al., 2021). The TrX solution was applied intranasally to the right OE for each fish for each experimental condition, and the left nose was used as an internal control tissue, which was not subjected to injury.

Following the TrX application, the nasal cavity was immediately washed out with a gentle stream of fresh water delivered from a Pasteur pipette and the fish were moved back to freshwater tanks for recovery. At 4 and 8 h timepoints after the lesion (hpl), the OEs were dissected, and 12 µm sections were taken for subsequent detection of *hbegfa* transcripts by *in situ*-hybridization procedure. Since the transcriptome profiling showed that *hbegfa* transcript levels reach a peak at 4 hpl but declined from a 15-fold upregulation at 4 hpl to only 2-fold higher than normal expression levels at 12 hpl (Figure 4.1.), tissue was also collected 8 hpl as a second time point for analysis.

Consistent with the transcriptome results, *hbegfa* signal levels were strongly upregulated at 4 hpl but declined at the 8 hpl timepoint when 1% TrX was used. For both timepoints, a large number of labeled cells/cell clusters, often in close proximity to the basal lamina (arrows in figure 4.3.) and around the SNS could be observed. In addition to basal cells, a few individual cells in intermediate and apical tissue layers could also be detected. The spatial pattern of signal distribution was more disorganized, and the strength of the signal was reduced at 8 hpl. In addition, treatment of the OE with the milder 0.1% concentration of TrX also induced *hbegfa* expression. *Hbegfa*-positive cells often formed a double layer of basal cells in the region of Krt5/Tp63-positive basal progenitors (Demirler et al., 2021) and are indicated by yellow and white arrowheads in Figure 4.3. However, the

staining pattern was more diffuse and often included isolated stretches of individual basal cells that were detected by the probe. Overall, the morphological structures of the labeled cells appear to be better preserved, as expected for the milder damage condition under which the tissue integrity is less severely affected. Although only a small number of isolated cells express *hbegfa* in the intact tissue, labeled cells in 0.1% TrX-treated OEs appear to preferentially locate around the ILC and in the basal-most layer. Instead of the larger cell clusters that can be observed in the 1% TrX treated tissue at 4 hpl, individual cells are observed in the control tissue (Figure 4.3, white arrowheads). In addition, the damaged tissue shows an elevated background signal compared to the control tissue. Nevertheless, a clear distinction of *hbegfa*-positive cells can be made close to basal layers, the SNS, and within the non-sensory region.

To quantitatively describe the changes in *hbegfa* expression, the percent area occupied by *hbegfa* signal in the injured OE was quantified and normalized to the area in intact control tissues. To do so, images of tissue sections were thresholded and analyzed by determining the area above threshold using the Image J software (Schindelin et al., 2012). The data for each experimental OE were divided by the total area of the respective tissue section and normalized to the signal area of untreated control OEs. Figure 4.4. represents the quantification of the mean \pm SEM (standard error means) of the *hbegfa* signal area for each condition and three tissue sections per condition. The area occupied by *hbegfa* signal following the mild 0.1% TrX exposure showed an overall 1.64 ± 0.10 -fold increase at 4 hpl. In contrast, the stronger 1% TrX exposure resulted in a more robust upregulation with a 4.25 ± 0.96 -fold increase at the same time point.

The area of *hbegfa* expression in 1% TrX-treated tissue declined at 8 hpl and reached only a 2.78 ± 0.67 -fold larger value than in control OEs. These results indicate that not only the total amount of mRNA levels per cells but also the spatial expression pattern of *hbegfa* changes transiently in the regenerating OE, suggesting that additional cells start to express *hbegfa* in response to injury. The results mirror the observation in the transcriptome data, which also show a peak of *hbegfa* expression at 4 hpl followed by a subsequent decline.

These results show that both strong and mild tissue damage result in an induction in *hbegfa* expression at 4 hpl and 8 hpl. However, *in situ*-hybridization against *hbegfa* by itself is not sufficient to pinpoint which cell types express the gene in response to injury.

Additional co-staining experiments that make use of cell type-specific markers for OE cell types will be necessary to further characterize *hbegfa*-expressing cells in the intact and injured OE.

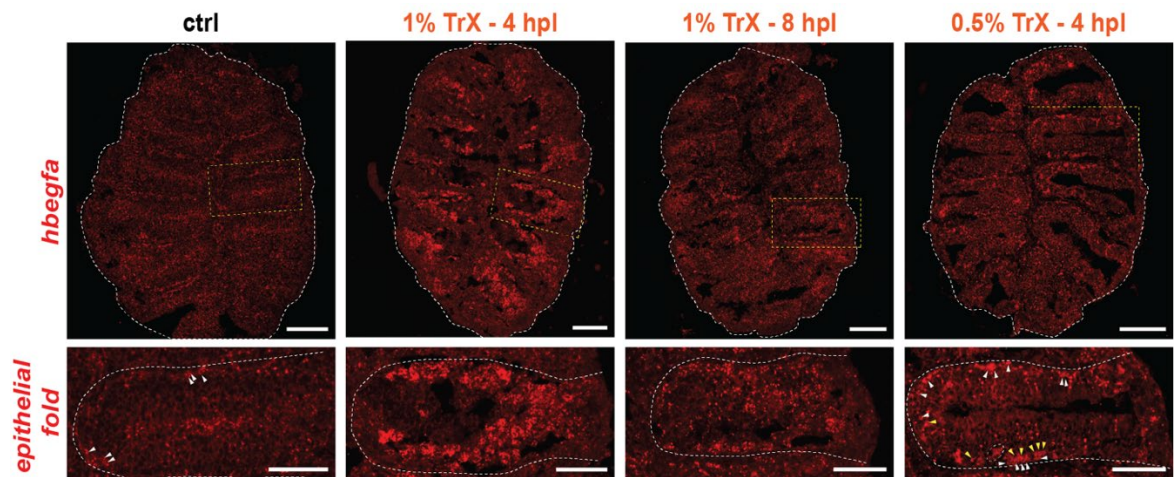


Figure 4.3. ISH against *hbegfa* (red) transcript on OE sections under physiological and different injury conditions. Dotted lines indicate the outline of OE sections (top). Higher power view of the region indicated by the yellow box (bottom). Scale bars: 25 μ m, 50 μ m.

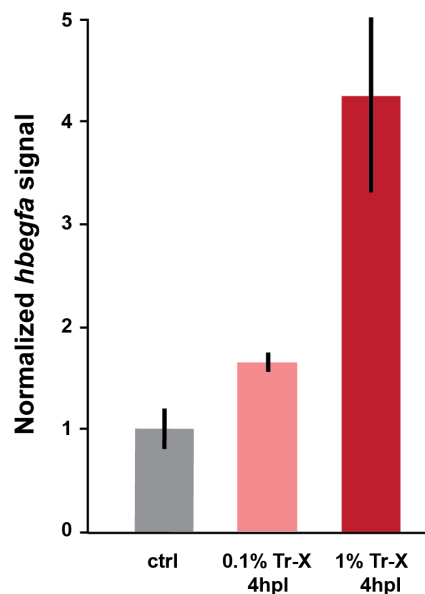


Figure 4.4. Quantification of *hbegfa* signal in the control and 4-hour post lesioned OE. The data represents the mean \pm SEM of three tissue sections for each condition and are normalized to the control signal area.

4.3. Summary Conclusion

Hbegfa is expressed in a small number of cells in the intact OE without a clear preference of the tissue distribution for these cells. However, more consistent labeling of *hbegfa*-positive cells could be detected around the basal layers of the OE, in addition to the presence of occasional cells in more apical layers.

The intensity of the *hbegfa* expression signal is correlated with the severity of the injury in the damaged tissue. The *hbegfa* signal is transient and higher at 4 hpl in comparison to 8 hpl. Thus, the OE shows higher *hbegfa* expression levels upon acute lesion as an early damage response in accordance with previous studies conducted on the zebrafish retina (Wan et al., 2012).

The morphology of individual cells can be resolved more clearly under milder damage conditions in which the integrity of the tissue is better conserved. Under these conditions, individual *hbegfa*-positive cells also do not show a specific tissue preference and can be identified in all regions of the OE. Compared to the damaged OE, much lower levels of *hbegfa* expression can be detected under physiological conditions.

4. 4. Identification of *hbegfa*-expressing cells in the intact OE

In situ-hybridization against *hbegfa* demonstrated a prevalent spatial expression pattern in the regenerating sensory region, preferentially in basal strata. However, the assay itself cannot reveal which of the various cell populations that constitute the OE expresses *hbegfa*. Therefore, to unequivocally identify *hbegfa*-positive cells, immunohistochemistry against the cell type-specific markers; Sox2, Tp63, CKII, Krt5 and HuC/D were combined with *in situ*-hybridization experiments in the intact OE.

4.4.1. Expression of *hbegfa* in Sox2-positive cells

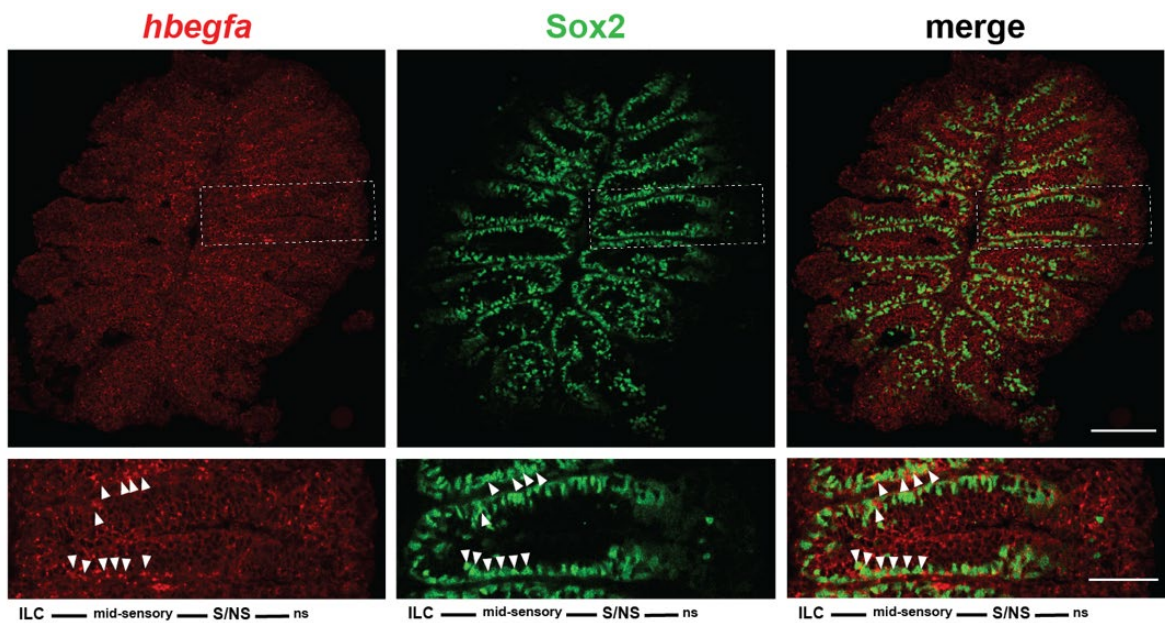
Sox2 has been described in the zebrafish OE as a general marker for non-neuronal cell types that are distributed along the entire basal layer of the epithelium, including the ILC and SNS (Demirler et al., 2020). Sox2 maintains the stemness state (Packard et al., 2016) and all of the three major groups of non-neuronal cell populations (i.e., HBCs, GBCs, and SCs) express Sox2 in the basal layer of the sensory OE but show distinct morphological

features with positional preferences that allows to distinguish different basal cell populations (Demirler et al., 2020).

Immunocytochemistry was performed together with *in situ*-hybridization on intact OE sections with the undifferentiated cell marker Sox2 in order to reveal whether Sox2-positive progenitor cells and/or SCs might be the source of *hbegfa* in the intact OE. To do so, an anti-Sox2 antibody was included in the staining procedure during the anti-DIG-AP antibody step of the *in situ*-hybridization protocol. The anti-Sox2 antibody was used at a 1:500 dilution and tissue sections were incubated overnight at 4°C. The standard *in situ*-hybridization protocol was continued and just after the detection of *in situ* signal by HNPP/FastRed, appropriate secondary antibodies were applied to visualize Sox2 expression. The tissue sections were incubated for 2 h at RT, similar to standard immunohistochemistry procedure, however, the slides harboring tissue sections were stored in DEPC-treated H₂O to preserve the signal for later analysis since prolonged PBS exposure has a tendency to reduce or eliminate the *in situ*-hybridization signal.

The results show that *hbegfa* signal can be detected around the nuclei of Sox2-positive cells in the intact tissue (arrowheads in the merged image in Figure 4.5.). Yet, additional cells that were positive for *hbegfa* but did not show no immunoreactivity for Sox2 expression could also be observed in more apical tissue layers. Although *hbegfa* signal and background do not generate a distinctive contrast in the intact tissue, the well-defined spatial pattern of Sox2 expression was obvious (Figure 4.5.).

The presence of *hbegfa*-expressing Sox2-negative cells suggests that *hbegfa* expression is not restricted to the three major non-neuronal cell populations of HBCs, GBCs, and SCs and may also include mature olfactory neurons.



4.4.2. Expression of *hbegfa* in Tp63-positive cells

Previous results showed that Sox2-positive cells stain positive for the *hbegfa* riboprobe. However, Sox2-positive cells include the diverse HBC, GBC, and SC subpopulations and Sox2 immunohistochemistry itself is not sufficient to discriminate between these cells. Thus, specific markers that individually label HBCs, GBCs and SCs need to be employed to further characterize *hbegfa*-expressing cells.

HBCs in the mouse OE express the transcription factor Tp63 under dormant conditions in the intact OE but cease Tp63 expression upon tissue lesion prior to entering mitotic activity in the mouse (Packard et al., 2011; Schnittke et al., 2015). HBC progenitors in the zebrafish OE also express Tp63, which can be used as an HBC marker in addition to Krt5 (Demirler et al., 2020). To further dissect the Sox2-positive cells that express *hbegfa*, immunohistochemistry against Tp63 was used under physiological conditions.

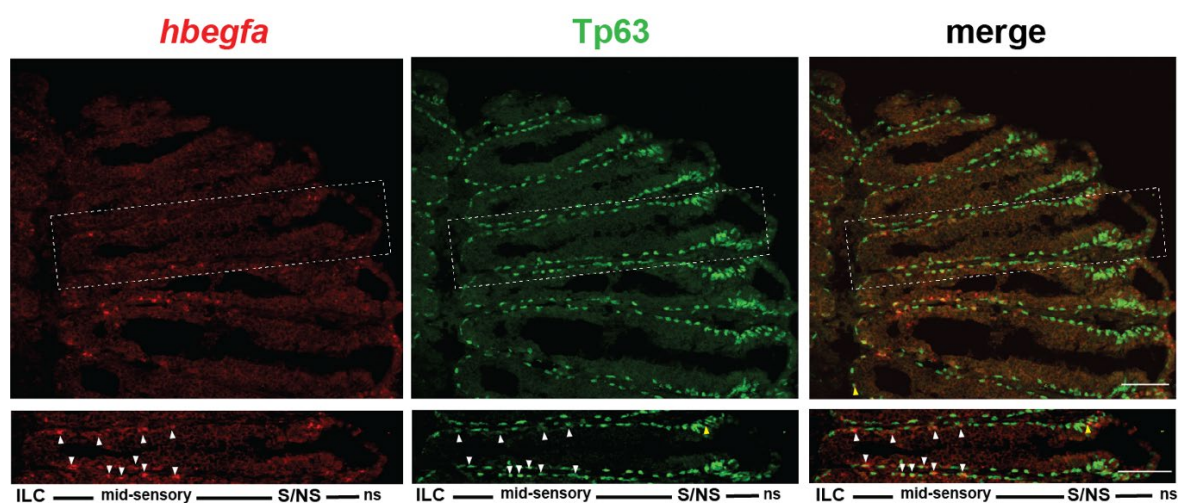


Figure 4.6. Combination of *in situ*-hybridization against *hbegfa* transcript (red) and immunohistochemistry against the transcription factors Tp63 (green) (Top Panel shows hemi-OE sections; Bottom Panel shows epithelial folds of same sections). Scale Bar:50 μ m

Tp63-positive cells occupy the basal layer in all positions of OE between the ILC and the peripheral edge of the tissue, albeit present with differential morphologies. Tp63-positive cells between the ILC and SNS show flat horizontal morphologies and form a single basal layer along the entire lamella. The morphologies of Tp63-positive cells become more spherical, eventually vertically elongated, and their density is increased within the non-sensory OE. Not all but some of these cells stain positive for the *hbegfa* riboprobe. Double-positive cells are depicted with white arrowheads in Figure 4.6. and shows a location preference towards the ILC and the mid-sensory region, while Tp63-positive cells in the non-sensory OE were generally devoid of *hbegfa* expression. In addition, cells that are only *hbegfa*-positive but do not stain for Tp63 can be observed at the SNS (yellow arrowhead). Thus, some Tp63-positive HBC progenitor cells express *hbegfa* under physiological condition while others do not. The reason for the heterogeneity of *hbegfa* expression in Tp63-positive HBCs remains unknown.

4.4.3. Expression of *hbegfa* in Krt5-positive cells

The previous results showed that *hbegfa* expression can mostly be observed in basal cell layers. In the intact zebrafish OE, HBCs and SCs were shown to occupy the basal layers (Demirler et al., 2020). Co-labeling of cells for *hbegfa* and Tp63 expression revealed that a subpopulation of Tp63-positive cells expresses *hbegfa*. However, Tp63 is dynamically

regulated upon injury in the mouse OE and is an important switch to break mitotic dormancy (Packard et al., 2011; Schnittke et al., 2015). In addition to Tp63, Krt5 is another reliable HBC marker that is not dynamically regulated upon injury. Immunohistochemistry against Krt5 was shown to specifically label HBC progenitors in basal layers of zebrafish OE (Sakızlı, 2017; Demirler, et al., 2020). Although the anti-Krt5 antibody recognizes the antigen effectively in regular immunohistochemistry experiments (Figure 4. 7.), anti-Krt5 antibody staining was not compatible with the harsh tissue treatment during *in situ*-hybridization and could not be included in the analysis. The reason for that incompatibility is most likely that the Krt5 protein does not survive Proteinase K treatment during the *in situ*-hybridization procedure.

On the other hand, the regular staining itself represents Krt5 positive HBCs which are presented with horizontal dimensions in the mid-sensory regions and occasionally elongated pyramidal morphologies towards the ILC as in Figure 4.7.

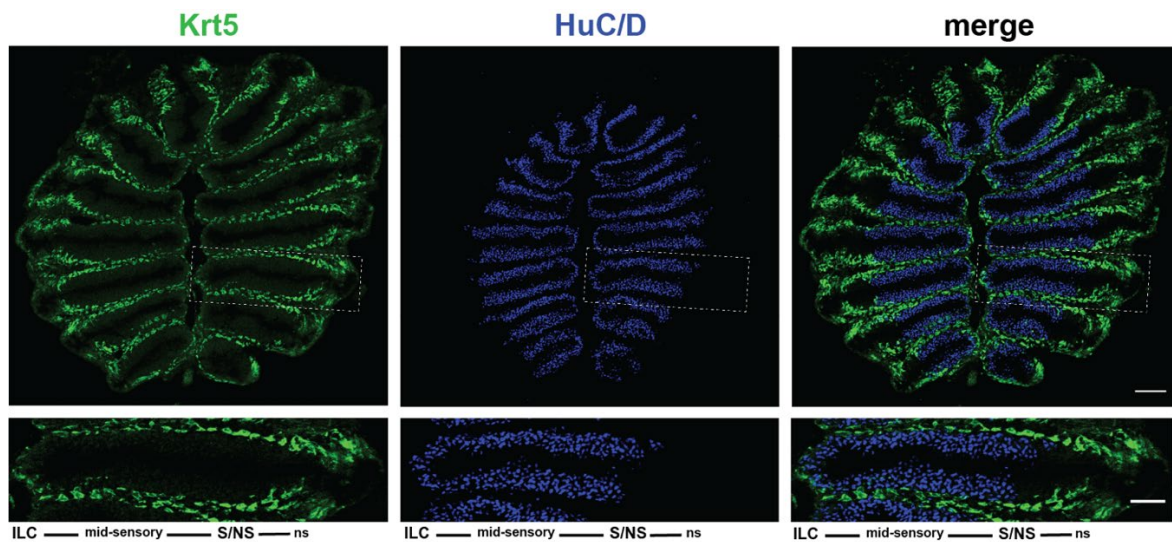


Figure 4.7. Anti-Krt5 (green) (the HBC marker) and anti- HuC/D (blue) IHC on intact OE. (Top Panel shows whole OE sections; Bottom Panel shows single epithelial folds of same sections). The images are provided by Zeynep Dokuzluoğlu. Scale Bar: 50 μ m, 25 μ m.

4.4.4. Expression of *hbegfa* in CKII-positive cells

Previous work conducted by our group revealed that CKII immunohistochemistry can be used as a cell type-specific marker for SCs (Bali, 2015). SCs are elongated cells that stretch the entire vertical dimension of the OE and possess basally located somata that form a layer that is located just above HBCs. Immunostaining against CKII-expression labels intracellular filaments and reveals somata that constitute the suprabasal layers of the Sox2-expressing cell pool (Demirler et al., 2020). Basal nuclei SCs is stained by Sox2 antibody, and perinuclear cytoplasm and their keratin filaments are stained with CKII marker (Figure 4.8.).

To assess whether SCs express *hbegfa*, *in situ*-hybridization was combined with immunohistochemistry against CKII. The contrast between background and *hbegfa* was not distinctive in Figure 4.9. therefore, it remains uncertain whether the labeled dots that could be observed in the intact tissue is a true biological signal or represents intense background. Yet, SCs were successfully labeled by CKII immunohistochemistry. Pyramidal cell bodies and keratin filaments are observable in the figure. Double positive SCs could not be detected in merged images and the results suggest SCs seem to lack *hbegfa* expression.

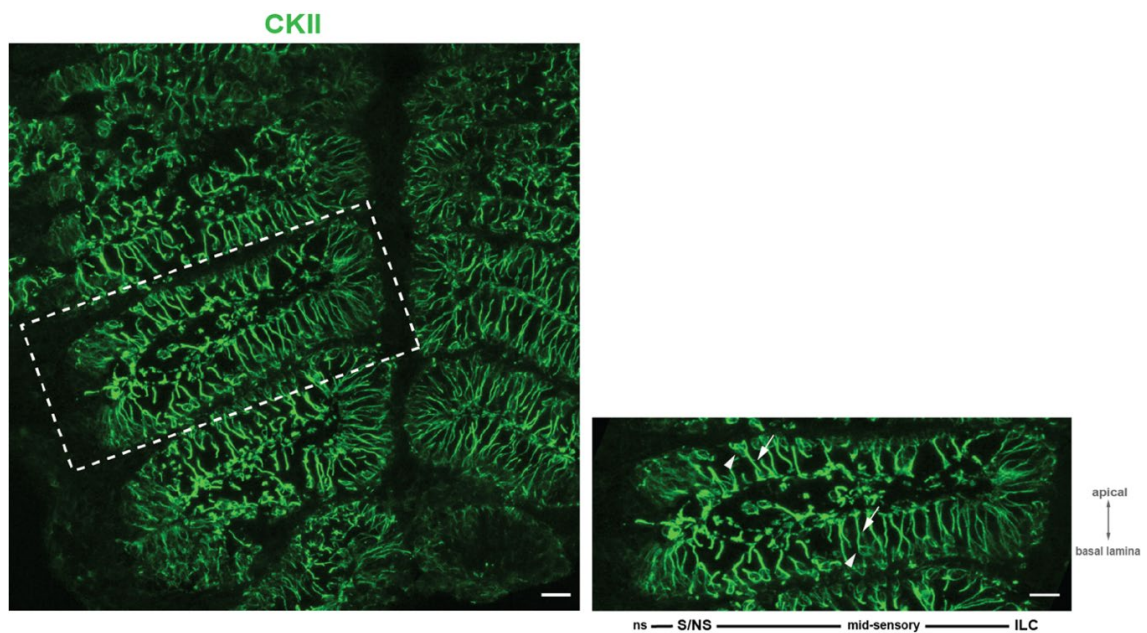


Figure 4.8. Immunohistochemistry against the SC marker CKII. A semi-section of an intact OE is shown on the left and a higher power view of the region indicated by the box is shown on the right. Scale bars: 100 μ m.

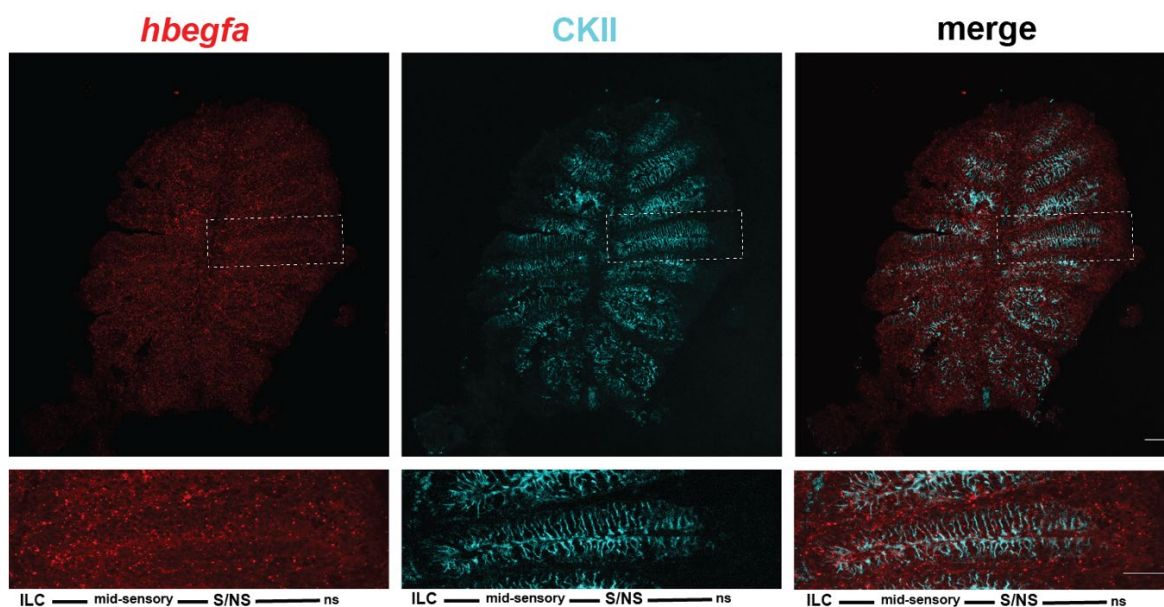


Figure 4.9. Combination of *in situ*-hybridization against *hbegfa* transcript (red) and IHC against the SC marker CKII (cyan) (Top Panel shows whole nose sections; Bottom Panel depicts single epithelial folds of same sections). Scale Bar: 50 μ m Scale Bar: 25 μ m

4.4.5. Expression of *hbegfa* in HuC/D-positive cells

Mature zebrafish OSNs can be labeled by the pan-neuronal RNA-binding protein HuC/D (Bayramlı et al., 2017). Immunostaining against HuC/D depicts the nuclei of OSNs in the OE and HuC/D expression can be observed in intermediate and apical layers of the OE under physiological conditions. Occupancy of HuC/D-positive OSNs starts from the ILCs and extends to the SNS. Since OSNs are not observed in the non-sensory region, HuC/D staining sharply separates sensory and non-sensory regions.

As for the other cell type specific markers, anti-HuC/D staining was combined with *in situ*-hybridization, to determine the source of *hbegfa* expression. *Hbegfa*-positive cells within the basal OE layer were detected to be HuC/D-negative at the ILC and SNS (yellow arrowheads), however, occasional individual double-positive cells could be observed in intermediate layers of OE (white arrowheads) suggesting that *hbegfa* expression is not limited to the non-neuronal cell populations. However, the abundance of *hbegfa*-expressing OSNs is sparse.

In the Figure 4. 10., it is interesting that in certain regions, the *hbegfa* expression at the basal layer is stronger and more distinctive compared to the rest of the tissue. The dynamic molecular nature of cells constituting the basal layer can lead to increased levels of expression regionally although such regional inductions in the intact OE regarding *hbegfa* expression were not observed in previous experiments. This result demonstrates that *hbegfa* is expressed by both neuronal and non-neuronal cell populations under physiological conditions and the level of expression may change within the tissue itself.

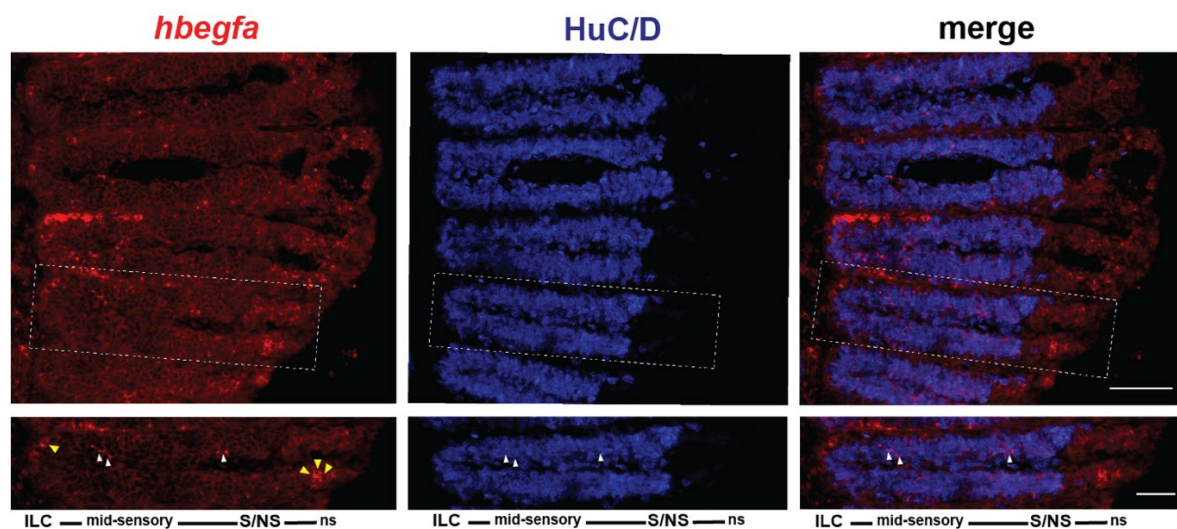


Figure 4.10. Combination of *in situ*-hybridization against *hbegfa* transcript (red) and IHC against the pan-neuronal marker HuC/D (blue) (Top Panel shows semi-OE sections; Bottom Panel shows single epithelial folds of same sections). Scale Bar: 50 μ m, 25 μ m.

4.5. Summary Conclusion

These above-mentioned results demonstrate that non-neuronal cells belonging to the Sox2-positive cell populations are the major source of *hbegfa* expression in the intact OE. These non-neuronal cells include HBCs and SCs. Unlike SCs, some Tp63-positive HBCs along the basal layer in the ILC and sensory region show detectable levels of *hbegfa* expression. In addition, occasional HuC/D-positive neuronal cells are found to express *hbegfa*. These recent results indicate that eventually members of all OE cell populations are potential source for *hbegfa* expression in the OE tissue.

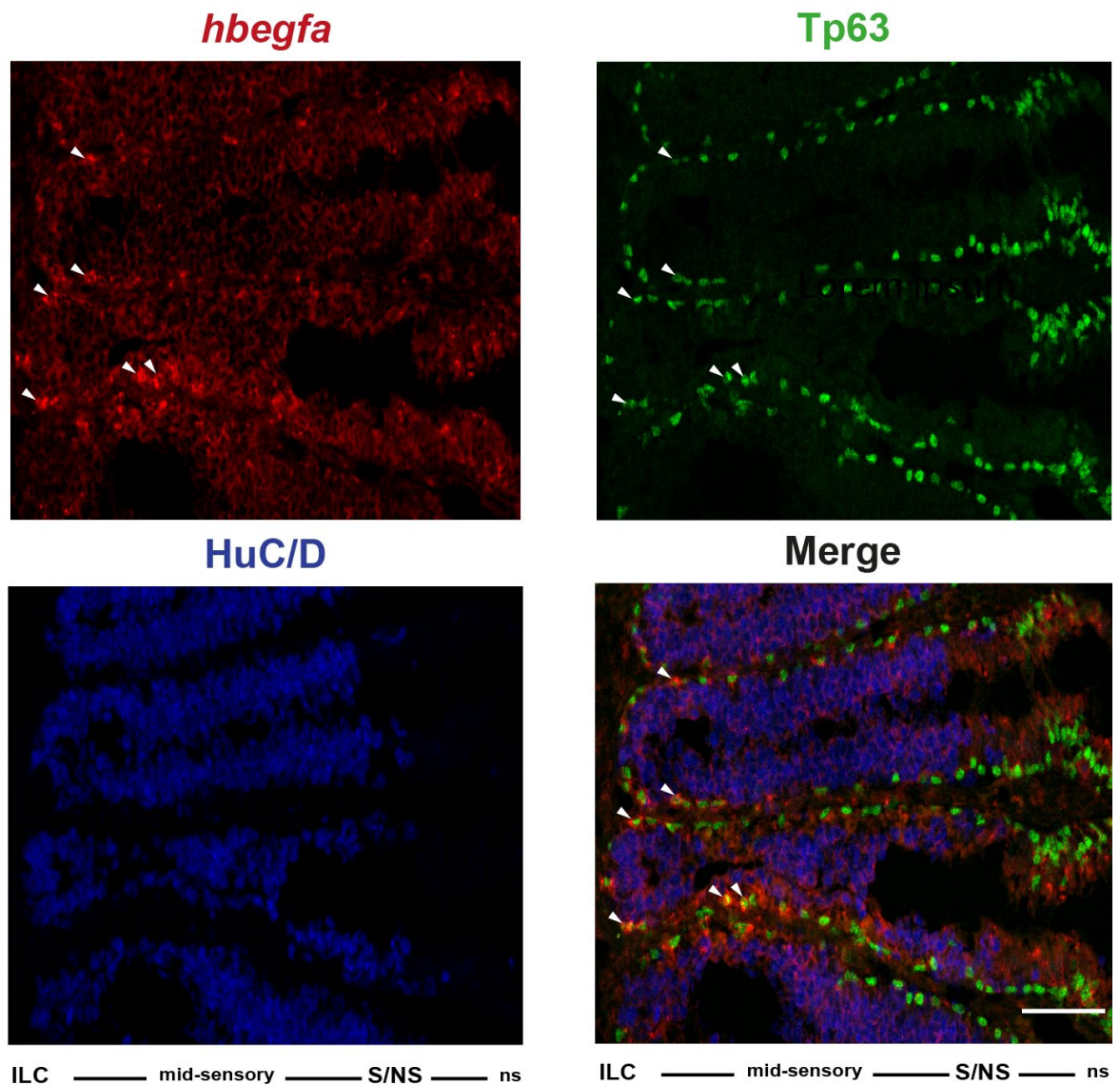


Figure 4.11. Combination of *in situ*-hybridization against *hbegfa* transcript (red) and immunohistochemistry against the HBC marker Tp63 (green) and pan-neuronal marker HuC/D (blue) on the intact OE. Scale Bar: 50 μ m Scale Bar: 25 μ m.

4. 6. Identification of *hbegfa*-expressing cells in damaged OE

The analysis of *hbegfa* expression so far showed that *hbegfa* is not limited to any specific cell population in the intact tissue and that all cell types constituting the olfactory tissue may express *hbegfa*. As a next step, the identify of *hbegfa* expressing cells under different damage conditions was analyzed to provide further insight into the role of HB-EGF in the regenerating zebrafish OE. Thus, *hbegfa* expression was analyzed by *in situ*-hybridization in combination with immunostaining against the cell type specific markers

Sox2 (general stem cell marker), CKII (sustentacular cell marker), Tp63 (HBC progenitor marker), and HuC/D (pan-neuronal marker) under different damage conditions.

4.6.1. Expression of *hbegfa* in Sox2-positive cells [4hpl]

As previously explained (Results 4.2.), the olfactory tissue was treated with 0.1% and 1% TritonX-100 solution to damage the OE with different severity and tissues were collected at 4 hpl since *hbegfa* expression showed a peak at 4 h after damage in the transcriptome data and expression analysis.

Despite the lack of strong contrast between the *hbegfa* signal and background fluorescence in the intact tissue, an unambiguously strong *hbegfa* signal could be detected in most of the cells that labeled positive for Sox2 immunohistochemistry in 1% TrX treated tissue (arrowheads in Figure 4.13. B part). In addition, the number of *hbegfa*/Sox2 double-positive cells appeared to be increased upon chemical lesion. Yet, as can be seen in figure 4.12, the tissue was severely damaged and individual *hbegfa*-expressing cells were difficult to discriminate even though a general induction in *hbegfa* expression was obvious. The standard damage protocol using 1% TrX severely affected the tissue morphology in a way that made tissue collection and cellular analysis challenging at 4 hpl. To overcome this limitation, subsequent experiments were carried out under milder conditions by irrigation with 0.1% TrX, during which the tissue integrity is largely conserved and the morphology of damaged cells that are labelled with the respective markers can be clearly observed.

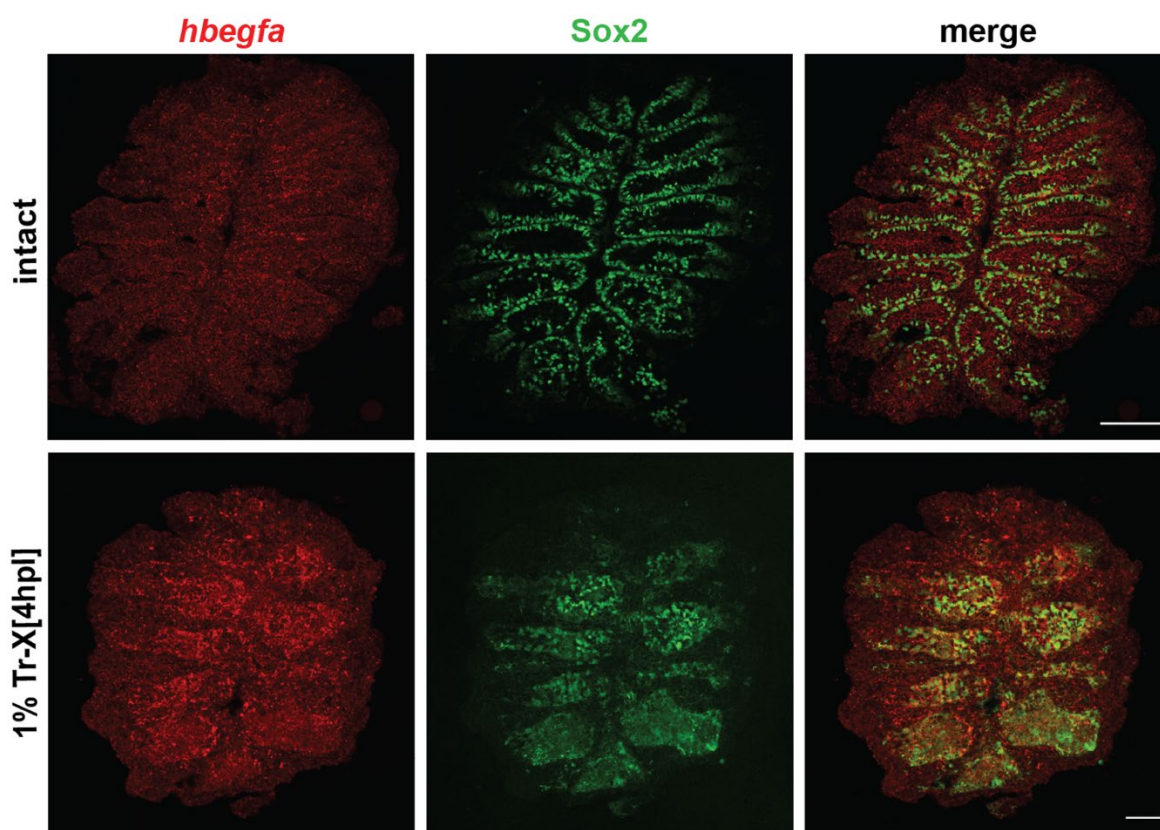


Figure 4.12. *In situ*-hybridization against *hbegfa* transcript (red) and IHC against Sox2 (green). Top panel shows untreated whole nose OE sections and bottom panel depicts 1% Tr-X treated OE sections at 4hpl. Scale Bar: 50 μ m Scale Bar: 25 μ m respectively.

A clear *hbegfa* signal could be detected around a few Sox2-positive cells with nuclear morphologies in the basal layers of the mid-sensory region in intact tissue (Figure 4.13 / A). In addition, occasional cells in the ILC showed clear *hbegfa* signals, however, these cells were not immunoreactive for the Sox2 marker as depicted by yellow arrowheads. Unlike the well-defined spatial pattern of Sox2 expression in the intact tissue, the expression pattern in the lesioned tissue was less organized and was mostly formed by dispersed cell clusters that occupied multiple tissue layers as shown in Figure 4.13. / B. The similarities in the spatial expression patterns and the occurrence of a high number of *hbegfa*/Sox2 double-positive cells upon injury suggest that *hbegfa* is largely expressed by one or more subsets of the non-neuronal basal populations in response to OE damage. However, not all *hbegfa* expressing cells co-labeled for Sox2 immunohistochemistry, which suggest that *hbegfa* expression in the lesioned OE is not restricted to non-neuronal populations and may also be sustained by mature neurons under stress conditions.

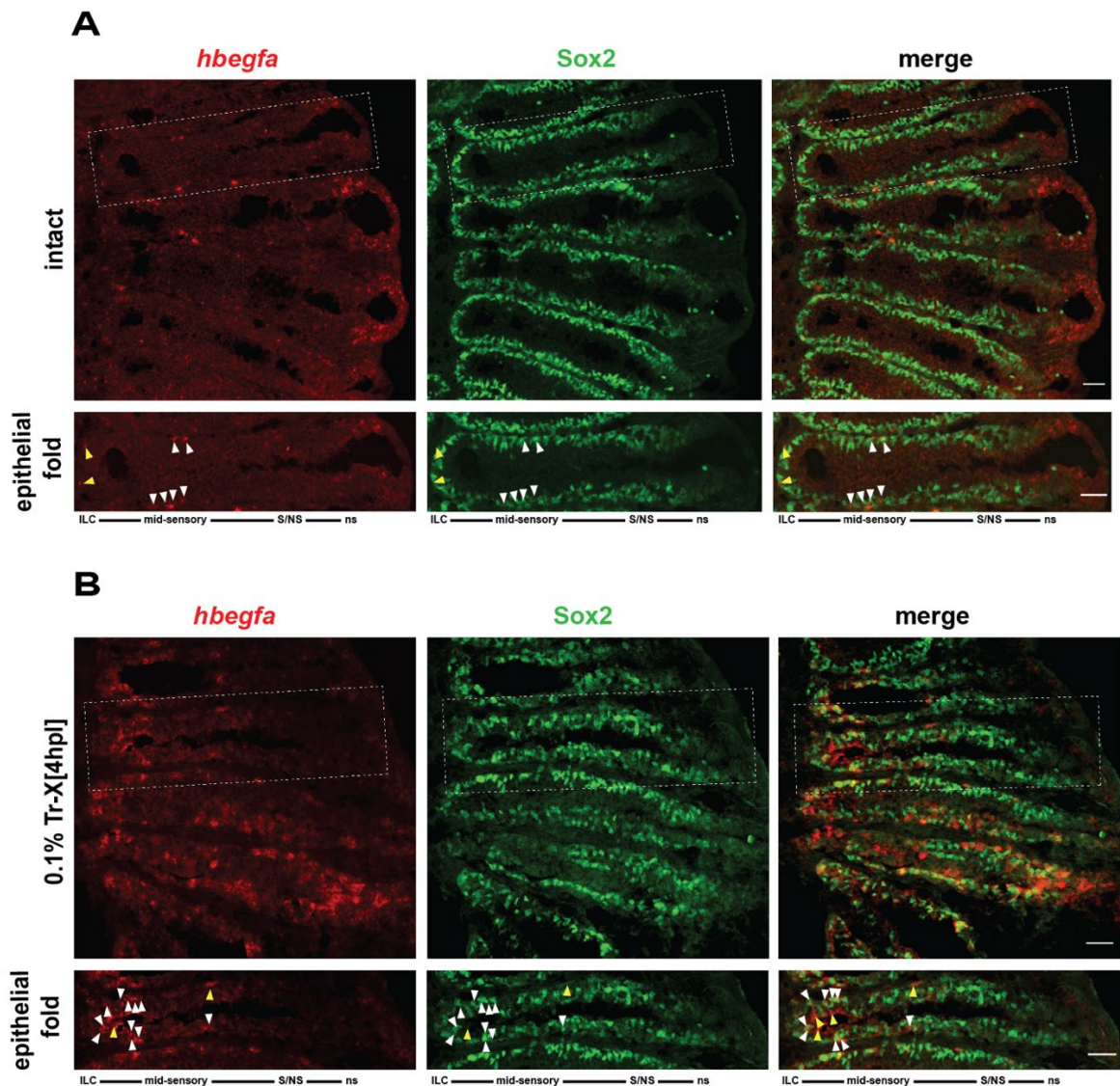


Figure 4.13. ISH against *hbegfa* transcript (red) and IHC against Sox2 (green) marker. **A.** Untreated hemi-OE sections (top) and higher power views of box (bottom). **B.** 0.1% Tr-X treated hemi-OE (top) and higher power views of box (bottom) at 4hpl. Scale Bars: 25 μ m.

4.6.2. Expression of *hbegfa* in CKII-positive cells [4hpl]

SCs expressing the cell marker CKII could be another source for *hbegfa* release under damage conditions. Immunohistochemistry against CKII showed that SCs are highly sensitive to the damage and that their morphology is severely disrupted. Although individual CKII-positive cells were difficult to detect, it was obvious that some SCs upregulated *hbegfa* expression under lesioned tissue (Figure 4.14.).

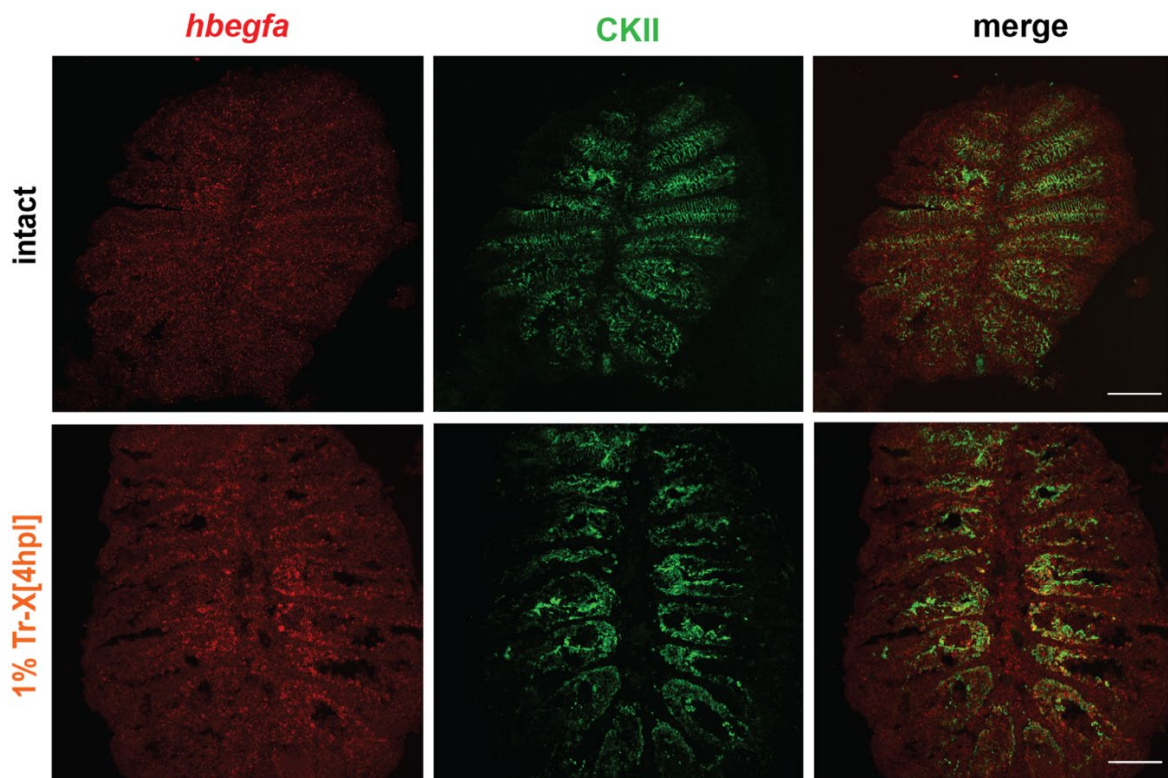


Figure 4.14. Combination of *in situ*-hybridization against *hbegfa* transcript (red) and IHC against SC marker CKII (green). Top panel shows untreated whole nose OE sections. Bottom panel shows 1% TrX treated whole nose OE sections at 4hpl. Scale Bar: 50 μ m.

In the intact tissue, only a few cells could be detected that are *hbegfa* / CKII double positive. In the lesioned tissue, the abundance of double-positive cells was increased, and these cells could be detected around the basal layers (arrowheads). However, all SCs were observed to lose their protruding keratin filaments due to the lesion. (Figure 4.15)

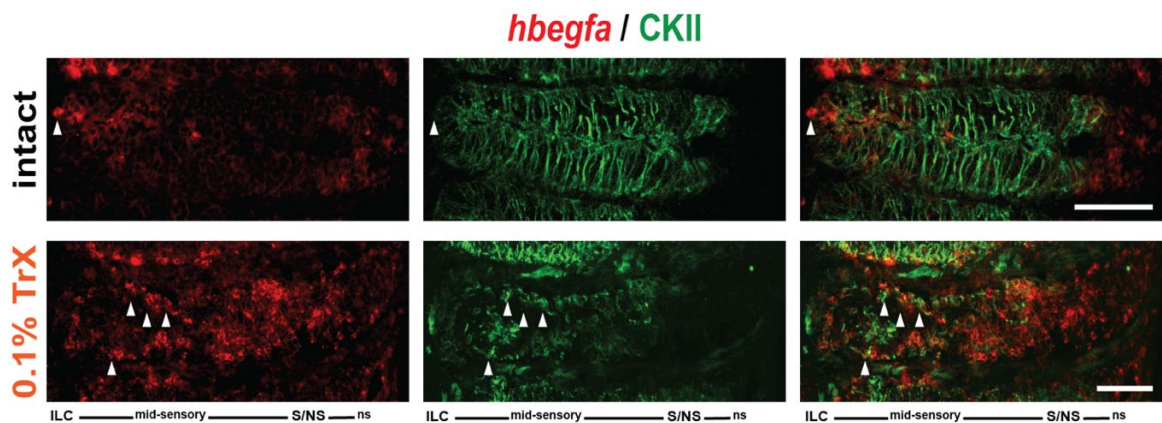


Figure 4.15. ISH against *hbegfa* transcript (red) and IHC against SC marker CKII (green). Top panel shows single epithelial fold of untreated OE sections and bottom panel depicts single epithelial fold of 1% TrX treated OE sections at 4hpl. Scale Bars: 50 μ m, 25 μ m.

4.6.3. Expression of *hbegfa* in Tp63-positive cells [4hpl]

The Sox2-positive non-neuronal cells also include Tp63-positive HBCs and, therefore, the tissue was also labeled against Tp63 under both strong and mild damage conditions. Both damage condition resulted in a noticeable induction of *hbegfa* expression (Figure 4.16 and Figure 4.17.) Under strong damage condition, the unspecific background staining was high, yet induction in *hbegfa* expression was still obvious in Tp63-positive cells in the core-sensory OE. However, not all tp63-positive cells were positive for *hbegfa* expression.

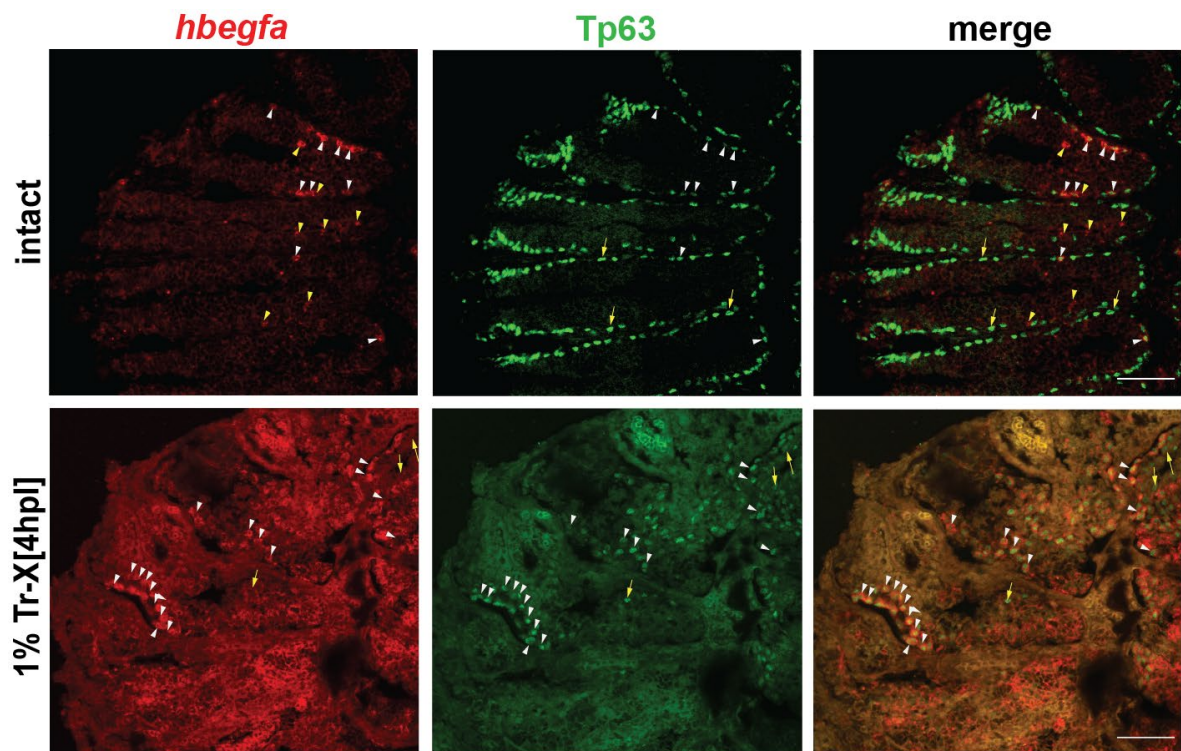


Figure 4.16. Combination of *in situ*-hybridization against *hbegfa* transcript (red) and IHC against transcription factor *tp63* (green). Top panel shows untreated semi-OE sections.

Bottom panel shows 1% Tr-X treated hemi-OE sections. Scale Bar: 25 μ m.

When the milder damage conditions were used, an induction of *hbegfa* signal can be clearly observed in dormant HBCs. The number of *hbegfa/tp63*-double positive cells was increased 4 h after 0.1 % TrX treatment. The newly induced *tp63*-positive could be observed in multiple layers of the OE both in the sensory OE and the ILC (white arrowheads in Figure 4.17). This may indicate that HBCs are about to respond to the injury by proliferating and migrate to more apical layers in the sensory region. Symmetrical HBC divisions can generate new HBCs to maintain the progenitor pool and takes place largely in the basal-most layers of the OE (Demirler et al., 2021). Asymmetric HBC division, on the other hand, occur in response to damage and give rise to transiently amplifying GBCs in suprabasal layers, which will give rise to OSNs (Demirler et al., 2021).

Again, the existence of *hbegfa*-positive/*tp63*-negative cells cannot be disregarded. *tp63* is dynamically regulated in HBCs the rodent OE and downregulated in actively dividing cells (Herrick et al., 2017). Thus, some of these cells may stain positive for the *Krt5* label, which, however, was incompatible with the *in situ*-hybridization conditions.

Alternatively, cells in more apical layers could possibly be OSNs (yellow arrowheads in Figure 4.17). Also, in the figure below, it was observed that Tp63-positive cells formed multiple layers in suprabasal regions and these (probably) injury responsive newly generated tp63 cells were not expressing *hbegfa* (yellow arrows).

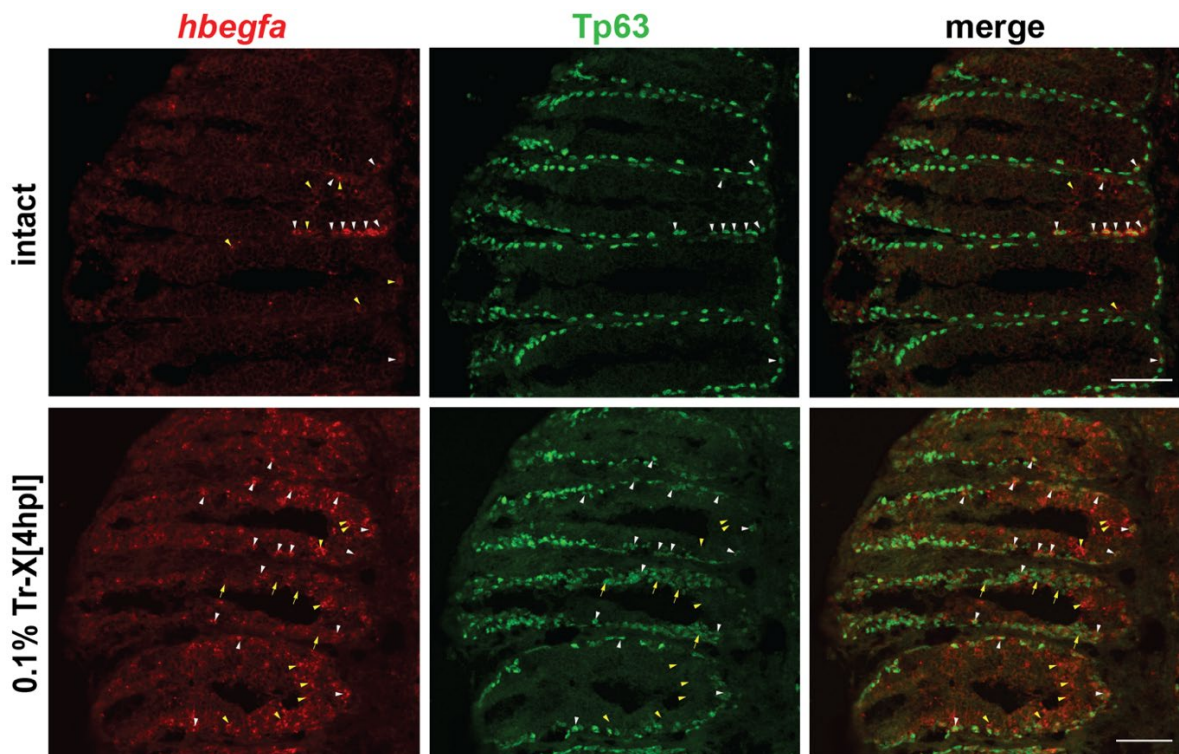


Figure 4.17. Combination of *in situ*-hybridization against *hbegfa* transcript (red) and IHC against transcription factor tp63 (green). Top panel shows untreated hemi-OE sections.

Bottom panel shows 1% Tr-X treated hemi-OE sections at Scale Bar: 25 μ m.

4.6.4. Expression of *hbegfa* in HuC/D-positive cells [4hpl]

Immunostaining against the cell-type specific marker HuC/D was used to visualize the nuclei of OSNs. HuC/D expression was observed in the intermediate and apical layers of the OE under physiological conditions as shown in previous results. Upon damage, the expression pattern is severely disrupted due to the loss of OSNs. Staining against HuC/D marker was also used as a criterion to evaluate the extent of the chemical lesion. Mild damage conditions caused a partial loss of OSNs in the OE, while strong damage caused the loss of almost the entire OSN population.

Under physiological conditions, OSNs are observed in sensory region and the S/NS border is sharply distinctive. A low number of *hbegfa*-positive OSNs can be observed. Treatment with 0.1% TrX caused the disruption of the OSN pattern in the sensory region, which was heterogeneous and affected some lamellae more than others (Figure 4.18 /B higher power view of white box). The strong induction of *hbegfa* expression upon injury also included a large number of surviving OSNs as indicated by white arrowheads in Figure 4.16. Yet not all the surviving OSNs expressed *hbegfa* (white arrows). Nevertheless, it can be concluded that a subpopulation of damaged OSNs is responsive to tissue damage and upregulate expression of *hbegfa*.

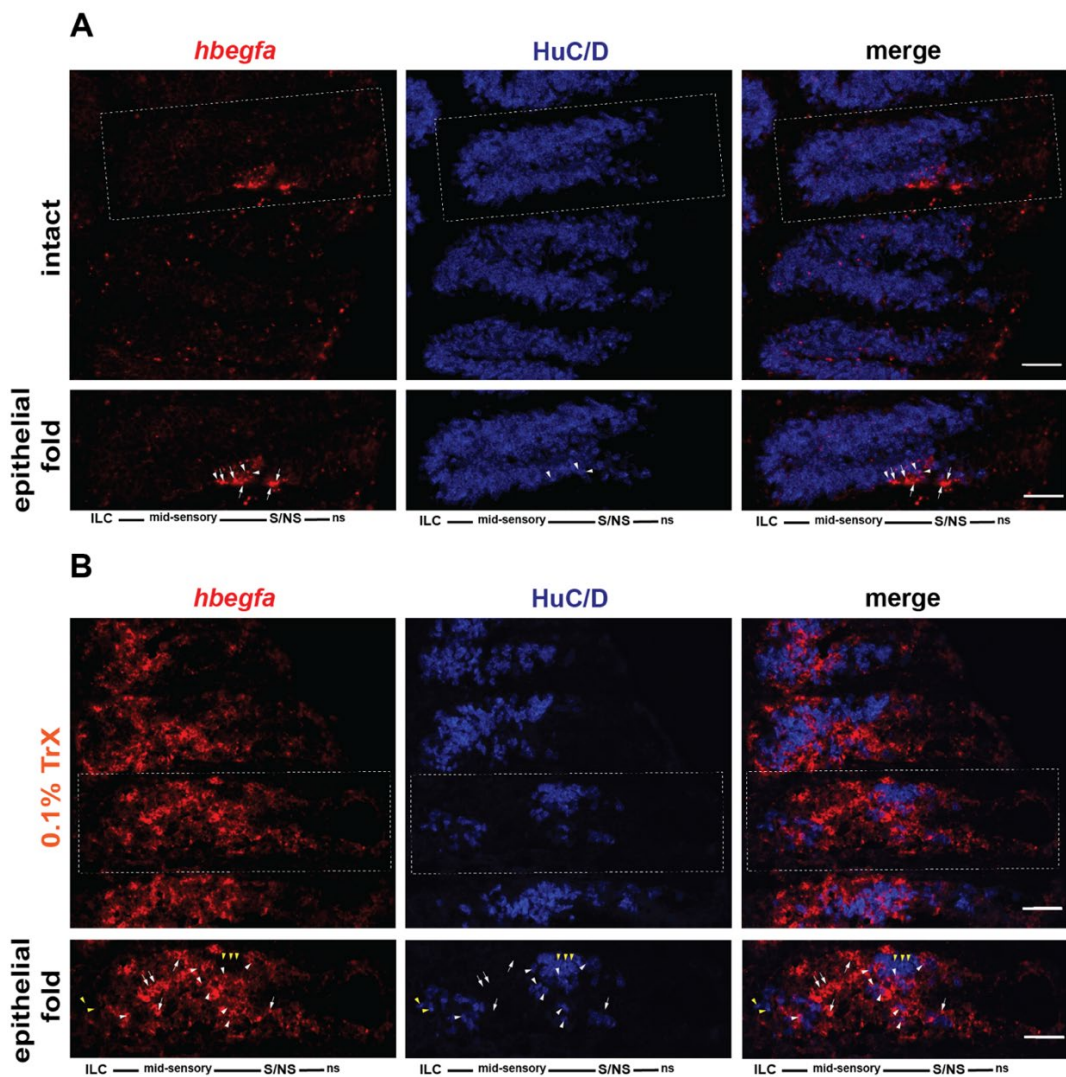


Figure 4.18. ISH against *hbegfa* transcript (red) and IHC against pan-neuronal marker HuC/D (blue). **A.** Intact hemi-OE sections and higher power views of white box. **B.** 0.1 %TrX treated hemi-OE sections at 4 hpl and higher power views of white box. Scale Bar: 50 μ m.

4.7. Summary Conclusion

In situ-hybridization against *hbegfa* transcripts and immunostaining against the cell type specific markers tp63, HuC/D, and Sox2 revealed that all cell types upregulate *hbegfa* expression in response to injury. *Hbegfa*/Sox2 double-positive cells can be observed in basal strata, whereas *hbegfa*/HuC/D double-positive cells are located in the more apical, including the apical-most layer of the OE. There were also several neuronal and nonneuronal cells that showed a clear *hbegfa* signal in the intact tissue, however, a distinctive induction was observed only after the tissue was chemically treated with TrX. Tp63-positive cells showed horizontally elongated morphologies in the ILC and in the basal layer of sensory region and more spherical morphologies were observed in mid-sensory and towards the SNS (arrowheads in Figure 4.20.). *Hbegfa*/tp63 double-positive cells could be detected at the basalmost layer of the OE and *hbegfa*/ HuC/D double-positive cells were mostly detected in the sensory region of the OE. Nonetheless, the distribution of cells giving *hbegfa* signal did not show an organized pattern and additional cells, that did not stain with the markers were detected to give only *hbegfa* signal (dashed spheres in Figure 4.20).

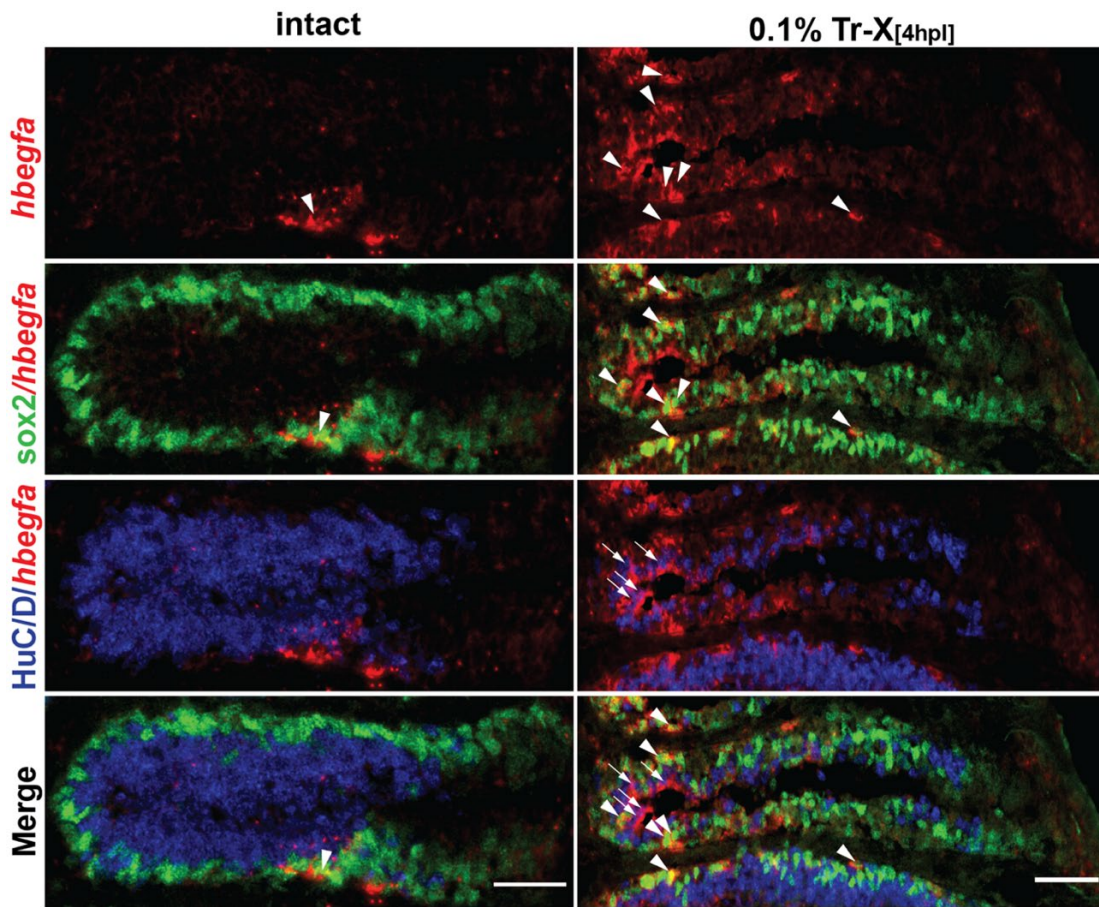


Figure 4.19. ISH against *hbegfa* transcripts (red) and IHC against pan-neuronal marker HuC/D (blue), and stem cell marker Sox2 (green). Arrowheads show *hbegfa*/Sox2 double-positive cells, arrows show *hbegfa*/HuC/D double-positive cells. Scale bars: 100 μm .

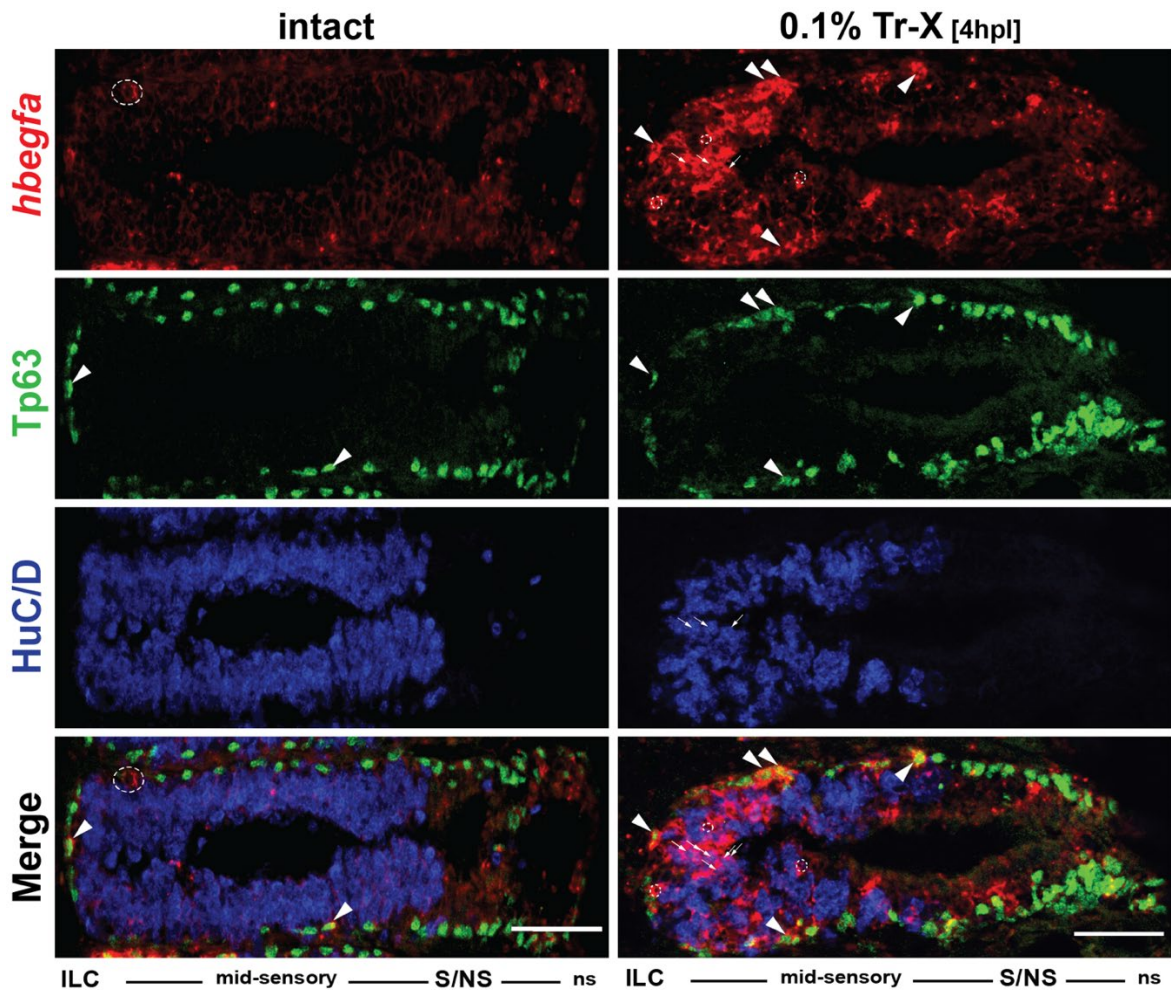


Figure 4.20. *In situ*-hybridization against *hbegfa* transcripts (red) and immunohistochemistry against the pan-neuronal marker HuC/D (blue), and the transcription factor tp63 (green). Scale bars: 100 μ m.

A quantitative analysis was conducted to assess the average percentages of co-expression of *hbegfa* with the different cell markers for individual epithelial folds. In untreated control samples, 17.5 % of *hbegfa*-positive cells were immunoreactive for the neuronal marker HuC/D, while the 41.7% of the population expressed Sox2. A separate assay showed that 52.1% of *hbegfa*-positive cells also expressed tp63 and therefore belonged to HBC progenitor pool. Unexpectedly, the percentages of different cell types under mild injury condition did not change dramatically. Around 20% of *hbegfa*-positive cells were positive for HuC/D and 46.5% and 52.6% of cells were positive for tp63 or Sox2, respectively. The summary data are illustrated in the graph in Figure 4.21 / C (Quantification of the number of *hbegfa*-positive cells per epithelial fold at 4 hpl expressed as fold change

relative to the untreated control OE at 4h. Box and Tukey style whiskers plot, the black bar depicts the median, p-values represent the results of a Tukey HSD post-hoc test on two-way ANOVA). An accurate quantitative analysis could not be performed for CKII-positive SC populations in the damaged tissue since the morphology of these cells was severely disrupted upon chemical lesion. Despite the inability to make a quantitative analysis for SCs, occasional co-labeling of *hbegfa* with CKII marker were observed in damage condition.

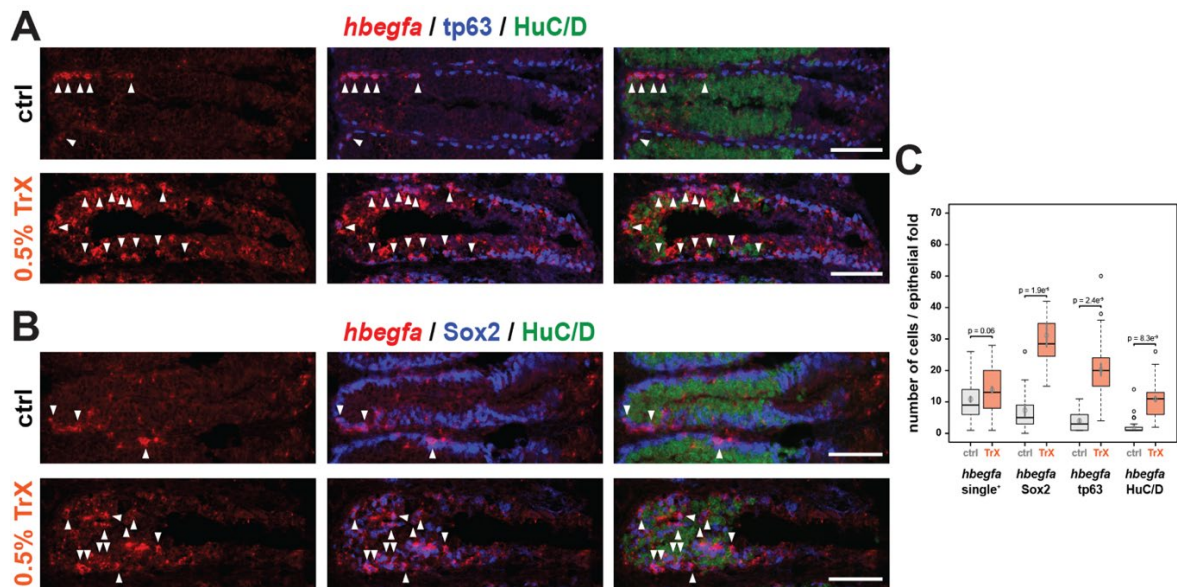


Figure 4.21. **A. B.** ISH against *hbegfa* transcripts (red) and IHC against HuC/D (green), tp63 (blue; top panels) and Sox2 (blue, bottom panels)[4hpl]. **C.** Quantification of the number of *hbegfa*-positive cells per epithelial fold at 4 hpl. Scale Bar: 50 μ m.

As a conclusion, the results showed that all major cell types, neuronal and non-neuronal, are responsive to mild and strong tissue damage and can be the source of HB-EGF release in the injured OE. It is likely, that cells, which are only *hbegfa*-positive but do not express any other cell type specific marker, belong to transition states of the OSN cell lineage.

4. 8. Generation of an *erbB1/egfra*- specific riboprobe

The *egfra* gene of the zebrafish is annotated in the NCBI database with the gene ID 378478 and the *egfra* transcript NM_1194424.1 with 6.169 bp length and containing 28 exons was selected for riboprobe design. The region within the last coding exon (depicted as green rectangular in Figure 4.22) was chosen as a candidate probe region taking care to

avoid repeated common transposon sequences and the TCR-18 (T-cell receptor sequence) sequences to ensure target sequence specificity. Regions corresponding to repeat elements can be expressed from other regions within the genome and would give false positive and unspecific signals during *in situ*-hybridization experiments. The template for the *egfra* probe region was checked for specificity using the Ncbi Blast tool and was found to align specifically with the *egfra* mRNA. Oligonucleotide primer sets were designed using the Ncbi Primer-Blast tool and the best choice among the primer sets were checked with OligoCalc (Kibbe, 2007). The *egfra* primer pair *egfra_F2*, *egfra_R2* (see 3.2.2. Table 1 for primer sequences), which spans a 450 bp region was selected as the best candidate with appropriate primer features and the primer positions are indicated on the transcript map created by SnapGene version 5.3.2. in Figure 4.22.

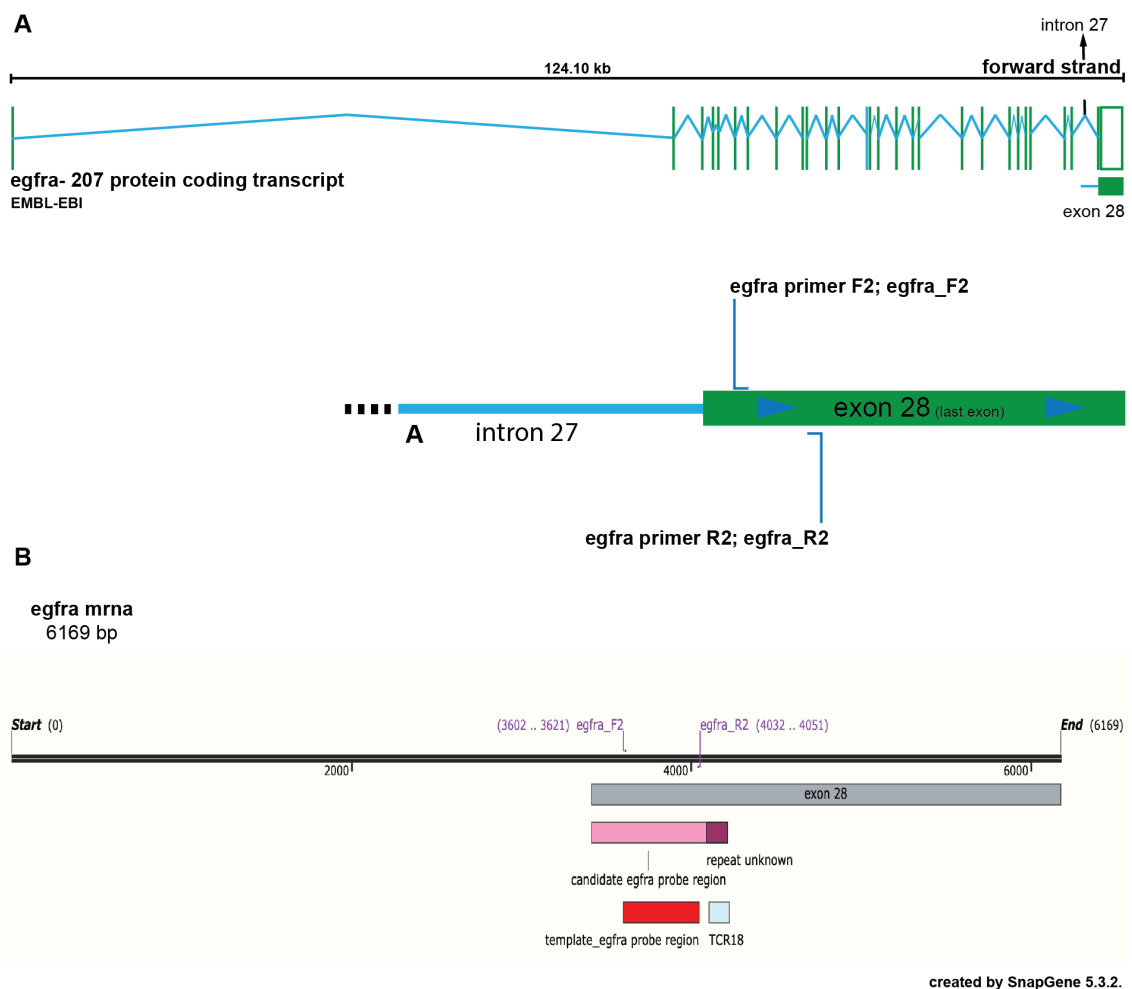


Figure 4.22. Representation of *egfra* transcript. **A.** *egfra*-207 protein coding transcript (by EMBL-EBI). Last exon of the transcript is depicted by green rectangular. **B.** *egfra* template transcript region with specifically designed primers are positioned on the mRNA sequence.

A 450 bp *egfra* DNA template sequence for antisense riboprobe synthesis was amplified from adult zebrafish gDNA by polymerase chain reaction (PCR) using Titanium Taq polymerase, which provides increased specificity and yield due to the included TaqStart® Antibody (Kellogg et al., 1994). The image of the gel electrophoresis analysis of PCR products is shown in Figure 4.23. The product in lane 7, amplified by the F2/R2 primer pair and Titanium Taq polymerase gave the least amplification of unspecific bands and was further purified with the PCR purification kit (Roche) and run again on a 1% agarose gel as demonstrated in Figure 4.23. The size of the amplicon met the expectation size of 450 bp. However, while loading the well with the sample, the tip stabbed the gel, therefore, the banding pattern was observed to be disturbed during visualization of the gel image.

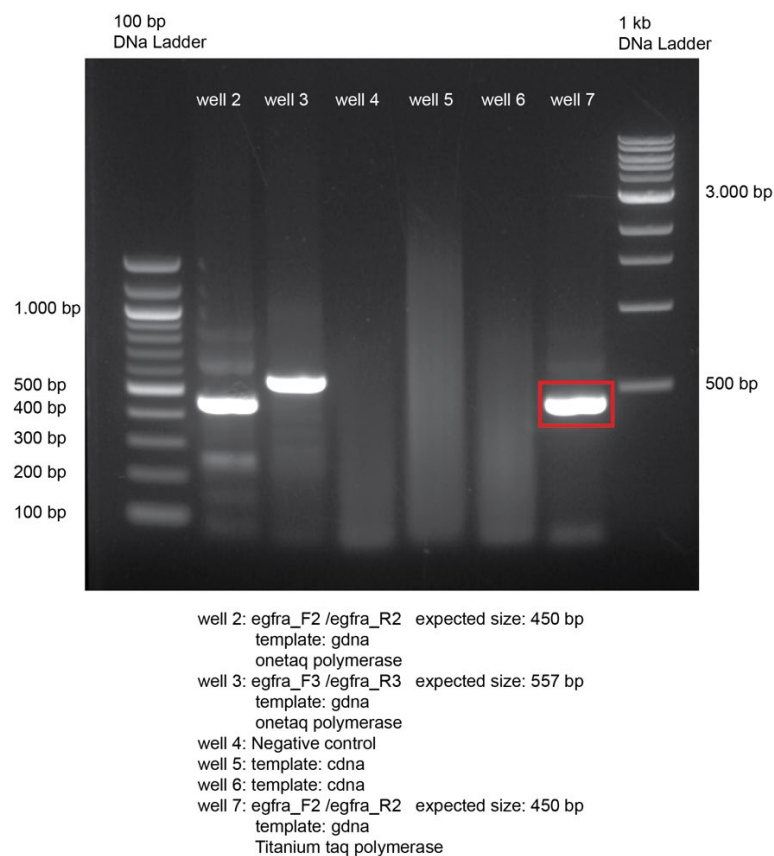


Figure 4.23. Amplification of *egfra* target region by polymerase chain reaction (PCR) with OneTaq® and Titanium Taq® Polymerases. Primer pairs; egfra_F2/ egfra_R2 and egfra_F3 / egfra_R3. Templates; zebrafish cdna and gdna.

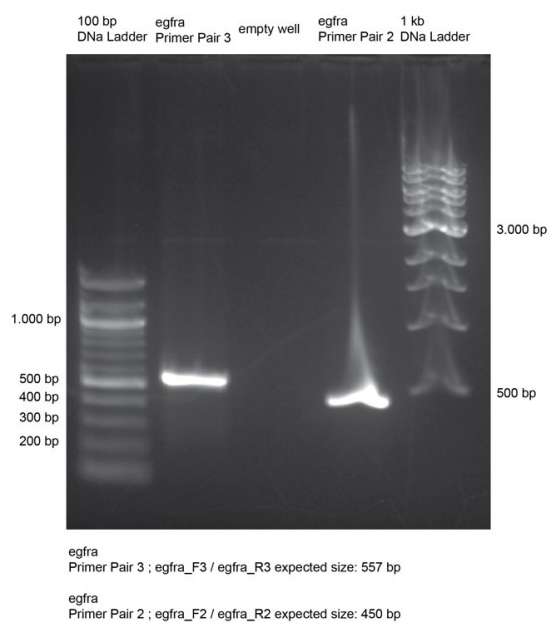


Figure 4.24. Gel image of specifically designed *egfra* primer pairs. Zebrafish gDNA was used as PCR template.

The purified PCR product was cloned into the pGEMT-easy plasmid vector (3015 bp) and transformed into DH5 α competent *E.coli* cells. Transformed bacteria was spread onto LB agar plates and colonies were allowed for growth at 37 $^{\circ}$ C overnight. Multiple colonies were selected and extruded plasmid DNA was digested with *Eco*RI restriction enzyme to check if the vector contains the desired insert as can be seen in Figure 4.25. All selected colonies contained inserts of appropriate size. Positive colonies were grown in LB Broth medium and plasmids were extracted with the MiniPrep (Roche) plasmid isolation kit. Isolated plasmid samples were subjected to DNA sequencing with *egfra* primer set 2 and T7 / SP6 general primers to check for insert directionality. The sequencing results showed that the sequence reads of the plasmid obtained from colony 7 were aligned with the target sequence as depicted in figure 4.24. This indicates that the desired *egfra* template was successfully inserted into the pGEMT-easy vector in reverse orientation relative to the T7 promoter, which was used for further *in vitro* transcription (Figure 4.26.). The concentration of the plasmid obtain from colony 7 was measured to be 319,5 ng/ μ l using a NanoDrop UV spectrophotometer (ThermoFisher Scientific). This isolated plasmid was linearized with the *Nco*I restriction enzyme, which is a unique cutter within the multiple cloning site of the plasmid map and linearizes the template from the SP6 side of the vector. The expected size of the linearized plasmid was 3.467 bp as calculated by SnapGene. The linearized plasmid

harboring the confirmed *egfra* probe region was purified and run again on a 1 % agarose gel to verify complete digestion to avoid run-around transcription. The results of the analysis is shown in figure 4.27. The upper band corresponds to the expected size of 3.467 bp, however, another band running at around 2 kb could be detected on the gel. This dim band most probably originates from single-stranded DNA caused by denaturation of the linearized plasmid during DNA purification and was neglected.

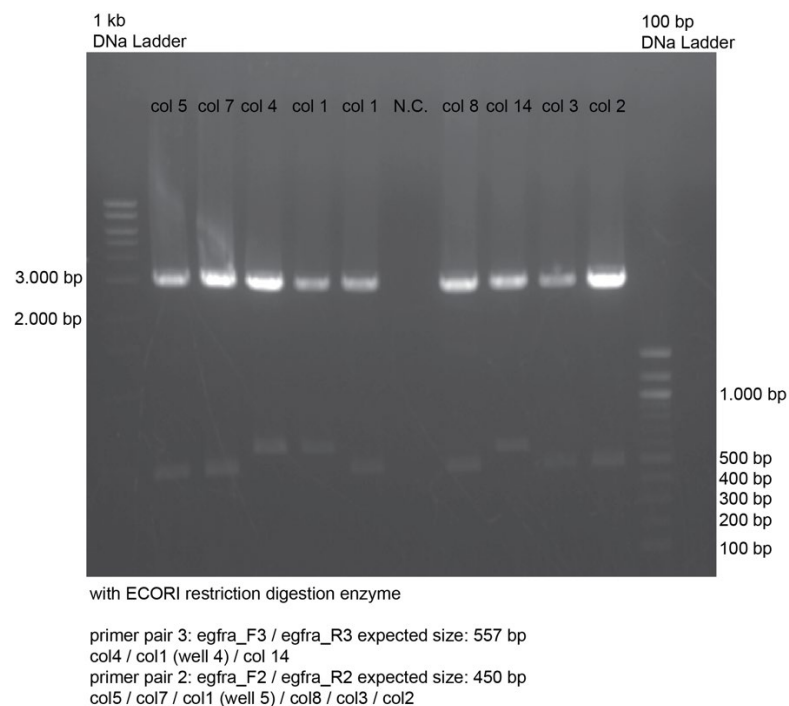


Figure 4.25. *EcoRI*-HF restriction digestion for *egfra* colonies. All selected colonies are positive regarding desired *egfra* insert.

The purified and linearized *egfra* probe plasmid was used as template for an *in vitro* transcription reaction for antisense riboprobe synthesis. A DIG-UTP-labeled antisense *egfra* riboprobe was synthesized using T7 polymerase and purified by ethanol precipitation before the sample was run on an agarose gel for control purposes. A bright band corresponding to the length of the synthesized RNA probe is indicated by a red box in figure 4.28. An additional weak band of 1.500 bp, most likely originating from incompletely digested template DNA, could also be detected. Nevertheless, the synthesized riboprobe was utilized for further *in situ*-hybridization experiments.

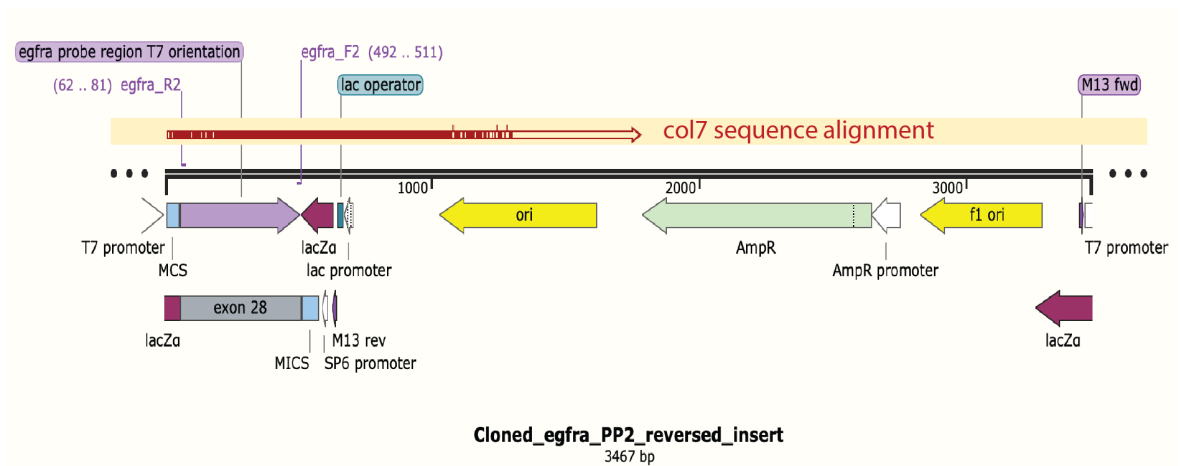


Figure 4.26. Representation of pGEMT-easy vector map with *egfra* probe region reversely inserted. *Egfra* primer pair 2 is positioned and sequence alignment for colony 7 is shown on the vector map. (Created with SnapGene version 5.3.2.)

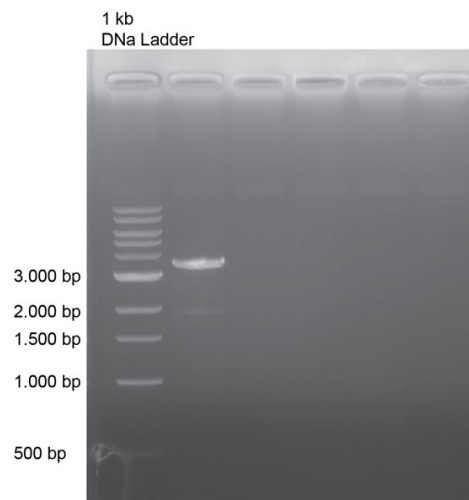


Figure 4.27 Agarose gel image of linearized *egfra* template in pGEMT-easy vector. Linearization by *Nco*I restriction digestion enzyme.

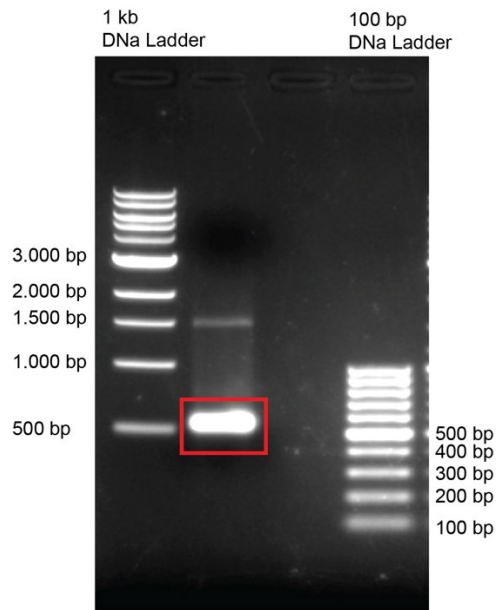


Figure 4.28. Gel electrophoresis of the synthesized *egfra* riboprobe.

4. 9. Expression pattern of *erbb1/egfra* in the intact zebrafish OE

HB-EGF preferentially binds to target cells that express epidermal growth factor (EGF) receptors of the *ErbB* family (Junttila et al, 2000; Iwamoto et al., 2017). In mammals, the *ErbB* family consists of four receptors; EGFR/ ErbB1, ErbB2, ErbB3 and ErbB4, however, the zebrafish genome contains six members due to a partial duplication of the genome, which resulted in *ErbB3a/b* and *ErbB4a/b* paralogs. Among these, ErbB1 and ErbB4 have been shown to bind HB-EGF specifically and preferentially. As a response to receptor binding, different downstream signaling pathways are activated, eventually resulting in transcription of target genes related to growth, proliferation, and survival (Iwamoto et al., 2017).

Transcriptome data generated by our lab revealed that all six *erbb* paralogs are expressed at different levels in the zebrafish OE. Of those *erbb2* and *erbb3a* show the highest level of expression while the HB-EGF-sensitive *erbb1/egfra* and *erbb4a/b* genes are expressed at intermediate or low levels. Upon OE damage, *erbb1/egfra* is the only isoform that is upregulated 2-fold, which makes it the most relevant candidate for HB-EGF signaling during induction of repair neurogenesis. Therefore, in this part of this study, I particularly focused on the analysis of the *erbb1* expression pattern in the zebrafish OE by *in situ*-

hybridization and the identification of expressing cell types by simultaneous labeling for cell type-specific markers.

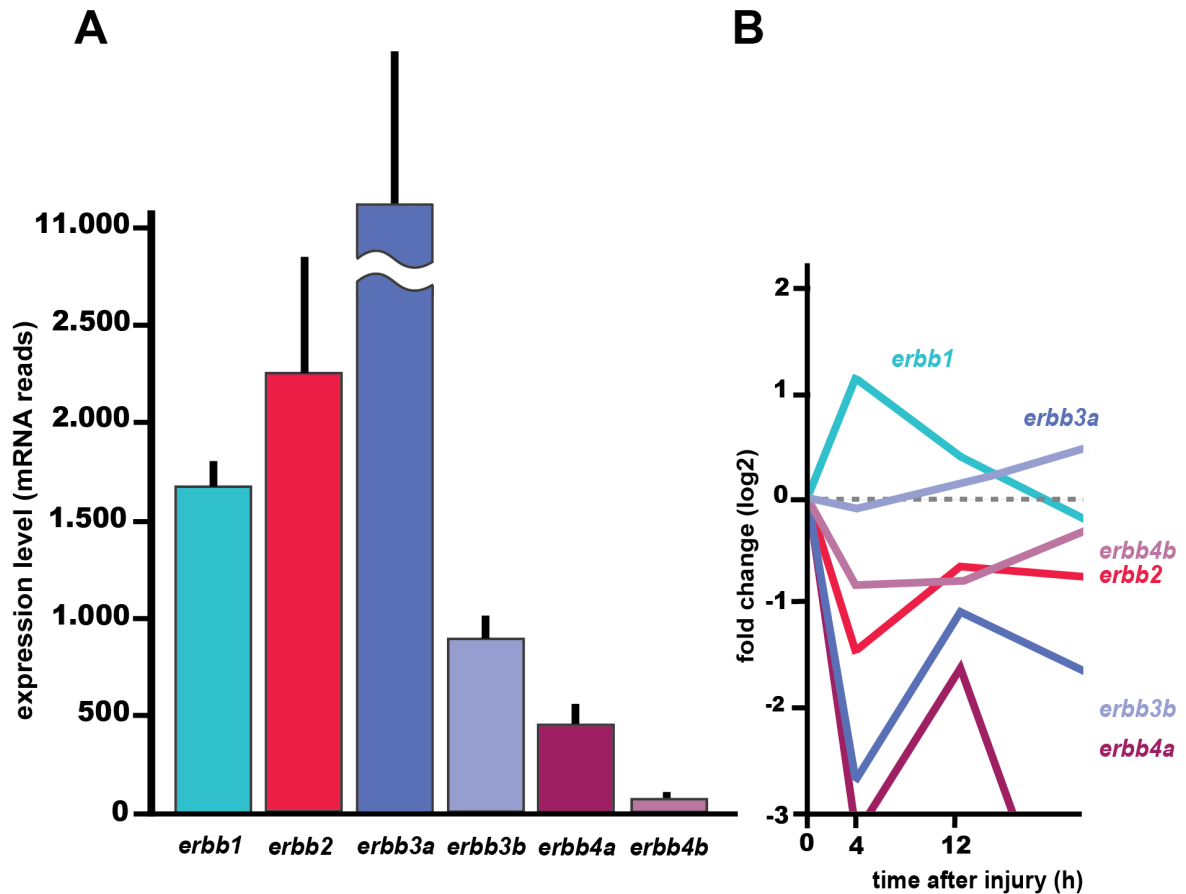


Figure 4.29. **A.** Baseline expression levels of EGF receptor family members in the intact zebrafish OE. **B.** Logarithmic fold changes in expression levels of EGF receptor family members upon 1% TrX 100 induced chemical lesion to the OE.

4.9.1. Expression of *erbb1/egfra*

Expression of *egfra* in the intact zebrafish OE was analyzed by *in situ*-hybridization. The result showed labeled cells in the apical and basal OE. Cells in the basal layer of the OE are indicated by the dashed line within the yellow box in figure 4.30. White arrowheads in the zoomed image depicts *egfra in situ*-hybridization signal in the cytoplasm of the basal cells. The expression can be seen as a punctuated pattern of red dots probably due to the low expression levels of *egfra* under physiological conditions. The result may indicate that dormant HBCs are a potential source of the *egfra* expression in the intact zebrafish OE. In

addition, a continuous band of apically located cells of unknown identity could be observed. The apical expression may explain, why exogenous HB-EGF stimulation effectively induces cell proliferation in the OE.

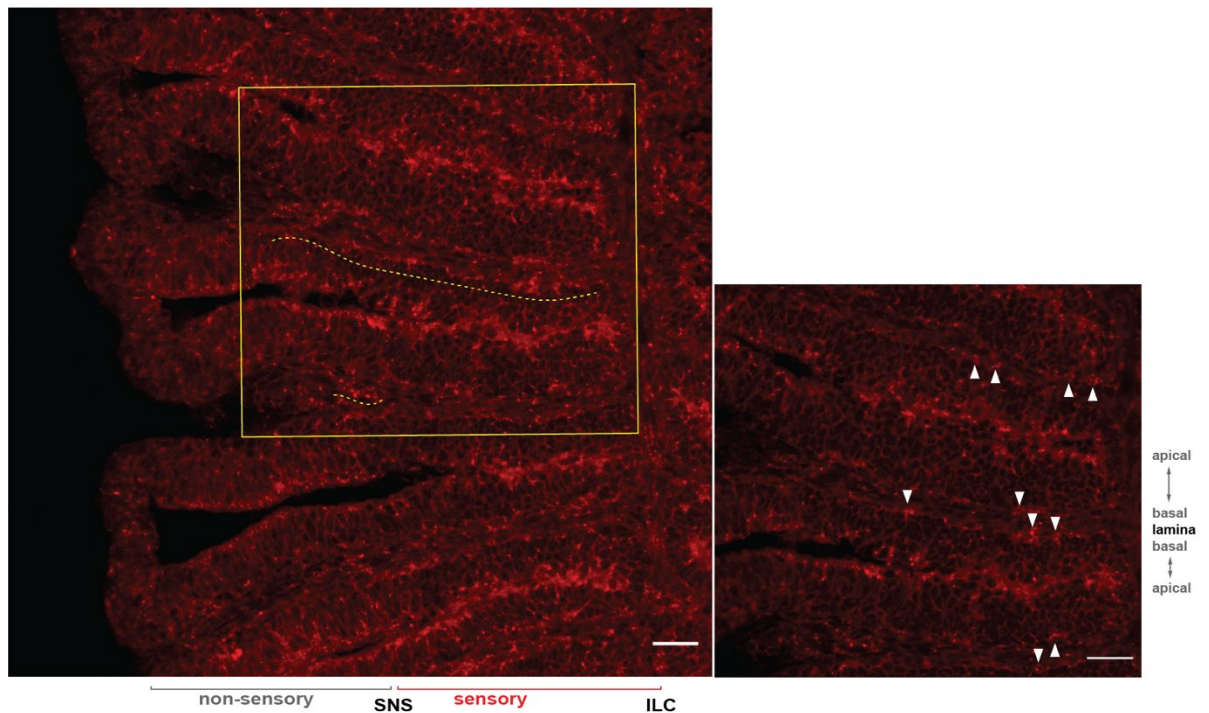


Figure 4.30. *Egfra* expression in the intact hemi-OE. Higher power view of the region shown in yellow box is represented at the right. Scale Bars 25 μ m.

4.9.2. Expression of *erbB1/egfra* combined with IHC

In situ-hybridization against the *egfra* riboprobe was combined with immunohistochemistry against the HBC progenitor marker tp63 and the pan neuronal marker HuC/D under physiological conditions to further identify *egfra*-expressing cells. Previous results suggested that HBCs and neurons are sources of HB-EGF expression under physiological and injury conditions.

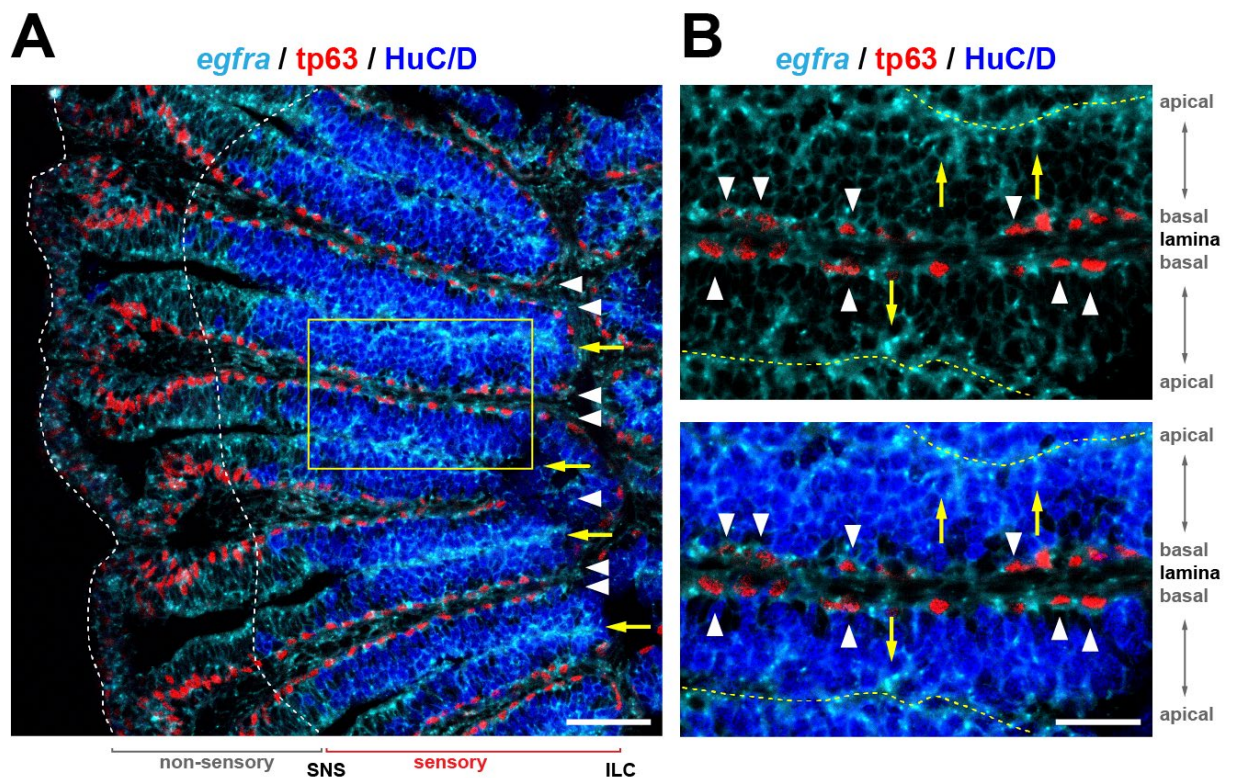


Figure 4.31. **A.** ISH with *egfra* antisense RNA riboprobe (cyan) and IHC against the HBC marker *tp63* (red) and OSN marker *HuC/D* (blue). A hemi-OE is shown. Scale bar: 50 μ m.

B. Higher power view of the region indicated by the yellow box in A. Scale bar: 25 μ m.

The low *egfra* signal was difficult to detect in the OE due to high background staining, however, when higher power images were analyzed in detail, some *tp63* expressing cells could be observed to show *egfra* signal at the basal layer (arrowheads). However, not all *tp63*-positive cells co-labeled for *egfra* expression. In addition, some *HuC/D* positive cells in apical layers (yellow arrows) were also found to express *egfra* transcript, which is shown in figure 4.31.

4.10. Summary Conclusion

Expression analysis of the *egfra* gene suggests that a high number of *tp63*-positive HBCs and some OSNs express the Erb1/EGFRA receptor and may be responsive to HB-EGF in the zebrafish OE under physiological conditions. However, additional *in situ*-hybridization experiments combined with cell type specific markers should be performed under damage conditions to further identify and characterize the HB-EGF-responsive cell

populations. The observations are in line with the literature, which reveals specific EGFR expression on the surface of the HBCs in rodents (Dai et al., 2018; Holbrook et al., 1995).

4. 11. Induction of *ascl1a*-expressing cells in the lesioned OE

Regenerative OSN neurogenesis goes along with the transient generation of *ascl1*-positive GBCs within the core sensory OE. In this part of my thesis, I focus on *ascl1a*-expressing cells under physiological and damaged conditions, which will also serve as an experimental strategy to correlate HB-EGF-induced neurogenesis with cellular events that take place during the tissue response to damage.

Achaete-acute like 1a (*ascl1a*; Mash1 in mammals) is a bHLH transcription factor that has been shown to be essential for neural differentiation during embryogenesis (Kim et al., 2011). *Ascl1a* is expressed by transit-amplifying spherical GBCs that are located more apically than HBCs in the basal OE of rodents and *ascl1* is currently their most defining molecular marker (Schwob et al., 1995). Previous studies by our group showed a specific localization of *ascl1a*-positive cells at the ILC and SNS border, thus, the zones at which proliferating activity related to constitutive OSN neurogenesis occurs. Therefore, *in situ*-hybridization against *ascl1a* was performed to investigate, whether GBC-like cells are generated in additional epithelial positions in response to damage.

4.11.1. Expression of *ascl1* in intact OE

In situ-hybridization against *ascl1a* was combined with the undifferentiated stem cell marker Sox2 and the HBC marker tp63 under physiological conditions. Strong *ascl1a* signal could be detected be concentrated around the SNS border and within the ILC. The ILC and SNS regions are the zones of proliferative activity in the intact tissue and *ascl1a* is one of the first fate determination genes expressed in the OE (Bayramlı et al., 2017). Some individual *ascl1a* expressing cells could also be detected in the sensory region, however, the outer non-sensory region of the OE was typically devoid of signal. *Ascl1a*-positive cells at the basal layer of OE were also positive for Sox2 (white arrowhead at the mid-sensory basal layer of OE in Figure 4.32).

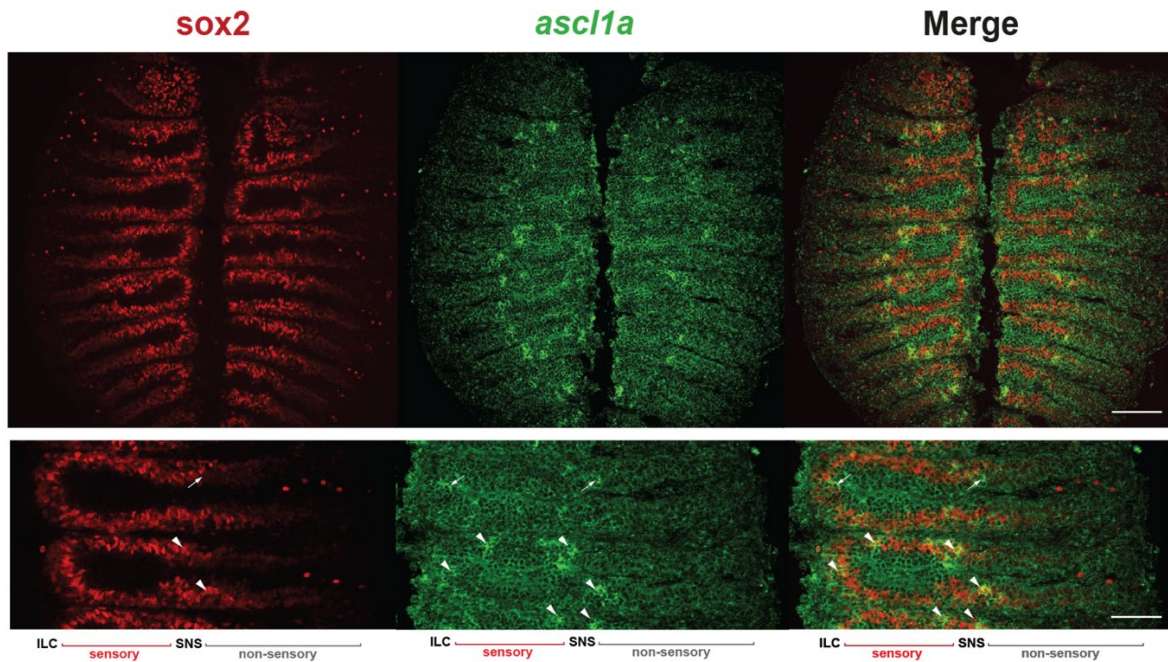


Figure 4.32. Expression of *ascl1a* (green) proneuronal gene and IHC against stem cell marker Sox2 (red). Upper panel shows the whole nose sections of untreated OE and bottom panel depicts higher power views of the same sections. Scale bars: 25 μm .

In addition to the prominent co-labeling of with Sox2 in most *ascl1a*-positive cells, a low number of *ascl1a* cells occupying the SNS were also detected to be Sox2 negative (arrow in Figure 4.32). This result suggests that cells may lose their stemness and enter a transition state in the OSN lineage and will later lose their *ascl1a* expression as they mature.

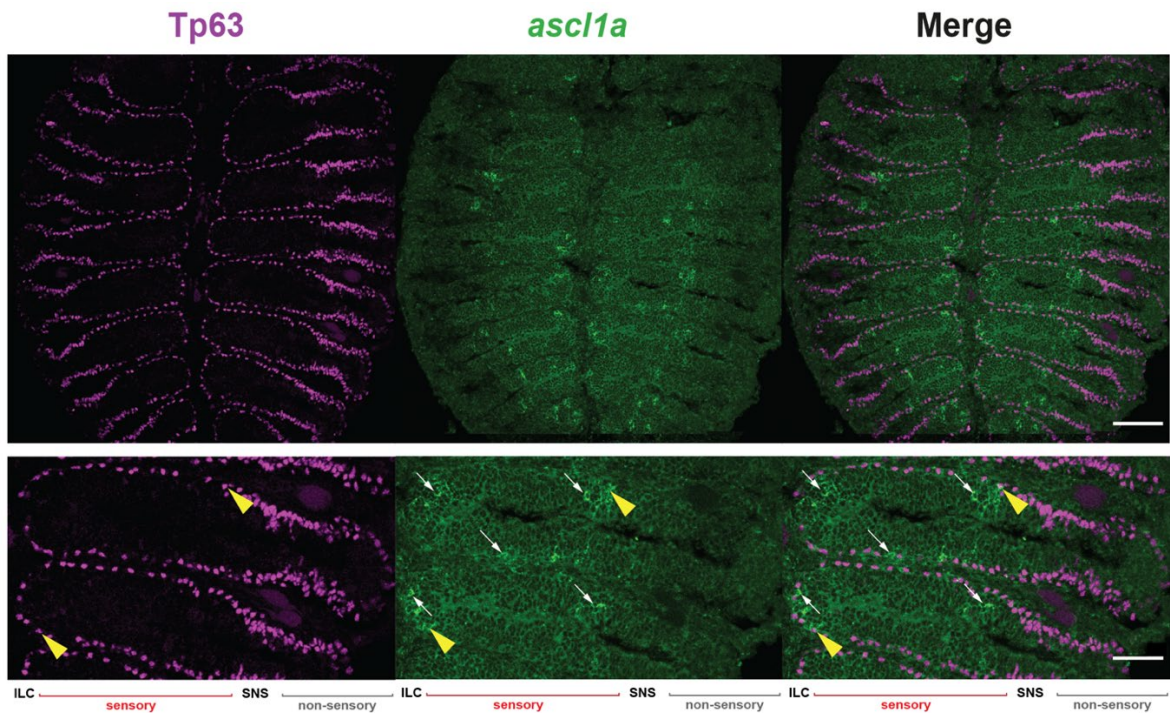


Figure 4.33. Expression pattern of *ascl1a* (green) and immunohistochemistry against HBC marker tp63 (magenta). Upper panel shows the whole nose sections of untreated OE and bottom panel depicts higher power views of the same sections. Scale bar: 25 μ m.

Ascl1-positive GBC-like progenitors undergoing multiple rounds of cell divisions before differentiating into neurons were described to be a result of early HBC activation in rodents (Schnittke, N. et al., 2015) and zebrafish (Kocagöz et al., 2021). Therefore, the immunoreactivity of *ascl1a*-positive cells for HBC marker tp63 were examined. A low number of tp63-positive cells stained double-positive for *ascl1*-expression at the ILC and SNS border (yellow arrowheads in Figure 4.33.), suggesting that some of the early GBCs may also be HBC-derived under physiological conditions. Yet, most *ascl1a*-positive cells at the ILC and more apical regions were devoid of the tp63 marker.

4.11.2. Expression of *ascl1a*-expressing cells in damaged (1% TrX Lesioned) OE

To examine whether the regenerative response stimulates neurogenesis in the OE that depends on transient generation of an *ascl1a*-positive GBC population, the spatial pattern of *ascl1a* expression was analyzed in the injured OE. Upon chemical lesion, *ascl1a*-expressing cells could be observed more frequently than in the intact tissue and without any apparent spatial restriction. *Ascl1a*/Sox2 double-positive cells occupy mostly the basal

layers of the lesioned OE, including suprabasal layers. The expression pattern observed under damage condition resembles the distribution pattern of *hbegfa* expressing cells in the lesioned OE.

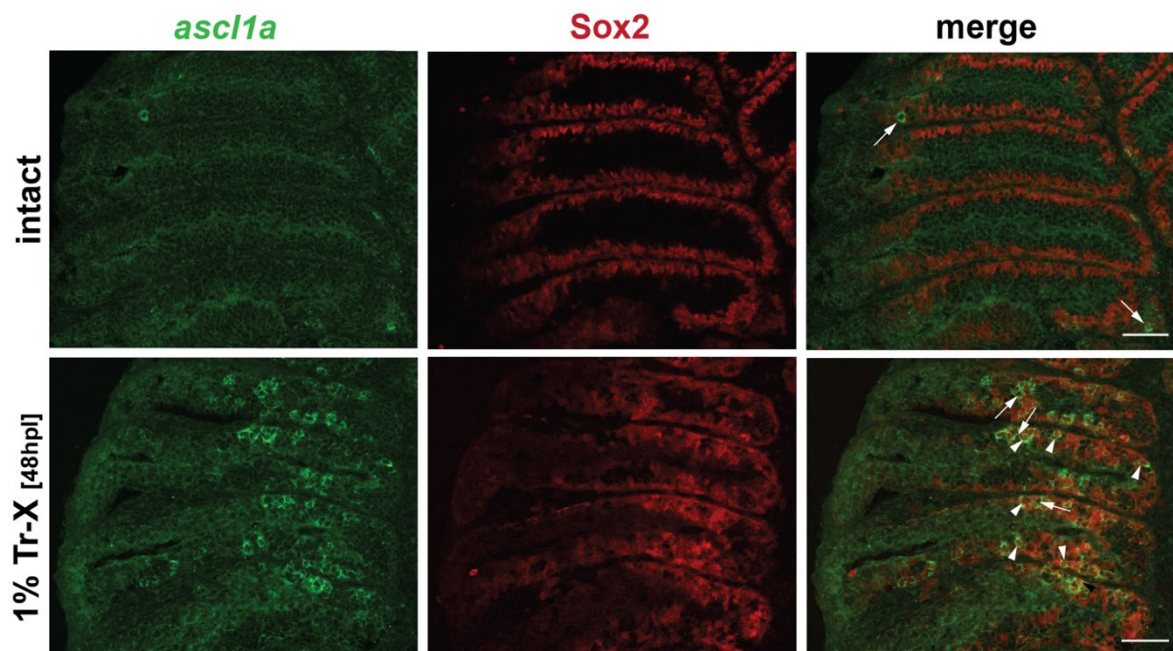


Figure 4.34. Expression pattern of *ascl1a* (green) and immunohistochemistry against Sox2 (red) stem cell marker. (Upper panel shows intact tissue sections, bottom panel shows *ascl1a* induction at 48 hpl). Scale bars: 20 μ m.

To further analyze the activity of *ascl1a*-positive cells in the regenerating OE, *in situ*-hybridization against *ascl1a* was combined with immunocytochemistry against pan-neuronal marker HuC/D under damage conditions at 24 h and 48 h post lesion.

Previous findings showed the absence of overlap between Huc/D-positive OSNs and *ascl1a*-expressing cells, however, occasional OSNs were found to be *ascl1a*-positive, suggesting that these neurons just reached maturity and have not lose their *ascl1a* expression at the time of analysis as shown by arrowheads in upper panel in Figure 4.33. Upon chemical lesion, the number of *ascl1a* expressing cells were found gradually increase over time and more *ascl1a*-positive cells could be identified at 48 h post lesion. The newly generated *ascl1a*-positive cells were usually devoid of Huc/D expression (arrows in Figure 4.35) with the exception of occasional double-positive cells near the ILC region.

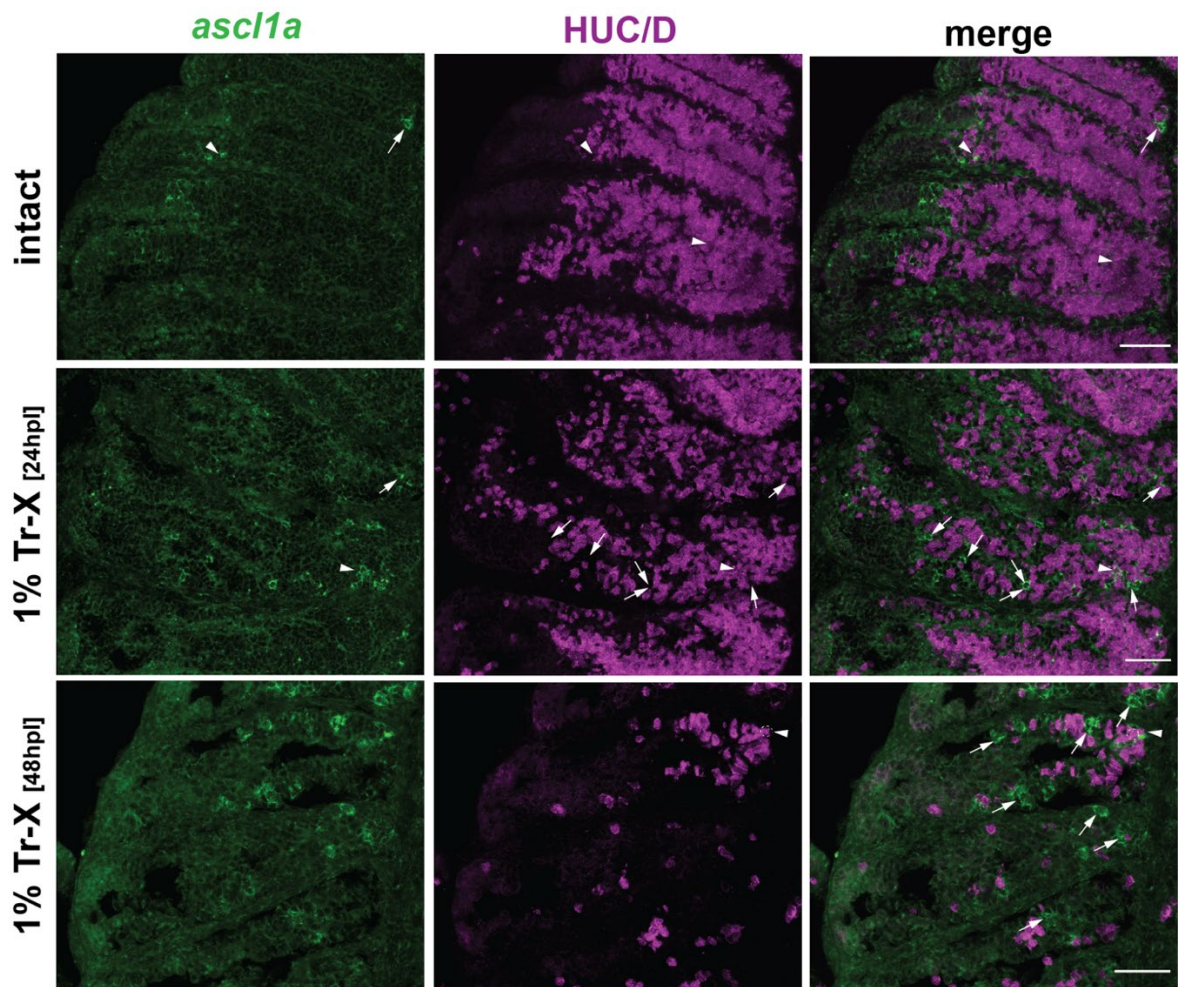


Figure 4.35. *In situ*-hybridization against *ascl1a* (green) combined with immunohistochemistry against HuC/D (magenta) in intact and damaged OE at 24 and 48 hpl. Scale bars: 50 μ m.

4.12. Summary Conclusion

The above-mentioned results show the occurrence of *ascl1a*-positive cells at ILC and SNS regions which are the active proliferative regions in the OE. *Ascl1a/ Sox2* double positive cells were found to form clusters at SNS, yet individual cells are mostly observed at the ILC under physiological conditions. Upon chemical damage to the tissue, *ascl1a/Sox2* double-positive cells could be found along the sensory region instead of spatial preference observed in intact tissue. Although, *ascl1a* expression is observed in active HBC-like cells in the literature, my results also showed that some dormant HBCs that are tp63-positive also express *ascl1a* at the basal layer or these HBCs probably reflect a transitions state. *Ascl1a*-expressing cells are induced upon chemical lesion and the number of newly generated *ascl1a*

cells is increased in response to tissue injury. Most newly generated *ascl1a* cells are devoid of mature OSN marker as expected.

Considering that the *ascl1a*-expressing fast cycling GBCs are also generated in the sensory region in the injured zebrafish OE and similarity between the spatial distributions of *ascl1a* and *hbegfa* expressing cells in the injured tissue suggests that HB-EGF may be involved in regenerative neurogenesis.

However, to have a better understanding and to directly to demonstrate the neurogenic role of HB-EGF, future experiments should be performed examining the *ascl1a* expression pattern upon intranasal stimulation to the OE with HB-EGF under physiological conditions.

5. DISCUSSION

Nervous tissue has only a limited capacity for structural and functional repair due to the limited number of active stem cell populations that support continuous neuronal turnover and tissue regeneration upon tissue injury (Gage and Temple, 2013). Nevertheless, the OE, has retained an unusually high capability to form new olfactory neurons in adult organisms, most likely because it is vulnerable to direct exposure to pollutants, heavy metals, chemical neurotoxicants, infectious agents, and direct physical injury (Moulton, 1975; Mackay-Sim and Kittel, 1991; Tierney et al., 2010). This makes continuous OSN neurogenesis and the capacity for functional and structural repair a necessity to maintain a sense of smell over the lifetime of the organism. Similar to the other epithelial tissues that show a high degree of cellular turnover, the OE is enriched with two functionally and morphologically distinct stem/progenitor cell populations that are responsible for the generation of new OSNs during tissue maintenance and repair. (Schwob et al., 2017; Yu and Wu, 2017). In the zebrafish OE, these progenitor cell populations have distinct but partially overlapping tissue distributions (Demirler et al., 2020; Kocagöz et al., 2021). GBCs exclusively occupy the ILC and SNS, while HBCs are uniformly distributed throughout the entire OE (Demirler et al., 2020). While GBCs continuously contribute to the formation of new OSNs under physiological conditions, HBCs function as dormant progenitors that are activated when the structural integrity of the OE is severely disrupted (Leung et al., 2007; Packard et al., 2011; Herrick et al., 2017; Kocagöz et al., 2021). These studies also indicated that HBC activity is regulated by cell-cell contacts as well as paracrine signals between non-neuronal cells or between OSNs and HBCs, however, the molecular signaling network that is involved in HBC activation under injury conditions has not been fully elucidated.

Our research group has identified the heparin-binding epidermal growth factor-like growth factor (HB-EGF) as a novel regulatory signaling molecule that appears to control HBC activity in the zebrafish OE. Preliminary findings provide evidence that HB-EGF plays a critical role during the initiation of injury-induced OSN neurogenesis and tissue regeneration. HB-EGF is transiently and rapidly upregulated by 4 h after experimental lesion to the tissue but expression immediately declines to the control levels within the next few hours (Kocagöz et al., 2021). Transcriptome profiling of the zebrafish olfactory epithelium

performed revealed that HB-EGF expression is increased 15-fold at 4 hpl and that expression levels drops to 4- and 2.3-fold by 12 hpl and 24 hpl, respectively.

In this thesis, I could show that *hbegfa* expression is detected to be significantly stronger in the OE at 4 hpl compared to 8 hpl after a lesion, which is consistent with the transcriptome data (Figure 4. 3.) and also in accordance with previous studies conducted on the zebrafish retina (Wan et al., 2012). *In situ*-hybridization for *hbegfa* suggests that the injury-induced expression is abundant among basal cells in the OE at 4 hpi in 1% Triton X-100 treated fish, however, this observation can be perceptual since damage condition also leads to a severed disruption of tissue integrity, which in turn would change the position of *hbegfa*-expressing cells at the time of analysis. Therefore, milder chemical injury conditions, using a 10-fold lower Triton X-100 concentration allowed for a better tissue structure and resulted in a more reliable positional identification of *hbegfa*-positive cells under damage conditions. Nevertheless, exposure to dilute TrX solution also induces a rapid proliferation response while maintaining the tissue integrity. Under these conditions, a clear localization of *hbegfa* positive cells to the basal layers, both around the SNS and within the non-sensory region, could be observed. Although, the positional pattern of *hbegfa*-expressing cells could be detected, the overall identity of these *hbegfa*-positive cells remained unknown. Therefore, *in situ*-hybridization was combined with immunohistochemistry assays against cell type-specific markers for neurons, glia cells, and horizontal basal cells to further identify *hbegfa*-expressing cells under both physiological and non-physiological conditions.

My results of *in situ*-hybridization against *hbegfa* transcripts and immunostaining against the cell type specific markers tp63, HuC/D, and Sox2 showed that non-neuronal cells belonging to the Sox2-positive cell populations constitute the majority of *hbegfa*-expressing cells in the untreated OE. These non-neuronal cells include HBCs and SCs (Demirler et al., 2020). However, contrary to SCs, only tp63-positive HBCs along the basal layer in the ILC and sensory region show detectable levels of *hbegfa* expression. In addition, occasional HuC/D-positive neuronal cells were found to express *hbegfa* in more apical regions, including the apical border of the OE. These results provide evidence that eventually all cell types of OE express *hbegfa* under physiological conditions. Despite this observation, not all individual cells of any of these cell populations were positive for *hbegfa*-expression and *hbegfa*-positive cells were scattered around the tissue. The reason for the spotty expression

of *hbegfa* in occasional cells is not known. A reasonable assumption would be that naturally occurring microlesions induce *hbegfa* expression around the site of damage or cellular stress. However, other factors, such as the age of cells or their exposure to distinct signaling molecules that may stimulate *hbegfa* expression cannot be ruled out.

In TrX treated tissues, however, a distinctive induction of *hbegfa* expression was detected. Under damage condition, tp63-positive cells demonstrated horizontally elongated morphologies within the ILC but more spherical morphologies in the core sensory region and towards the SNS (Figure 4.18). It has been shown that HBCs change their morphology upon entering mitotic activity (Brann and Firestein, 2015; Demirler et al., 2021). Thus, the morphological change that was observed in the injured zebrafish OE may also reflect the activation of HBCs. Interestingly, *hbegfa*/tp63 double-positive cells, which were more numerous in the basal layer of the injured OE, also showed this morphological change. As before, *hbegfa*/HuC/D double-positive neurons were mostly detected in apical positions of the sensory region of the OE. Nevertheless, as in the intact tissue, the distribution of these cells lacked an organized pattern and additional cells only expressing *hbegfa* could also be observed (Figure 4.18). These findings revealed that all cell types of zebrafish OE upregulate *hbegfa* expression as an early damage response and the relative proportions of Sox2-positive, Huc/D-positive, and tp63-positive cells did not change between injury and intact conditions despite becoming overall more numerous.

The identity of the *hbegfa*-positive cells that did not stain with any of the markers remains unknown. Unfortunately, keratin 5 immunohistochemistry could not be performed because it was not compatible with the *in situ*-hybridization protocol despite the general good performance of antibody in regular staining. This may be presumably due to the proteinase K treatment during the *in situ*-hybridization, which is necessary for tissue permeabilization. In the intact tissue keratin 5 and tp63 are both expressed by HBCs in rodents (Herrick et al., 2015) and zebrafish (Kocagöz et al., 2021) but tp63 expression is downregulated in activated HBCs (Schnittcke et al., 2015). Thus, tp63 staining on the injured zebrafish OE may miss some activated HBCs, which could account for the unknown population of *hbegfa*-positive cells. Another complication was that SCs could not be identified with high confidence in the injured OE, even under mild damage conditions. While a fraction of SCs clearly expresses *hbegfa*, proportion of *hbegfa*-positive cells among the SC population could not be quantified. In the zebrafish retina, glia cells are the major

source of *hbegfa* expression following injury (Wan et al., 2012). Thus, it would be interesting to see whether this principle is also conserved in the zebrafish OE. Yet, additional SC markers that stain nuclear structures will be required for this analysis.

Nevertheless, a quantitative analysis was conducted to assess the average percentages of co-expression of *hbegfa* with the above-mentioned cell markers. The findings of this analysis showed that all major cell types, both neuronal and non-neuronal, are responsive to mild and strong tissue damage and are the potential source of HB-EGF release in the injured OE. An alternative explanation for the occurrence of cells that are *hbegfa*-positive but do not express any other cell type specific marker could be that these cells are in a transition state of the OSN cell lineage (Schwob et al., 2017; Wu and Yu, 2017).

GBCs that undergo neuronal commitment are characterized by the expression of proneural genes and neurogenic transcription factors such as *Ascl1* and *Neurod1* (Beites et al., 2005; Packard et al., 2011). In the zebrafish OE, neuronally committed GBC-like cells at the ILC and SNS are mitotically active and also express *ascl1a* as an early marker (Bayramlı et al., 2017). In this study, my results show that *ascl1a*-positive cells occupy predominantly the ILC and SNS regions which are the active proliferative regions in the OE. This result is in accordance with previous findings (Bayramlı et al., 2017). *Ascl1a* expressing Sox2-positive cells are found to form clusters at the SNS and individual cells are mostly observed at the ILC in intact OE. Following chemical tissue injury, however, *ascl1a*/Sox2 double-positive cells could be found within the sensory region in contrast to the strong spatial preference of these cell populations observed in intact tissue. Interestingly, my results also showed that some dormant HBCs that are tp63-positive also express *ascl1a* at the basal layer, although *ascl1a* expression is limited to transit-amplifying active basal cells in the literature (Schwob et al., 2017). These HBCs probably are in different stages of lineage progression rather than quiescent. Thus, *ascl1a* gene expression is activated before the loss of tp63 expression occurs. *Ascl1a*-expressing cells are induced upon chemical lesion and the number of newly generated *ascl1a* cells is increased in response to tissue injury. Most newly generated *ascl1a* cells were detected to be HuC/ D negative as expected since mature neurons are known to be devoid of *ascl1a* expression (Schwob et al., 2017; Bayramlı et al., 2017). As a conclusion of the analysis, the *ascl1a*-expressing fast cycling GBCs are generated in the sensory region in the injured zebrafish OE and similarity between the spatial distributions of *ascl1a* and *hbegf* expressing cells following injury propose the possible

involvement of HB-EGF in regenerative neurogenesis. On a larger scale, these results also indicate that the damage response in the zebrafish OE is mechanistically similar to the response of the rodent OE to tissue injury.

However, no direct conclusion could be drawn regarding the neurogenic role of HB-EGF from the experiments conducted so far. Future studies investigating *ascl1a* expression pattern upon HB-EGF intranasal administration to the OE in the absence of damage could be used to address this issue.

5.1. HB-EGF as a molecular signal in tissue regeneration

Heparin-binding epidermal growth factor-like growth factor is initially synthesized as a type I transmembrane protein that undergoes ectodomain shedding, which is stimulated by ADAMs and other matrix metalloproteinases (MMPs), ADAM 9, 10, 17 and MMP 3 and 7 in particular (Suzuki et al., 1997; Izumi et al., 1998; Asakura et al., 2002; Sunnarborg et al., 2002; Yan et al., 2002; Yu et al., 2002). The soluble form of HB-EGF harbors six cysteine residues, which are known as EGF-like domain and is thought to be necessary for EGF family members to bind and activate EGFR signaling pathway (Carpenter et al., 1991; Thomson et al., 1994). Through activation of EGFR signaling network, HB-EGF can stimulate the tissue repair and regeneration in a variety of tissues including liver, intestine, lung, kidney and brain (Dao et al., 2018). Several other studies have also demonstrated the stimulatory role of HB-EGF in retinal progenitors both in the avian and murine retina, as well as in the zebrafish retina following tissue injury. (Todd et al., 2005; Wan et al., 2012). In the human retina, HB-EGF expression has been shown in patients having proliferative vitreoretinopathy but not in normal controls (Hollborn et al., 2005).

Previous investigations in our lab have showed that HB-EGF is transiently and rapidly upregulated as early as 4hpl after experimental lesion to the olfactory tissue. The transcript levels declined to control levels within 24 hpl. This rapid and transient increase in gene expression in olfactory tissue can be explained by the activity of a positive-feedback loop during the regenerative response. Supportive evidence comes from studies demonstrating the action of HB-EGF in an autocrine manner in which HB-EGF promotes subsequent transcription of HB-EGF through binding and activating EGF receptor thereby establish positive-feedback loop. (Iwamoto et al., 2016). A similar auto-stimulatory loop has

been described in the zebrafish retina (Wan et al., 2012) and preliminary observations in the OE suggest that this principle is conserved (Şireci, unpublished).

Some systemically administered growth factors have been shown to trigger neurogenesis (Wagner et al., 1999). HB-EGF is found to be among these factors and HB-EGF has been demonstrated to have a crucial role in neurogenesis both in *in vivo* and *in vitro* studies (Jin et al., 2003; Cantarella et al., 2008). Previous studies conducted in our laboratory also showed an increased cellular proliferation upon intranasal administration of recombinant HB-EGF and OSN neurogenesis in the sensory region of OE (Kocagöz et al., 2021), showing evidence regarding the stimulatory role of HB-EGF in the zebrafish OE.

The formation of HB-EGF and its extracellular release as a signaling molecule are directly affected by the molecular changes in extracellular matrix, particularly by the levels of metalloproteases under non-physiological conditions. Coherently, regulation of metalloprotease activity by inhibitors suppresses the regenerative proliferation significantly (Kocagöz et al., 2021; Şireci, unpublished). Results of the previous studies reveal that HB-EGF is potent to initiate cellular proliferation and its metalloprotease-mediated activity is involved in the OE regeneration following extensive injury. The reduced proliferative activity upon the use of metalloprotease inhibitors in the injured OE (Kocagöz et al., 2021) suggests the necessity of proHB-EGF cleavage and its subsequent paracrine activity for the regenerative response.

5.2. EGFR expression in the zebrafish olfactory system

HB-EGF is originally formed as a single-pass transmembrane protein, proHB-EGF, that is activated by ectodomain shedding through matrix-metalloproteases of a disintegrin and metalloprotease (ADAM) family (Singh and Harris, 2005; Taylor et al., 2014). The soluble active form of the HB-EGF ectodomain activates tyrosine kinase membrane receptors constituted by ErbB1 homodimer (also known as EGFR) or ErbB1/ErbB4 heterodimer complexes (Abud et al., 2021). The OE regeneration through EGFR signaling has been demonstrated in the mouse OE (Chen et al., 2020). The neural- glial cell adhesion molecule (NRCAM), which is not a member of EGF superfamily, has been shown to involved in the process (Chen et al., 2020).

At the intracellular level, network of signaling pathways namely, mitogen-activated protein kinase, MAPK/ ERK, Notch, the Janus kinase/signal transducer and activator of transcription, JAK/ STAT and the phosphatidylinositol 3-kinase/Akt, PI3K have been shown to stimulate cell survival and proliferation (Singh and Harris, 2005; Wee and wang, 2017; Chen et al., 2020; Abud et al., 2021). Downstream signaling network of the activated EGF receptor through the binding of HB-EGF activates the above-mentioned signaling pathways, however the fine-tuning of the response may be more complex (Wan et al., 2014; Wee and Wang, 2017). Another study of HB-EGF also demonstrated that HB-EGF predominantly activate EGFR- MAPK- signaling (Lemmon and Schlesinger, 2010; Schneider and Wolf, 2009). Wan and his colleagues have shown that HB-EGF treated Müller glia reenter the cell cycle and grow into all cell types of retinal tissue (Wan et al., 2012). Another study also concluded that EGF-treated mouse retina results in the stimulation of MG proliferation under damaged conditions (Karl et al., 2008). These studies show differential response of normal and damaged mouse retina which could be due to the injury-induced activation of the EGFR (Close et al., 2006) through downstream signaling networks.

The paracrine (or autocrine) stimulation of cellular proliferation by HB-EGF acts through EGFR signaling. In rodent models, EGFR expression has been observed characteristically in HBCs (Holbrook et al., 1995; Chen et al., 2020) however, to date, its functional importance has not been investigated comprehensively. Thus, it was necessary to show whether EGFR is also specifically expressed by HBC-like cells in the zebrafish OE. In this context, according to results of this study, expression analysis of the *egfra* gene by the use of specifically designed *egfra* riboprobe in *in situ*-hybridization experiments demonstrated that a high number of tp63-positive HBCs at the basal layers of OE and some OSNs express the ErbB1/EGFRA receptor at the apical layers of the tissue. These cell populations may be responsive to HB-EGF in the zebrafish OE under physiological conditions. The region-specific expression profile of *egfra* in the absence of damage would be explained by the basal levels of *hbegfa* expression that is also detected on these quiescent progenitors However, additional *in situ*-hybridization experiments combined with cell type specific markers should be performed under damage conditions to further identify and characterize the HB-EGF-responsive cell populations. The observations are parallel with the literature, which reveals specific EGFR expression on the surface of the HBCs in rodents (Duan et al., 2018; Holbrook et al., 1995; Krishna et al., 1996; Chen et al., 2020). In addition

to the identification of receptor- expressing cells by ISH and IHC assays, analysis of the activation of HBC-like cells upon HB-EGF administration by the use of anti-Krt5 and anti-BrdU immunostaining assays would allow us to characterize the specific stimulatory effect of HB-EGF on this particular dormant cell population. The observation of an apical rim of *egfra*-positive cells may also explain the potential of nasally administered HB-EGF to stimulate HBC proliferation (Kocagöz et al., 2021). In this scenario, apical cells stimulated by HB-EGF would upregulate HB-EGF expression, which in turn activates *egfra*-expressing HBCs.

Investigating HB-EGF-induced downstream pathways in the OE is a challenging task, since EGFR activates a large number of diverse signaling pathways mentioned above. As these pathways are highly intermingled, activation of EGFR acts on an entire molecular network that control various physiological tasks, such as cell growth, proliferation, and differentiation. Because components within EGFR-mediated signaling pathways have been important target molecules of pharmacological cancer research, the effects of different downstream pathways on the OE regeneration can be easily examined by the use of various specific inhibitors. Preliminary studies from our group reveals that pharmacological inhibition of either of the three downstream pathways, JAK-STAT, PI3K/AKT, and ERK-MAPK pathways, by the use of specific inhibitors, prevents HBC activation and therefore disrupts OE regeneration and results in similar tissue phenotypes observed after metalloprotease inhibition by Marimastad molecule (Alkiraz and Dokuzluoğlu, unpublished data; Kocagöz et al., 2021). Detailed analysis of these pharmacological manipulations and their effects on the tissue would reveal the importance of HB-EGF-mediated pathways in the OE regeneration.

Additional studies, using loss-of-function strategies, such as disruption of signaling activity by cell-specific HB-EGF or EGFR knockout lines may allow to clarify the functional significance of the early rapid *hbegfa* expression and distinguish cellular subsets contributing to the late proliferation response.

5.3. Relationship between EGF signaling and other signaling pathways in the context of regeneration

Understanding the molecular regulations of the stem/progenitor cell activity is necessary to have better insights regarding the mechanisms of neurogenesis and their innate potential for nervous system repair. Activation of stem/progenitor cells in the nervous system has been shown to be regulated by several signaling cascades, such as Notch and Wnt/ β -catenin (Kizil et al. 2012; Herrick et al., 2017). Moreover, Wang et al identified a HB-EGF/ MAPK/ *Ascl1a* / Notch / *hb-egfa* signaling loop in which Notch inhibition resulted in HB-EGF production in the damaged retina of zebrafish (Wan et al., 2012). This signaling loop has been shown to maintain steady level of HB-EGF leading to sufficient number of Müller glia recruitment to the injury site and regenerates the retina (Wan et al., 2012).

ErbB transactivation has been shown to involve Wnt signals, which bind to frizzled (Fz) receptors of the Wnt pathway and stimulates EGFR tyrosine kinase activity through metalloproteinase-mediated cleavage of EGF-like ligands (Civenni et al., 2003). In addition, another study revealed that EGFR signaling can promote the Wnt/ β -catenin signaling through the stabilization and subsequent nuclear accumulation of β -catenin, which depends on several EGFR-regulated mediators including ERK and MAPK (Krejci et al., 2012). Previous studies performed by the former lab member, S.Eski proposed that the canonical Wnt/ β -catenin signaling pathway may have a critical role in the regulation or in triggering the stem/progenitor cell activity during neurogenesis in the zebrafish OE (Eski, 2019). Wnt/ β -catenin signaling also appears to be critical and is both necessary and sufficient for HBC activation (Eski, thesis, 2019). Thus, HB-EGF/EGFR signaling in the fish OE may also converge on this conserved pathway to promote mitotic activity in HBCs.

In addition, it was found that sonic hedgehog (SHH) signaling pathway activation in neural stem cells and in HeLa cells resulted in EGFR transactivation together with the transient activation of the MAPK/ERK signaling cascade in NCS cell proliferation (Reinchisi et al., 2013). Concomitantly, the detailed investigation regarding the crosstalk between EGFR signaling and other signaling pathways, such as Notch, Wnt and SHH, is required to improve our understanding in the context of tissue regeneration. Future research is required to show the possible involvement and necessity of these pathways in the cellular

proliferation in OE neurogenesis. The use of ligand specific inhibitors or receptor specific inhibitors under physiological conditions would shed light on this issue.

REFERENCES

- Abud, H. E., Chan, W. H., & Jardé, T. (2021). Source and Impact of the EGF Family of Ligands on Intestinal Stem Cells. *Frontiers in cell and developmental biology*, *9*, 685665.
- Aguirre, A., Dupree, J. L., Mangin, J. M., & Gallo, V. (2007). A functional Role for EGFR Signaling in Myelination and Remyelination. *Nature Neuroscience*, *10*(8), 990–1002.
- Ahuja G, Bozorg Nia S, Zapilko V, Shiriagin V, Kowatschew D, Oka Y, Korsching SI. (2014) Kappe Neurons, a Novel Population of Olfactory Sensory Neurons. *Sci Rep* 4:4037.
- Altman, J. (1969). Autoradiographic and Histological Studies of Postnatal Neurogenesis. IV. Cell Proliferation and Migration in the Anterior Forebrain, with Special Reference to Persisting Neurogenesis in the Olfactory Bulb. *The Journal of Comparative Neurology*, *137*(4), 433–457.
- Altman, J., & Das, G. D. (1965). Autoradiographic and Histological Evidence of Postnatal Hippocampal Neurogenesis in Rats. *The Journal of Comparative Neurology*, *124*(3), 319–335.
- Alunni, A., & Bally-Cuif, L. (2016). A Comparative View of Regenerative Neurogenesis in Vertebrates. *Development (Cambridge, England)*, *143*(5), 741–753.
- Anderson, R. M., Bosch, J. A., Goll, M. G., Hesselton, D., Dong, P. D., Shin, D., Chi, N. C., Shin, C. H., Schlegel, A., Halpern, M., & Stainier, D. Y. (2009). Loss of Dnmt1 Catalytic Activity Reveals Multiple Roles for DNA Methylation During Pancreas Development and Regeneration. *Developmental biology*, *334*(1), 213–223.
- Andersson, O., Adams, B. A., Yoo, D., Ellis, G. C., Gut, P., Anderson, R. M., German, M. S., & Stainier, D. Y. (2012). Adenosine Signaling Promotes Regeneration of Pancreatic β Cells *in vivo*. *Cell Metabolism*, *15*(6), 885–894.

- Asakura M, Kitakaze M, Takashima S, Liao Y, Ishikura F, Yoshinaka T, et al. Cardiac Hypertrophy is Inhibited by Antagonism of ADAM12 Processing of HB-EGF; Metalloproteinase Inhibitors as a New Therapy. *Nat Med* 2002;8:35–40.
- Bali, B. (2015). *The Role of Sustentacular Cells in Adult Neurogenesis*. Boğaziçi University.
- Bayramlı, X., Kocagöz, Y., Sakizli, U., & Fuss, S. H. (2017). Patterned Arrangements of Olfactory Receptor Gene Expression in Zebrafish are Established by Radial Movement of Specified Olfactory Sensory Neurons. *Scientific Reports*, 7(1), 5572.
- Bayramlı, K. (2016). *Neurogenesis and Migration of Specified Chemosensory Neurons in the Adult Zebrafish Olfactory Epithelium*. Boğaziçi University.
- Becker, C. G. and Becker, T. (2008). Adult Zebrafish as a Model for Successful Central Nervous System Regeneration. *Restor. Neurol. Neurosci.* 26, 71-80.
- Beites C. L., Kawauchi S., Crocker C. E., Calof A. L. (2005). Identification and Molecular Regulation of Neural Stem Cells in the Olfactory Epithelium. *Exp. Cell Res.* 306, 309-316.
- Boldrini, M., Fulmore, C. A., Tartt, A. N., Simeon, L. R., Pavlova, I., Poposka, V., Mann, J. J. (2018). Human Hippocampal Neurogenesis Persists throughout Aging. *Cell Stem Cell*, 22(4), 589–599.e5.
- Brignull, H. R., Raible, D. W., & Stone, J. S. (2009). Feathers and Fins: Non-mammalian Models for Hair Cell Regeneration. *Brain Research*, 1277, 12–23.
- Calvo-Ochoa, E., & Byrd-Jacobs, C. A. (2019). The Olfactory System of Zebrafish as a Model for the Study of Neurotoxicity and Injury: Implications for Neuroplasticity and Disease. *International Journal of Molecular Sciences*, 20(7), 1639.
- Calvo-Ochoa E, Byrd-Jacobs CA, Fuss SH. Diving into the Streams and Waves of Constitutive and Regenerative Olfactory Neurogenesis: Insights from Zebrafish. *Cell Tissue Res.* 2021 Jan; 383(1): 227-253.

- Cantarella, C., Cayre, M., Magalon, K., & Pascale, D. (2008). Intranasal HB-EGF Administration Favors Adult SVZ Cell Mobilization to Demyelinated Lesions in Mouse Corpus Callosum. *Developmental Neurobiology*, *68*(2), 223–236.
- Çapar, S. (2015). *Olfactory Neurogenesis Following Acute Injury*. Boğaziçi University.
- Carpentier, P. A., & Palmer, T. D. (2009). Immune Influence on Adult Neural Stem Cell Regulation and Function. *Neuron*, *64*(1), 79–92.
- Carter, L. A., MacDonald, J. L., & Roskams, A. J. (2004). Olfactory Horizontal Basal Cells Demonstrate a Conserved Multipotent Progenitor Phenotype. *The Journal of Neuroscience: The Official Journal of the Society for Neuroscience*, *24*(25), 5670–5683.
- Carpenter G. (1999). Employment of the Epidermal Growth Factor Receptor in Growth Factor-independent Signaling Pathways. *The Journal of Cell Biology*, *146*(4), 697–702.
- Cau, E., Gradwohl, G., Fode, C., & Guillemot, F. (1997). Mash1 Activates a Cascade of bHLH Regulators in Olfactory Neuron Progenitors. *Development*, *124*(8).
- Celik A, Fuss SH, Korsching SI. Selective Targeting of Zebrafish Olfactory Receptor Neurons by the Endogenous OMP Promoter. *Eur J Neurosci*. 2002 Mar; *15*(5):798-806.
- Chapouton, P., Skupien, P., Hesl, B., Coolen, M., Moore, J. C., Madelaine, R., ... Bally-Cuif, L. (2010). Notch Activity Levels Control the Balance Between Quiescence and Recruitment of Adult Neural Stem Cells. *The Journal of Neuroscience: The Official Journal of the Society for Neuroscience*, *30*(23), 7961–7974.
- Chen, M., Tian, S., Yang, X., Lane, A. P., Reed, R. R., & Liu, H. (2014). Wnt-Responsive Lgr5+ Globose Basal Cells Function as Multipotent Olfactory Epithelium Progenitor Cells. *Journal of Neuroscience*, *34*(24), 8268–8276.

- Chen, X., Fang, H., & Schwob, J. E. (2004). Multipotency of Purified, Transplanted Globose Basal Cells in Olfactory Epithelium. *The Journal of Comparative Neurology*, 469(4), 457–474.
- Chen, Z. H., Luo, X. C., Yu, C. R., & Huang, L. (2020). Matrix Metalloprotease-mediated Cleavage of Neural Glial-related Cell Adhesion Molecules Activates Quiescent Olfactory Stem Cells via EGFR. *Molecular and Cellular Neurosciences*, 108, 103552.
- Chojnacki, A., & Weiss, S. (2008). Production of Neurons, Astrocytes and Oligodendrocytes from Mammalian CNS Stem Cells. *Nature Protocols*, 3(6), 935–940.
- Civenni G, Holbro T, Hynes NE. Wnt1 and Wnt5a Induce Cyclin D1 Expression Through ErbB1 Transactivation in HC11 Mammary Epithelial Cells. *EMBO Rep*. 2003; 4:166–171.
- Close, J.L., Gumuscu, J. Liu, B, T. A. Reh Epidermal Growth Factor Receptor Expression Regulates Proliferation in the Postnatal Rat Retina Glia, 54 (2006), pp. 94-104. *The Journal of Neuroscience: The Official Journal of the Society for Neuroscience*, 28(2), 434–446.
- Costanzo, R. M. (1985). Neural Regeneration and Functional Reconnection Following Olfactory Nerve Transection in Hamster. *Brain Research*, 361(1–2), 258–266.
- Curado, S., & Stainier, D. Y. (2010). DeLiver'in Regeneration: Injury Response and Development. *Seminars in Liver Disease*, 30(3), 288–295.
- Currais A., Hortobagyi T., Soriano S. (2009). The Neuronal Cell Cycle as a Mechanism of Pathogenesis in Alzheimer's Disease. *Aging (Albany NY)* 1, 363–371.
- Dai, Q., Duan, C., Ren, W., Li, F., Zheng, Q., Wang, L., Li, W., Lu, X., Ni, W., Zhang, Y., Chen, Y., Wen, T., Yu, Y., & Yu, H. (2018). Notch Signaling Regulates Lgr5⁺ Olfactory Epithelium Progenitor/Stem Cell Turnover and Mediates Recovery of Lesioned Olfactory Epithelium in Mouse Model. *Stem Cells (Dayton, Ohio)*, 36(8), 1259–1272.

- Dangles, O., Irschick, D., Chittka, L., & Casas, J. (2009). Variability in Sensory Ecology: Expanding the Bridge Between Physiology and Evolutionary Biology. *The Quarterly Review of Biology*, 84(1), 51–74.
- Das, S., & Basu, A. (2008). Inflammation: A New Candidate in Modulating Adult Neurogenesis. *Journal of Neuroscience Research*, 86(6), 1199–1208.
- Dao, D. T., Anez-Bustillos, L., Adam, R. M., Puder, M., & Bielenberg, D. R. (2018). Heparin-Binding Epidermal Growth Factor-Like Growth Factor as a Critical Mediator of Tissue Repair and Regeneration. *The American Journal of Pathology*, 188(11), 2446–2456.
- Demirler, M. C., U. Sakizli, B. Bali, Y. Kocagöz, S. E. Eski, A. Ergönen, A. S. Alkiraz, X. Bayramli, T. Hassenklöver, I. Manzini and S. H. Fuss, “Purinergic Signaling Selectively Modulates Maintenance but Not Repair Neurogenesis in the Zebrafish Olfactory Epithelium”, *FEBS Journal*, Vol. 287, No. 13, pp. 2699– 2722, 2020.
- Diep, C. Q., Ma, D., Deo, R. C., Holm, T. M., Naylor, R. W., Arora, N., Wingert, R. A., Bollig, F., Djordjevic, G., Lichman, B., Zhu, H., Ikenaga, T., Ono, F., Englert, C., Cowan, C. A., Hukriede, N. A., Handin, R. I., & Davidson, A. J. (2011). Identification of Adult Nephron Progenitors Capable of Kidney Regeneration in Zebrafish. *Nature*, 470(7332), 95–100.
- Dooley, K., & Zon, L. I. (2000). Zebrafish: A Model System for the Study of Human Disease. *Current Opinion in Genetics & Development*, 10(3), 252–256.
- Dorseman, A. C., Soulé, S., Weger, M., Bourdon, E., Lefebvre d'Hellencourt, C., Meilhac, O., & Diotel, N. (2017). Impaired Constitutive and Regenerative Neurogenesis in Adult Hyperglycemic Zebrafish. *The Journal of Comparative Neurology*, 525(3), 442–458.

- Edlund, J. A., Chaumont, N., Hintze, A., Koch, C., Tononi, G., & Adami, C. (2011). Integrated Information Increases with Fitness in the Evolution of Animals. *PLoS Computational Biology*, 7(10).
- Eierhoff, T., Hrincius, E. R., Rescher, U., Ludwig, S., & Ehrhardt, C. (2010). The Epidermal Growth Factor Receptor (EGFR) Promotes Uptake of Influenza A Viruses (IAV) Into Host Cells. *PLoS Pathogens*, 6(9), e1001099.
- Eriksson, P. S., Perfilieva, E., Björk-Eriksson, T., Alborn, A.-M., Nordborg, C., Peterson, D. A., & Gage, F. H. (1998). Neurogenesis in the Adult Human Hippocampus. *Nature Medicine*, 4(11), 1313–1317.
- Engeszer, R.E., Barbiano, L.A., Ryan, M.J., and Parichy, D.M. (2007) Timing and Plasticity of Shoaling Behaviour in the Zebrafish, *Danio rerio*. *Animal Behaviour*. 74(5):1269-1275.
- Eski, S., E., *The role of Wnt Signaling During Regenerative Neurogenesis in the Zebrafish Olfactory Epithelium*, 2019, Boğaziçi University.
- Fang, Y., Vilella-Bach, M., Bachmann, R., Flanigan, A., & Chen, J. (2001). Phosphatidic Acid-mediated Mitogenic Activation of mTOR Signaling. *Science (New York, N.Y.)*, 294(5548), 1942–1945.
- Feng J., El-Assal O.N., Besner G.E. Heparin-binding EGF-like Growth Factor (HB-EGF) and Necrotizing Enterocolitis. *Semin Pediatr Surg*. 2005; 14:167–174.
- Fleisch, C, Valerie.; Fraser, Brittany; Allison w., Ted (2010). Investigating Regeneration and Functional Interaction of CNS Neurons: Lessons from Zebrafish Genetics and Other Fish Species., 1812(3), 0–380.
- Gage F. H. (2000). Mammalian Neural Stem Cells. *Science (New York, N.Y.)*, 287(5457), 1433–1438.

- Gage H., Fred, Temple, Sally, Neural Stem Cells: Generating and Regenerating the Brain, Neuron, Volume 80, Issue 3, 2013, Pages 588-601, ISSN 0896-6273.
- Ganz, J., Kaslin, J., Hochmann, S., Freudenreich, D., & Brand, M. (2010). Heterogeneity and Fgf Dependence of Adult Neural Progenitors in the Zebrafish Telencephalon. *Glia*, 58(11), n/a-n/a.
- Gauthier-Fisher, A., Lin, D. C., Greeve, M., Kaplan, D. R., Rottapel, R., & Miller, F. D. (2009). Lfc and Tctex-1 Regulate the Genesis of Neurons from Cortical Precursor cells. *Nature Neuroscience*, 12(6), 735–744.
- Streisinger, G. et al. (1981) Production of Clones of Homozygous Diploid Zebrafish (*Brachy danio rerio*). *Nature* 291, 293–296.
- Gemberling, M., Bailey, T. J., Hyde, D. R., & Poss, K. D. (2013). The Zebrafish as a Model for Complex Tissue Regeneration. *Trends in Genetics: TIG*, 29(11), 611–620.
- Goldman, S. A., & Nottebohm, F. (1983). Neuronal Production, Migration, and Differentiation in a Vocal Control Nucleus of the Adult Female Canary Brain. *Proceedings of the National Academy of Sciences of the United States of America*, 80(8), 2390–2394.
- Goldman, S. (2005). Stem and Progenitor Cell-based Therapy of the Human Central Nervous System. *Nature Biotechnology*, 23(7), 862–871.
- Goldman D. Muller Glial Cell Reprogramming and Retina Regeneration. *Nature Reviews Neuroscience*. 2014; 15:431–42.
- Goldshmit, Y., Sztal, T. E., Jusuf, P. R., Hall, T. E., Nguyen-Chi, M., & Currie, P. D. (2012). Fgf-dependent Glial Cell Bridges Facilitate Spinal Cord Regeneration in Zebrafish. *The Journal of Neuroscience: The Official Journal of the Society for Neuroscience*, 32(22), 7477–7492.
- Ghosh, S., & Hui, S. P. (2016). Regeneration of Zebrafish CNS: Adult Neurogenesis. *Neural Plasticity*, 2016, 5815439.

- Gorsuch RA, Hyde DR. Regulation of Muller Glial Dependent Neuronal Regeneration in the Damaged Adult Zebrafish Retina. *Exp Eye Res.* 2014; 123:131–40.
- Gould, E., Reeves, A. J., Fallah, M., Tanapat, P., Gross, C. G., & Fuchs, E. (1999). Hippocampal Neurogenesis in Adult Old World Primates. *Proceedings of the National Academy of Sciences of the United States of America*, 96(9), 5263–5267.
- Grandel, H., Kaslin, J., Ganz, J., Wenzel, I., & Brand, M. (2006). Neural Stem Cells and Neurogenesis in the Adult Zebrafish Brain: Origin, Proliferation Dynamics, Migration and Cell Fate. *Developmental Biology*, 295(1), 263–277.
- Green PA, Van Valkenburgh B, Pang B, Bird D, Rowe T, Curtis A (2012) Respiratory and Olfactory Turbinal Size in Canid and Arctoid Carnivorans. *J Anat* 221:609–621.
- Gritti, A., Parati, E. A., Cova, L., Frolichsthal, P., Galli, R., Wanke, E., Faravelli, L., Morassutti, D. J., Roisen, F., Nickel, D. D., & Vescovi, A. L. (1996). Multipotential Stem Cells from the Adult Mouse Brain Proliferate and Self-renew in Response to Basic Fibroblast Growth Factor. *The Journal of Neuroscience: the Official Journal of the Society for Neuroscience*, 16(3), 1091–1100.
- Guo, Z., Packard, A., Krolewski, R. C., Harris, M. T., Manglapus, G. L., & Schwob, J. E. (2010). Expression of Pax6 and Sox2 in Adult Olfactory Epithelium. *The Journal of Comparative Neurology*, 518(21), 4395–4418.
- Gurtner, G., Werner, S., Barrandon, Y. et al. Wound repair and regeneration. *Nature* 453, 314 – 321 (2008).
- Hans, S., Kaslin, J., Freudenreich, D., and Brand, M. (2009) Temporally Controlled Site-Specific Recombination in Zebrafish. *PLoS One*. 4(2): e4640.
- Hansen, A., & Zeiske, E. (1993). Development of the Olfactory Organ in the Zebrafish, *Brachy Danio rerio*. *The Journal of Comparative Neurology*, 333(2), 289–300.
- Hansen, A.; Zeiske, E. (1998). *The Peripheral Olfactory Organ of the Zebrafish, Danio rerio: an Ultrastructural Study. Chemical Senses*, 23(1), 39–48.

- Hansen, A., Rolen, S. H., Anderson, K., Morita, Y., Caprio, J., & Finger, T. E. (2003). Correlation Between Olfactory Receptor Cell Type and Function in the Channel Catfish. *The Journal of Neuroscience: The Official Journal of the Society for Neuroscience*, 23(28), 9328–9339.
- Hernandez, P. A., Graham, C. H., Master, L. L., & Albert, D. L. (2006). The Effect of Sample Size and Species Characteristics on Performance of Different Species Distribution Modeling Methods. *Ecography*, 29(5), 773–785.
- Herrick, D. B., Guo, Z., Jang, W., Schnittke, N., & Schwob, J. E. (2018). Canonical Notch Signaling Directs the Fate of Differentiating Neurocompetent Progenitors in the Mammalian Olfactory Epithelium. *The Journal of Neuroscience: The Official Journal of the Society for Neuroscience*, 38(21), 5022–5037.
- Herrick, D. B., Lin, B., Peterson, J., Schnittke, N., & Schwob, J. E. (2017). Notch1 Maintains Dormancy of Olfactory Horizontal Basal Cells, a Reserve Neural Stem Cell. *Proceedings of the National Academy of Sciences of The United States of America*, 114(28), E5589–E5598.
- Holbrook EH, Iwema CL, Peluso CE, Schwob JE. The Regeneration of P2 Olfactory Sensory Neurons is Selectively Impaired Following Methylbromide Lesion. *Chem Senses*. 2014; 39:601–616.
- Hollborn M, Tenckhoff S, Jahn K, Iandiev I, Biedermann B, Schnurrbusch UE, Limb GA, Reichenbach A, Wolf S, Wiedemann P, et al. Changes in Retinal Gene Expression in Proliferative Vitreoretinopathy: Glial Cell Expression of HB-EGF. *Mol Vis*. 2005; 11:397–413.
- Hynes, N.E., Lane H.A. ERBB Receptors and Cancer: The Complexity of Targeted Inhibitors *Nat. Rev. Cancer*, 5 (2005), pp. 341-354.
- Ihunwo, A. O., Tembo, L. H., & Dzamalala, C. (2016). The Dynamics of Adult Neurogenesis in Human Hippocampus. *Neural Regeneration Research*, 11(12), 1869–1883.

- Inoue, H., Sakaue, T., Ozawa, T., & Higashiyama, S. (2013). Spatiotemporal Visualization of proHB-EGF Ectodomain Shedding in Living Cells. *Journal of Biochemistry*, *154*(1), 67–76.
- Iqbal, T., & Byrd-Jacobs, C. (2010). Rapid Degeneration and Regeneration of the Zebrafish Olfactory Epithelium after Triton X-100 Application. *Chemical Senses*, *35*(5), 351–361.
- Iwamoto, R. and E. Mekada, HB-EGF (Heparin-Binding EGF-like Growth Factor), Springer, New York, NY, New York, NY., 2016.
- Izumi Y, Hirata M, Hasuwa H, Iwamoto R, Umata T, Miyado K, et al. A Metalloprotease-Disintegrin, MDC9/meltrin-gamma/ADAM9 and PKCdelta are Involved in TPA-induced Ectodomain Shedding of Membrane-anchored Heparin-binding EGF-like Growth Factor. *EMBO J* 1998; *17*:7260–72.
- Jin, K., X. O. Mao, Y. Sun, L. Xie, L. Jin, E. Nishi, M. Klagsbrun and D. A. Greenberg, “Heparin-Binding Epidermal Growth Factor-Like Growth Factor: Hypoxia-Inducible Expression in Vitro and Stimulation of Neurogenesis *in vitro* and *in vivo*.”, *The Journal of Neuroscience: The Official Journal of the Society for Neuroscience*, Vol. 22, No. 13, pp. 5365–5373, jul 2002.
- Jin, K., Sun, Y., Xie, L., Peel, A., Mao, X. O., Bateur, S., & Greenberg, D. A. (2003). Directed Migration of Neuronal Precursors into the Ischemic Cerebral Cortex and Striatum. *Molecular and Cellular Neuroscience*, *24*(1), 171–189.
- Johansson, B. B. (2007). Regeneration and Plasticity in the Brain and Spinal cord. *Journal of Cerebral Blood Flow & Metabolism*, *27*, 1417–1430.
- Johnson, S. L., & Weston, J. A. (1995). Temperature-sensitive Mutations that Cause Stage-Specific Defects in Zebrafish Fin Regeneration. *Genetics*, *141*(4), 1583–1595.

- Kan, N.G., Junghans, D., and Izpisua Belmonte, J.C. (2009) Compensatory Growth Mechanisms Regulated by BMP and FGF Signaling Mediate Liver Regeneration in Zebrafish After Partial Hepatectomy. *FASEB journal: Official Publication of the Federation of American Societies for Experimental Biology*. 23(10):3516-3525.
- Kaplan, M. S., & Hinds, J. W. (1977). Neurogenesis in the Adult Rat: Electron Microscopic Analysis of Light Radioautographs. *Science (New York, N.Y.)*, 197(4308), 1092–1094.
- Karl MO, Hayes S, Nelson BR, Tan K, Buckingham B, Reh TA. Stimulation of Neural Regeneration in the Mouse Retina. *Proc Natl Acad Sci U S A*. 2008; 105:19508–19513.
- Kaslin, J., Ganz, J., & Brand, M. (2008). Proliferation, Neurogenesis and Regeneration in The Non-mammalian Vertebrate Brain. *Philosophical Transactions of the Royal Society of London. Series B, Biological Sciences*, 363(1489), 101–122.
- Kawahara, N., K. Mishima, S. Higashiyama, N. Taniguchi, A. Tamura and T. Kirino, “The Gene for Heparin-Binding Epidermal Growth Factor-Like Growth Factor is Stress-Inducible: Its Role in Cerebral Ischemia”, *Journal of Cerebral Blood Flow and Metabolism*, Vol. 19, No. 3, pp. 307–320, 1999.
- Kellogg, D. E., Rybalkin, I., Chen, S., Mukhamedova, N., Vlasik, T., Siebert, P. D., & Chenchik, A. (1994). TaqStart Antibody: "hot start" PCR Facilitated by a Neutralizing Monoclonal Antibody Directed Against Taq DNA Polymerase. *BioTechniques*, 16(6), 1134–1137.
- Kibbe WA. 'OligoCalc: an Online Oligonucleotide Properties Calculator'. (2007) *Nucleic Acids Res*. 35: May 25.
- Kim, C.-H., Ueshima, E., Muraoka, O., Tanaka, H., Yeo, S.-Y., Huh, T.-L., & Miki, N. (1996). Zebrafish *elav/HuC* Homologue as a very Early Neuronal Marker. *Neuroscience Letters*, 216(2), 109–112.

- Kim, E. J., Ables, J. L., Dickel, L. K., Eisch, A. J., & Johnson, J. E. (2011). *Ascl1* (*Mash1*) Defines Cells with Long-term Neurogenic Potential in Subgranular and Subventricular Zones in Adult Mouse Brain. *PLoS One*, 6(3), e18472.
- Kirsche, W., & Kirsche, K. (1961). Experimentelle Untersuchungen zur Frage der Regeneration und Funktion des Tectum Opticum von *Carassius Carassius* L. *Zeitschrift Fuer Mikroskopisch-Anatomische Forschung*, (67), 140–182.
- Kizil, C., & Brand, M. (2011). Cerebroventricular Microinjection (CVMI) into Adult Zebrafish Brain is an Efficient Misexpression Method for Forebrain Ventricular Cells. *PLoS One*, 6(11), e27395.
- Kizil, C., Kaslin, J., Kroehne, V., & Brand, M. (2012). Adult Neurogenesis and Brain Regeneration in Zebrafish. *Developmental Neurobiology*, 72(3), 429–461.
- Knobloch, M., & Jessberger, S. (2017). Metabolism and Neurogenesis. *Current Opinion in Neurobiology*, 42, 45–52.
- Krejci, P., Aklian, A., Kaucka, M., Sevcikova, E., Prochazkova, J., Masek, J. K., Mikolka, P., Pospisilova, T., Spoustova, T., Weis, M., Paznekas, W. A., Wolf, J. H., Gutkind, J. S., Wilcox, W. R., Kozubik, A., Jabs, E. W., Bryja, V., Salazar, L., Vesela, I., & Balek, L. (2012). Receptor Tyrosine Kinases Activate Canonical WNT/ β -catenin Signaling via MAP kinase/LRP6 Pathway and Direct β -catenin Phosphorylation. *PLoS One*, 7(4), e35826.
- Kroehne, V., Freudenreich, D., Hans, S., Kaslin, J., & Brand, M. (2011). Regeneration of The Adult Zebrafish Brain from Neurogenic Radial Glia-type Progenitors. *Development (Cambridge, England)*, 138(22), 4831–4841.
- Krolewski, R. C., Packard, A., Jang, W., Wildner, H., & Schwob, J. E. (2012). *Ascl1* (*Mash1*). Knockout Perturbs Differentiation of Nonneuronal Cells in Olfactory Epithelium. *PLoS One*, 7(12), e51737.
- Kuhn, H. G., Dickinson-Anson, H., & Gage, F. H. (1996). Neurogenesis in the Dentate Gyrus of the Adult Rat: Age-related Decrease of Neuronal Progenitor Proliferation.

The Journal of Neuroscience: The Official Journal of the Society for Neuroscience, 16(6), 2027–2033.

Lemmon, M.A., Schlessinger, J., 2010. Cell Signaling by Receptor Tyrosine Kinases. *Cell* 141 (7), 1117–1134.

Lentz, T. L. and Erulkar, Solomon D. (2020, November 10). *Nervous System. Encyclopedia Britannica*.

Leung, C. T., Coulombe, P. A., & Reed, R. R. (2007). Contribution of Olfactory Neural Stem Cells to Tissue Maintenance and Regeneration. *Nature Neuroscience*, 10(6), 720–726.

Libert, S., Zwiener, J., Chu, X., Vanvoorhies, W., Roman, G., & Pletcher, S. D. (2007). Regulation of Drosophila Life Span by Olfaction and Food-derived Odors. *Science (New York, N.Y.)*, 315(5815), 1133–1137.

López-Schier, H., & Hudspeth, A. J. (2006). A Two-step Mechanism Underlies the Planar Polarization of Regenerating Sensory Hair Cells. *Proceedings of the National Academy of Sciences of the United States of America*, 103(49), 18615–18620.

Ma, D. K., Bonaguidi, M. A., Ming, G. L., & Song, H. (2009). Adult Neural Stem Cells in the Mammalian Central Nervous System. *Cell Research*, 19(6), 672–682.

Mackay-Sim, A., & Kittel, P. W. (1991). On the Life Span of Olfactory Receptor Neurons. *European Journal of Neuroscience*, 3(3), 209–215.

Mackay-Sim, A., & Kittel, P. (1991). Cell Dynamics in the Adult Mouse Olfactory Epithelium: A Quantitative Autoradiographic Study. *The Journal of Neuroscience: The Official Journal of the Society for Neuroscience*, 11(4), 979–984.

Marques, Ines J.; Lupi, Eleonora; Mercader, Nadia (2019). *Model Systems for Regeneration: Zebrafish. Development*, 146(18), dev167692.

- Mattoon, D. R., Lamothe, B., Lax, I., & Schlessinger, J. (2004). The Docking Protein Gab1 is the Primary Mediator of EGF-stimulated Activation of the PI3K/Akt Cell Survival Pathway. *BMC biology*, 2, 24.
- McCampbell, K. K., & Wingert, R. A. (2014). New Tides: Using Zebrafish to Study Renal Regeneration. *Translational Research: The Journal of Laboratory and Clinical Medicine*, 163(2), 109–122.
- Ming, G., & Song, H. (2005). Adult Neurogenesis in the Mammalian Central Nervous System. *Annual Review of Neuroscience*, 28(1), 223–250.
- Ming, G. L., & Song, H. (2011). Adult Neurogenesis in the Mammalian Brain: Significant Answers and Significant Questions. *Neuron*, 70(4), 687–702.
- Mira, H., Andreu, Z., Suh, H., Lie, D. C., Jessberger, S., Consiglio, A., Gage, F. H. (2010). Signaling Through BMP-IA Regulates Quiescence and Long-term Activity of Neural Stem Cells in the Adult Hippocampus. *Cell Stem Cell*, 7(1), 78–89.
- Mishima K, Higashiyama S, Nagashima Y, Miyagi Y, Tamura A, Kawahara N, Taniguchi N, Asai A, Kuchino Y, Kirino T. Regional Distribution of Heparin-binding Epidermal Growth Factor-like Growth Factor mRNA and Protein in Adult Rat Forebrain. *Neurosci Lett*. 1996; 213:153–156.
- Miyoshi, H., Takahashi, M., Gage, F., & Verma, I. (1997). Stable and Efficient Gene Transfer into the Retina Using an HIV-based Lentiviral Vector. *Proceedings Of The National Academy Of Sciences*, 94(19), 10319-10323.
- Monje, M. L. (2003). Inflammatory Blockade Restores Adult Hippocampal Neurogenesis. *Science*, 302(5651), 1760–1765.
- Mori, K., Nagao, H., & Yoshihara, Y. (1999). The Olfactory Bulb: Coding and Processing of Odor Molecule Information. *Science (New York, N.Y.)*, 286(5440), 711–715.
- Morrison, S. J., & Spradling, A. C. (2008). Stem Cells and Niches: Mechanisms that Promote Stem Cell Maintenance Throughout Life. *Cell*, 132(4), 598–611.

- Moulton, D. G. (1975). Cell Renewal in the Olfactory Epithelium of the Mouse. In J. P. Denton, D. A. and Coughlan (Ed.) (Vol. V, pp. 111–114). New York: Academic Press.
- Owji S, Shoja MM. The History of Discovery of Adult Neurogenesis. *Clin Anat.* 2020 Jan;33(1):41-55.
- Packard, A., Lin, B., & Schwob, J. E. (2016). Sox2 and Pax6 Play Counteracting Roles in Regulating Neurogenesis within the Murine Olfactory Epithelium. *PloS One*, 11(5), e0155167.
- Packard, A., Schnittke, N., Romano, R.-A., Sinha, S., & Schwob, J. E. (2011). DeltaNp63 Regulates Stem Cell Dynamics in the Mammalian Olfactory Epithelium. *The Journal of Neuroscience: The Official Journal of the Society for Neuroscience*, 31(24), 8748–8759.
- Paton, J. A., & Nottebohm, F. N. (1984). Neurons Generated in the Adult Brain are Recruited into Functional Circuits. *Science (New York, N.Y.)*, 225(4666), 1046–1048.
- Prasad C., Brinda; Reed R., Randall (1999). Chemosensation: Molecular Mechanisms in Worms and Mammals. 15(4), 150–153.
- Poss, K. D., Wilson, L. G., & Keating, M. T. (2002). Heart Regeneration in Zebrafish. *Science (New York, N.Y.)*, 298(5601), 2188–2190.
- Puschmann, T. B., Zandén, C., Lebkuechner, I., Philippot, C., de Pablo, Y., Liu, J., & Pekny, M. (2014). HB-EGF Affects Astrocyte Morphology, Proliferation, Differentiation, and the Expression of Intermediate Filament Proteins. *Journal of Neurochemistry*, 128(6), 878-889.
- Raab, G., & Klagsbrun, M. (1997). Heparin-binding EGF-like Growth Factor. *Biochimica et biophysica acta*, 1333(3), F179–F199.

- Radulescu, A., Zorko, N., Yu, X. *et al.* Preclinical Neonatal Rat Studies of Heparin-Binding EGF-Like Growth Factor in Protection of the Intestines from Necrotizing Enterocolitis. *Pediatr Res* 65, 437–442 (2009).
- Ramon y Cajal, S. (1928). *Degeneration and Regeneration of the Nervous System. Degeneration and Regeneration of the Nervous System*. Oxford, England: Clarendon Press.
- Reinchisi, G., Parada, M., Lois, P., Oyanadel, C., Shaughnessy, R., Gonzalez, A., & Palma, V. (2013). Sonic Hedgehog Modulates EGFR Dependent Proliferation of Neural Stem Cells During Late Mouse Embryogenesis Through EGFR Transactivation. *Frontiers in Cellular Neuroscience*, 7, 166.
- Rock, R. B., Gekker, G., Hu, S., Sheng, W. S., Cheeran, M., Lokensgard, J. R., & Peterson, P. K. (2004). Role of Microglia in Central Nervous System Infections. *Clinical Microbiology Reviews*, 17(4), 942–64, table of contents.
- Rowena Spence; Gabriele Gerlach; Christian Lawrence; Carl Smith (2008). *The Behaviour and Ecology of the Zebrafish, Danio rerio.*, 83(1), 13–34.
- Sakızlı, U. (2018). *The Contribution of Purinergic Signaling to Olfactory Neurogenesis in Zebrafish*. Boğaziçi University.
- Sato, Y., N. Miyasaka and Y. Yoshihara, “Mutually Exclusive Glomerular Innervation by Two Distinct Types of Olfactory Sensory Neurons Revealed in Transgenic Zebrafish”, *Journal of Neuroscience*, Vol. 25, No. 20, pp. 4889–4897, 2005.
- Schneider, M.R., Wolf, E., 2009. The Epidermal Growth Factor Receptor Ligands at a Glance. *J. Cell. Physiol.* 218 (3), 460–466.
- Schindelin, J., Arganda-Carreras, I., Frise, E., Kaynig, V., Longair, M., Pietzsch, T., Preibisch, S., Rueden, C., Saalfeld, S., Schmid, B., Tinevez, J. Y., White, D. J., Hartenstein, V., Eliceiri, K., Tomancak, P., & Cardona, A. (2012). Fiji: An Open-source Platform for Biological-image Analysis. *Nature Methods*, 9(7), 676–682.

- Schultz, E. W. (1941). Regeneration of Olfactory Cells. *Experimental Biology and Medicine*, 46(1), 41–43.
- Schnittke, N., D. B. Herrick, B. Lin, J. Peterson, J. H. Coleman, A. I. Packard, W. Jang and J. E. Schwob, “Transcription Factor P63 Controls the Reserve Status but Not the Stemness of Horizontal Basal Cells in the Olfactory Epithelium”, *Proceedings of the National Academy of Sciences of the United States of America*, Vol. 112, No. 36, pp. E5068–E5077, 2015.
- Schwartz Levey, M., Chikaraishi, D. M., & Kauer, J. S. (1991). Characterization of Potential Precursor Populations in the Mouse Olfactory Epithelium Using Immunocytochemistry and Autoradiography. *The Journal of Neuroscience: The Official Journal of the Society for Neuroscience*, 11(11), 3556–3564.
- Schwob, J. E. (2002). Neural Regeneration and the Peripheral Olfactory System. *The Anatomical Record*, 269(1), 33–49.
- Schwob, J. E., Jang, W., Holbrook, E. H., Lin, B., Herrick, D. B., Peterson, J. N., & Hewitt Coleman, J. (2017). Stem and Progenitor Cells of the Mammalian Olfactory Epithelium: Taking Poietic License. *Journal of Comparative Neurology*, 525(4), 1034–1054.
- Schwob, J. E., Youngentob, S. L., & Mezza, R. C. (1995). Reconstitution of the Rat Olfactory Epithelium After Methylbromide-induced Lesion. *The Journal of Comparative Neurology*, 359(1), 15–37.
- Schultz, E. W. (1941). Regeneration of Olfactory Cells. *Proceedings of the Society for Experimental Biology and Medicine*, 46(1), 41–43.
- Shen, Y., Ruan, L., Lian, C., Li, R., Tu, Z., & Liu, H. (2019). Discovery of HB-EGF binding Peptides and Their Functional Characterization in Ovarian Cancer Cell Lines. *Cell Death Discovery*, 5, 82.
- Singh, A. B., & Harris, R. C. (2005). Autocrine, Paracrine and Juxtacrine Signaling by EGFR Ligands. *Cellular Signaling*, 17(10), 1183–1193.

- Spinazzola, J. M., & Kunkel, L. M. (2016). Pharmacological Therapeutics Targeting the Secondary Defects and Downstream Pathology of Duchenne Muscular Dystrophy. *Expert Opinion on Orphan Drugs*, 4(11), 1179–1194.
- Song, H.-G., Young Kwon, J., Soo Han, H., Bae, Y.-C., & Moon, C. (2008). First Contact to Odors: Our Current Knowledge about Odorant Receptor. *Sensors*, 8(10), 6303–6320.
- Sorrells, S. F., Paredes, M. F., Cebrian-Silla, A., Sandoval, K., Qi, D., Kelley, K. W., Alvarez-Buylla, A. (2018). Human Hippocampal Neurogenesis Drops Sharply in Children to Undetectable Levels in Adults. *Nature*, 555(7696), 377–381.
- Stenkamp D. L. (2007). Neurogenesis in the Fish Retina. *International Review of Cytology*, 259, 173–224.
- Streisinger, G. et al. (1986) Segregation Analyses and Gene-centromere Distances in Zebrafish. *Genetics* 112, 311–319.
- Streisinger, G., Walker, C., Dower, N. et al. Production of Clones of Homozygous Diploid Zebrafish (*Brachydanio rerio*). *Nature* 291, 293–296 (1981).
- Sunnarborg SW, Hinkle CL, Stevenson M, Russell WE, Raska CS, Peschon JJ, et al. Tumor Necrosis Factor-alpha Converting Enzyme (TACE) Regulates Epidermal Growth Factor Receptor Ligand Availability. *J Biol Chem* 2002;277(12):838–45.
- Suzuki M, Raab G, Moses MA, Fernandez CA, Klagsbrun M. Matrix Metalloproteinase-3 Releases Active Heparin-binding EGF-like Growth Factor by Cleavage at a Specific Juxtamembrane Site. *J Biol Chem* 1997;272(50):31730–7.
- Taylor, S. R., Markesbery, M. G., & Harding, P. A. (2014). Heparin-binding Epidermal Growth Factor-like Growth factor (HB-EGF) and Proteolytic Processing by a Disintegrin and Metalloproteinases (ADAM): a Regulator of Several Pathways. *Seminars in Cell & Developmental biology*, 28, 22–30.

- Tham, W. W. P., Stevenson, R. J., & Miller, L. A. (2009). The Functional Role of the Medial Dorsal Thalamic Nucleus in Olfaction. *Brain Research Reviews*, 62(1), 109–126.
- Thompson SA, Higashiyama S, Wood K, Pollitt NS, Damm D, McEnroe G, Garrick B, Ashton N, Lau K, Hancock N: Characterization of Sequences within Heparin-binding EGF-like Growth Factor that Mediate Interaction with Heparin. *J Biol Chem* 1994, 269:2541–2549.
- Tierney, K.B.; Baldwin, D.H.; Hara, T.J.; Ross, P.S.; Scholz, N.L.; Kennedy, C.J. Olfactory Toxicity in Fishes. *Aquat. Toxicol.* 2010, 96, 2–26.
- Todd, L., Volkov, L. I., Zelinka, C., Squires, N., & Fischer, A. J. (2015). Heparin-binding EGF-like Growth Factor (HB-EGF) Stimulates the Proliferation of Müller Glia-derived Progenitor Cells in Avian and Murine retinas. *Molecular and Cellular Neurosciences*, 69, 54–64.
- Tolino M. A., Block E. R. And Klarlund J. K. (2011) Brief Treatment with Heparin-binding EGF-like Growth Factor, but not with EGF, is Sufficient to Accelerate Epithelial Wound Healing. *Biochim. Biophys. Acta* 1810,875-8781810,875.
- Veldman, M. B., & Lin, S. (2008). Zebrafish as a Developmental Model Organism for Pediatric Research. *Pediatric Research*, 64(5), 470–476.
- Wagner, S., A. L. Gresser, A. T. Torello and C. Dulac, “A Multireceptor Genetic Approach Uncovers an Ordered Integration of VNO Sensory Inputs in the Accessory Olfactory Bulb”, *Neuron*, Vol. 50, No. 5, pp. 697–709, 2006.
- Wakisaka N, Miyasaka N, Koide T, Masuda M, Hiraki-Kajiyama T, Yoshihara Y (2017) An Adenosine Receptor for Olfaction in Fish. *Curr Biol* 27:1437–1447.e4.
- Wan, J., Ramachandran, R., & Goldman, D. (2012). HB-EGF Is Necessary and Sufficient for Müller Glia Dedifferentiation and Retina Regeneration. *Developmental Cell*, 22, 334–347.

- Wan, J., Zhao, X.-F., Vojtek, A., & Goldman, D. (2014). Retinal Injury, Growth Factors, and Cytokines Converge on β -catenin and pStat3 Signaling to Stimulate Retina Regeneration. *Cell Reports*, *9*(1), 285–297.
- Wang, Y.-Z., Yamagami, T., Gan, Q., Wang, Y., Zhao, T., Hamad, S., Zhou, C. J. (2011). Canonical Wnt signaling Promotes the Proliferation and Neurogenesis of Peripheral Olfactory Stem Cells During Postnatal Development and Adult Regeneration. *Journal of Cell Science*, *124*(9), 1553–1563.
- Wan, J., & Goldman, D. (2016). Retina Regeneration in Zebrafish. *Current Opinion in Genetics & Development*, *40*, 41–47.
- Wee, P., & Wang, Z. (2017). Epidermal Growth Factor Receptor Cell Proliferation Signaling Pathways. *Cancers*, *9*(5), 52.
- Westerfield, M. (1995). *The Zebrafish Book. A Guide for the Laboratory Use of Zebrafish (Danio rerio)* (3rd ed.).
- Weth, F., Nadler, W., and Korsching, S. (1996) Nested Expression Domains for Odorant Receptors in Zebrafish Olfactory Epithelium. *Proceedings of the National Academy of Sciences of the United States of America*. *93*(23):13321-13326.
- Weuste, M., A. Wurm, I. Iandiev, P. Wiedemann, A. Reichenbach and A. Bringmann, “HB-EGF: Increase in the Ischemic Rat Retina and Inhibition of Osmotic Glial Cell Swelling”, *Biochemical and Biophysical Research Communications*, Vol. 347, No. 1, pp. 310–318, 2006.
- Williams, J.A., & Holder, N. (2000). Cell Turnover in Neuromasts of Zebrafish Larvae. *Hearing Research*, *143*, 171-181.
- Yan Y, Shirakabe K, Werb Z. The Metalloprotease Kuzbanian (ADAM10) Mediates the Transactivation of EGF Receptor by G Protein-coupled Receptors. *J Cell Biol* 2002; *158*:221–6.
- Yu WH, Woessner JF, McNeish JD, Stamenkovic I. CD44 Anchors the Assembly of Matrilysin/MMP-7 with Heparin-binding Epidermal Growth Factor Precursor and

- ErbB4 and Regulates Female Reproductive Organ Remodeling. *Genes Dev* 2002; 16:307–23.
- Yu, C. R., & Wu, Y. (2017). Regeneration and Rewiring of Rodent Olfactory Sensory Neurons. *Experimental Neurology*, 287(Pt 3), 395–408.
- Zhang, R. L., Zhang, Z. G., & Chopp, M. (2005). Neurogenesis in the Adult Ischemic Brain: Generation, Migration, Survival, and Restorative Therapy. *The Neuroscientist*, 11(5), 408–416.
- Zhang, R., Oyajobi, B. O., Harris, S. E., Chen, D., Tsao, C., Deng, H.-W., & Zhao, M. (2013). Wnt/ β -catenin Signaling Activates Bone Morphogenetic Protein 2 Expression in Osteoblasts. *Bone*, 52(1), 145–156.
- Zhao, X.-F., Wan, J., Powell, C., Ramachandran, R., Myers, M. G., & Goldman, D. (2014). Leptin and IL-6 Family Cytokines Synergize to Stimulate Müller Glia Reprogramming and Retina Regeneration. *Cell Reports*, 9(1), 272–284.
- Zupanc, G. K. (2001). Adult Neurogenesis and Neuronal Regeneration in the Central Nervous System of Teleost Fish. *Brain, Behavior and Evolution*, 58(5), 250–275.
- Zupanc, G. K. H., & Horschke, I. (1995). Proliferation Zones in the Brain of Adult Gymnotiform Fish: A Quantitative Mapping Study. *The Journal of Comparative Neurology*, 353(2), 213–233.

APPENDIX A: EQUIPMENT, CHEMICALS and REAGENTS

Table A.1. List of equipment

Equipment	Manufacturer
05-090-128 Mini Centrifuges	Fisher Scientific, Korea
-20°C Freezer	Uğur, Turkey
-80°C Freezer, Farma 723	Thermo Elektron Corp., USA
4°C Room	Birikim Elektrik, Turkey
37°C Room	Birikim Elektrik, Turkey
Agarose Gel Tank, Mini Sub Cell GT Cell	BioRad, China
Aquatic Habitats	Pentair Aquatic Eco-systems, Inc., USA
Beaker	IsoLab, Germany
C1000 Thermal Cycler	Bio-Rad, USA
Capillary glass (1.00 mm × 0.75 mm × 10'')	Sutter Instrument, Co., USA
Centrifuge 5424, 5417R	Eppendorf, Germany
Colibri Microvolume spectrometer	Titertek Berthold, Germany
Coplin Staining Jar with Cover	VWR, USA
Confocal Microscope, SP5-AOBS	Leica Microsystems, USA
Confocal Microscope, SP5-AOBS Software LAS AF	Leica Microsystems, USA
Cryostat CM3050S	Leica Biosystems, Germany

Table A.1. List of equipment (cont.)

Dishwasher, Melabor G 7783	Miele, Germany
Dual Intensity Transilluminator	UVP, USA
Electrical Balance, TE412	Sartorius, Germany
Filter tips (10, 20, 100, 200, 1000 μ l)	Griener Bio-One, Germany
Fiji Image J Software	Developed at NIH
Forceps, FST	Dumont, Switzerland
Gel Doc XR Gel Documentation System	BioRad, China
GEloader tips, 0.5-20 μ l	Eppendorf, Germany
Glass bottle	Isolab, Germany
Graduate cylinder	Isolab, Germany
Ice Flaker	Brema, Italy
IKA Color Squid magnetic stirrer	IKA works, Inc., USA
Incubator 1	Weiss, Gallenkamp, UK
Incubator 2	Nüve, Turkey
Incubated Benchtop Orbital Shaker	Thermo Scientific, USA
<i>In vitro</i> transcription kit	Roche, Germany
Laboratory Hybridization Oven, G2545A	Agilent Technologies, USA
Magnetic stirrer and heater, RH B 2	IKA works, Inc., USA
Microcentrifuge tubes 1.5 ml	Capp ApS, Denmark
Microwave oven	Vestel, Turkey

Table A.1. List of equipment (cont.)

Microinjector, FemtoJet	Eppendorf, Germany
Microinjection Needles, Nanoject II	Warner Instruments, USA
Orbital shaker, Rotamax 120	Heidolph, Germany
P-97 Micropipette Puller	Sutter Instrument, Co., USA
Parafilm™	Parafilm, USA
PCR® strip Tubes	Axygen, USA
Petri Dishes, 60 ×15 mm	TPP Tecjno Plastic Products AG, Switzerland
pH-meter, pH315i	WTW, Germany
Prism 7.0	GrpPad, USA
Refrigerator	Arçelik, Turkey
Serological pipettes (5ml, 10 ml, 25ml, 50 ml)	Greiner Bio-One, Germany
Shake 'n' stack hybridization oven, 6240	Thermo Fisher Scientific, USA
Single channel micropipettes (10, 20, 100, 200, 1000 µl)	Eppendorf, Germany
Stemi 2000-C stereomicroscope	Zeiss, Germany
Super PAP Pen	Liquid Blocker, Japan
Superfrost Plus slides	VWR, Germany
Superfrost slides	Thermo Fisher Scientific, USA
Swiftlock Front loading Autoclave	Astell, UK

Table A.1. List of equipment (cont.)

Syngene G:Box Chemi XRQ Chemiluminescence and Fluorescence System	Syngene, UK
Syringe filter, 0.22 μm , 99722	TPP, Switzerland
SZ61 stereomicroscope	Olympus, USA
Tissue-Plus O.C.T. compound	Fisher HealthCare, USA
Universal Incubator	Binder, Germany
Vortex- Genie 2	Scientific Industries, Inc., USA
Water Bath, WNB 7	Memmert, Germany

Table A.2. List of chemicals and reagents

Chemical / Reagent	Manufacturer
1 kb DNA ladder, N3232	New England Biolabs, USA
100 bp DNA ladder, N3231	New England Biolabs, USA
5- Bromo-2'- Deoxyuridine (BrdU) BioChemica A2139, 0005	AppliChem, Germany
6X DNA Loading Dye, B7021S	New England Biolabs, USA
10X RNA Loading Dye,	
pGEM®-T Easy Vector System	Promega, USA

Table A.2. List of chemicals and reagents (cont.)

T4 DNA Ligase, M0202L	New England Biolabs, USA
dNTP	New England Biolabs, USA
α -DIG-Alkaline Phosphatase Fab Fragments	Roche, Germany
Acetic Anhydride	Merck, Germany
Agarose Universal PeqGOLD	VWR, USA
Absolute Ethanol (Ethyl alcohol), 34870	Sigma-Aldrich, USA
Advantage 2 PCR Kit, 639207	Clontech by Takara Biotechnologies, USA
Alexa Flour® 488, A28175	Life Technologies, USA
Alexa Flour® 555	Life Technologies, USA
Alexa Flour® 647	Life Technologies, USA
Anti-mouse-CytII antibody,	Life Technologies, USA
Anti-mouse-HuC/D antibody, 1661237	Life Technologies, USA
Anti-rabbit-Krt5 antibody,	Life Technologies, USA
Anti-rabbit-Sox2 antibody,	Life Technologies, USA
Anti-rabbit-tp63 antibody,	Life Technologies, USA
Blocking reagent	Roche, USA
Calcium Sulfate	Sigma-Aldrich, USA
Citric Acid, C8532	Sigma-Aldrich, USA
EDTA Disodium Salt, E5134	Sigma-Aldrich, USA

Table A.2. List of chemicals and reagents (cont.)

Endonuclease EcoRI, R0101S and buffer	New England Biolabs, USA
Endonuclease Sall, R0138S and buffer	New England Biolabs, USA
Ethidium Bromide, E1510-1ml	Sigma Life Sciences, USA
Fast HNPP Fluorescent Detection Kit, 11 758 888 001	Sigma-Aldrich, USA
Formamide	Sigma Life Sciences, USA
Formamide	Roche, Germany
High Pure PCR Product Purification Kit	Roche, USA
High Pure Plasmid Isolation (MiniPrep) Kit	Roche, USA
High Pure Plasmid Isolation (MidiPrep) Kit	Roche, USA
Hydrochloric acid (HCl)	Merck, Germany
<i>In vitro</i> Transcription Kit	Roche, Germany
LB Agar, SL08394	Sigma Life Sciences, USA
LB Broth EZMix™, L7658	Sigma Life Sciences, USA
Maleic Acid,141882	Pancreac Quimica SA, Spain
MS-222 (Ethyl 3-aminobenzoate methanesulfate salt)	Sigma-Aldrich, USA
NcoI-HF and buffer	New England Biolabs, USA
OneTaq® Polymerase, M0480L	New England Biolabs, USA

Table A.2. List of chemicals and reagents (cont.)

Magnesium Chloride (MgCl ₂), 25mM, A3511	Promega, USA
Optimum Cutting Temperature Compound (OCT), 4583	Sakura Finetek, USA
Parafilm, PM-996	Bemis Curwood, Sigma-Aldrich, USA
Paraformaldehyde, P6148-1kg	Sigma-Aldrich, USA
Phenol Red, A7615,01001	AppliChem, USA
Phosphate Buffered Saline (PBS) Tablet, P4417	Sigma-Aldrich, USA
Potassium Chloride (KCl), P9541	Sigma-Aldrich, USA
Proteinase K	Roche, USA
Sodium Chloride (NaCl), S7653	Sigma-Aldrich, USA
Sodium Hydroxide (NaOH), S8045	Sigma-Aldrich, USA
Sodium Acetate (NaOAc), S8625	Sigma-Aldrich, USA
Tri-ethylamine (TEA)	Merck Millipore, USA
Trizma® Base, T6066	Sigma-Aldrich, USA
Triton™ X-100, A4975	AppliChem, USA
Tween®20, 11332465001	Roche, USA

Table A.3. Solutions and Buffers

Buffer / Solution	Preparation / Content
Diethylpyrocarbonate (DEPC) Treated Distilled Water	<ul style="list-style-type: none"> - On 1.0 L dH₂O, add 1.0 ml of DEPC - Stir overnight at RT - Sterilize and deactivate by autoclave
4M Lithium Chloride Solution (LiCl)	<ul style="list-style-type: none"> - Dissolve 17.0g LiCl powder in 100 ml dH₂O final volume - Add 100 µl DEPC into the solution and stir overnight at RT - Sterilize and deactivate DEPC by autoclaving
4% Paraformaldehyde Solution (PFA)	<ul style="list-style-type: none"> - Dissolve 4g PFA in 75 ml dH₂O_{DT} in water bath at 60-65°C - Add a few droplets of NaOH until the solution becomes transparent - Add 10ml 10X PBS_{DT} and mix well to get a clear solution without any precipitation at the bottom of the Erlenmeyer flask - Adjust pH to exactly 7.4 by slowly adding concentrated HCl - Add dH₂O_{DT} up to 100 ml final volume - Filtrate the solution via vacuum filtration or 0.22 µm filter and let it cool down at 4°C

Table A.3. Solutions and Buffers (cont.)

10X Blocking Stock Solution	<ul style="list-style-type: none"> - Slowly add 10g of DIG Blocking Reagent in 100 ml previously prepared Maleic acid buffer while it is shaking on a heater - Solution should not be boiled - Sterilize by autoclaving
1M Citric Acid Solution	<ul style="list-style-type: none"> - Dissolve 14,705g Citric Acid in dH₂O_{DT}
1% Triton-X Damage Solution	<ul style="list-style-type: none"> - Mix 395 μl 1X PBS, 100 μl Phenol red (0.05% final) and 5 μl Triton-X and shake well until you get clear reddish-purple solution
0.1% Triton-X Damage Solution	<ul style="list-style-type: none"> - Dilute 1% Triton-X damage solution by 1X PBS to 0.1% final concentration
1M Maleic Acid Buffer Solution	<ul style="list-style-type: none"> - Dissolve 0,876g NaCl and 1.161g Maleic Acid in 80 ml dH₂O_{DT} - Adjust pH to 7.5 by slowly adding concentrated NaOH - Add dH₂O_{DT} up to 100 ml final volume - Sterilize by autoclaving

Table A.3. Solutions and Buffers (cont.)

10X PBS Buffer Stock Solution	<ul style="list-style-type: none"> - Dissolve 50 Sigma-Aldrich PBS tablets in dH₂O_{DT}, to a final 500 ml solution <ul style="list-style-type: none"> - Adjust pH to 7.4 - Add 500 µl of DEPC - Stir overnight, sterilize and deactivate DEPC by autoclave 10X Buffer composition: <ul style="list-style-type: none"> - 1.37M NaCl - 0.1M phosphate buffer (Na₂HPO₄) - 0.027M KCl - pH:7.4 AT 25°C
1X PBST	<ul style="list-style-type: none"> - Add 100 ml 10X PBS stock solution and adjust final volume to 1.0L by adding dH₂O_{DT} - Add 5 ml Tween-20 (Final concentration of Tween-20 is 0.05%)
1M Sodium Chloride Solution (NaCl)	<ul style="list-style-type: none"> - Dissolve 5,844g NaCl in 100 ml dH₂O_{DT} - Sterilize by autoclaving
10N Sodium Hydroxide Solution (NaOH)	<ul style="list-style-type: none"> - Dissolve slowly 40g NaOH beads in 75 ml dH₂O_{DT} in a plastic beaker - Adjust final volume to 100 ml by adding dH₂O_{DT}

Table A.3. Solutions and Buffers (cont.)

20X SSC Stock Solution	<ul style="list-style-type: none"> - Add 87.65g NaCl (3.0M final), 44.1g Sodium Citrate Tribasic Dihydrate (300mM final) and dissolve in 400 ml dH₂O_{DT} - Adjust pH to 7.0 with HCl - Add dH₂O_{DT} up to 500 ml final volume <ul style="list-style-type: none"> - Add 500 µl of DEPC - Stir overnight, sterilize and deactivate DEPC by autoclave
10X Tris-Acetate-EDTA (TAE) Stock Buffer	<ul style="list-style-type: none"> - Tris pH:8 at final 400mM concentration - EDTA final concentration 10mM - Adjust pH to 8.0 by acetic acid
0.2M Ethylenediaminetetraacetic acid (EDTA)	<ul style="list-style-type: none"> - Dissolve 7.45g EDTA in 80 ml dH₂O - Add magnetic stirrer into the solution and add NaOH bead one-by-one into the solution while shaking - Adjust pH to 8.0 and stabilize - Add dH₂O up to 100 ml final volume <ul style="list-style-type: none"> - Add 100 µl DEPC into the solution and stir overnight at RT - Sterilize and deactivate DEPC by autoclaving

Table A.3. Solutions and Buffers (cont.)

1M Tris-HCl Buffer solution, pH:7.5	<ul style="list-style-type: none"> - Dissolve 30.28g Trizma® base in 200 ml dH₂O_{DT} - Adjust pH to 7.5 by slowly adding concentrated HCl - Add dH₂O_{DT} up to 250 ml final volume - Shake well and sterilize by autoclave
1M Tris-HCl Buffer solution, pH:8.0	<ul style="list-style-type: none"> - Dissolve 60.55g Trizma® base in 400 ml dH₂O_{DT} - Adjust pH to 8.0 by slowly adding concentrated HCl - Add dH₂O_{DT} up to 500 ml final volume <p>Shake well and sterilize by autoclave</p>
LB Broth Medium, Lennox	<ul style="list-style-type: none"> - Dissolve 20.6g Sigma-Aldrich LB Broth EZMix™ in 1.0 ml dH₂O - Sterilize by autoclaving

Table A.3. Solutions and Buffers (cont.)

LB Broth Medium with Agar, Lennox	<ul style="list-style-type: none"> - Dissolve 35.6g Sigma-Aldrich LB Broth EZMix™ with agar in 1.0 ml dH₂O - Sterilize by autoclaving - Add desired antibiotics (ampicillin in this study) when the solution cools down to 55°C - Disperse on the plastic petri dishes and up-side down - Store plates after the temperature decreases to RT at 4°C room for later processing
<i>In situ</i> -Hybridization Solution	<ul style="list-style-type: none"> - Formamide final concentration 50% - 20X Stock Solution to final concentration 5X - Heparin final concentration 50µg/ml - Total yeast tRNA final concentration 250µg/ml - Riboprobe final concentration 3µg/ml - Tween-20 final concentration 0.05% <ul style="list-style-type: none"> - 1M Citric acid final concentration 9.2mM
<i>In situ</i> -Hybridization Detection Solution	<ul style="list-style-type: none"> - NaCl final concentration 100mM <ul style="list-style-type: none"> - Tris-HCl, pH:8 final concentration 100 mM - MgCl₂ final concentration 10mM